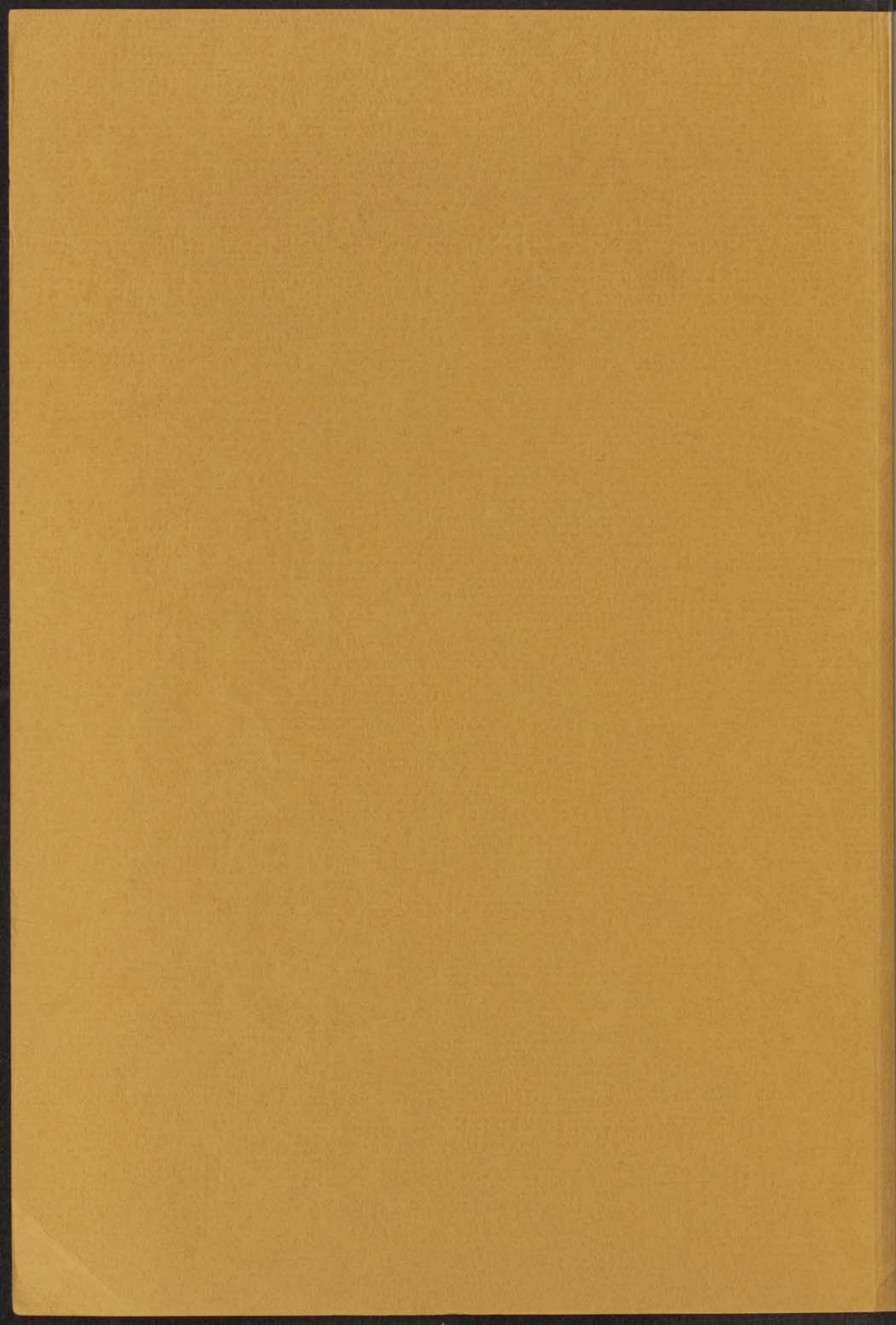


SOME EXPERIMENTS ON  
HEAT TRANSFER AND MAGNETISM  
BELOW  $1^{\circ}$  K



A. R. MIEDEMA



18 JUN 1960



kast dissertaties



SOME EXPERIMENTS ON HEAT TRANSFER  
AND MAGNETISM BELOW  $1^{\circ}$  K





SOME EXPERIMENTS ON  
HEAT TRANSFER AND MAGNETISM  
BELOW  $1^{\circ}$  K



PROEFSCHRIFT

TER VERKRIJGING VAN DE GRAAD VAN DOCTOR IN DE  
WIS- EN NATUURKUNDE AAN DE RIJKSUNIVERSITEIT  
TE LEIDEN, OP GEZAG VAN DE RECTOR MAGNIFICUS  
MR J. V. RIJPPERDA WIERDSMA, HOOGLERAAR IN DE  
FACULTEIT DER RECHTSGELEERDHEID, PUBLIEK TE  
VERDEDIGEN OP DONDERDAG 1 DECEMBER 1960  
TE 16 UUR

DOOR

ANDRIES RINSE MIEDEMA

GEBOREN TE LEEUWARDEN IN 1933

1960

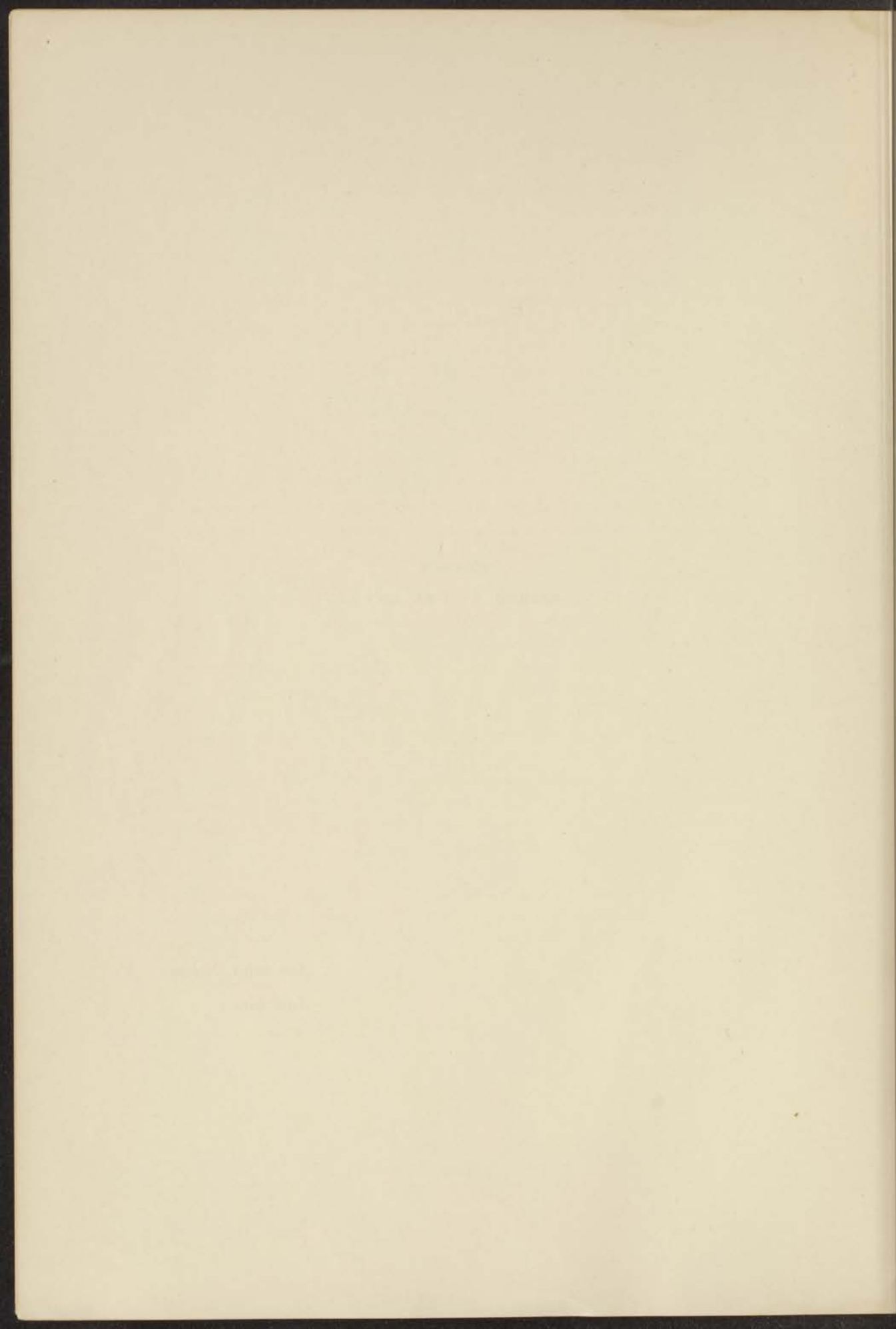
N.V. DRUKKERIJ HOLLAND - AMSTERDAM



*Promotor :*  
Prof. Dr C. J. GORTER

*Aan mijn Ouders*

*Aan Lies*



Teneinde te voldoen aan de wens van de Faculteit der Wis- en Natuurkunde volgt hier een kort overzicht van mijn academische studie.

Na 5 jaar het onderwijs aan de Dalton H.B.S. te 's Gravenhage gevolgd te hebben, begon ik in September 1951 mijn studie aan de Rijksuniversiteit te Leiden. Het candidaatsexamen D legde ik in October 1954 af. Bij mijn intrede in het Kamerlingh Onnes Laboratorium werd ik ingedeeld bij de werkgroep voor adiabatische demagnetisatie, die onder leiding stond van Dr M. J. STEENLAND.

Drs J. A. BEUN heeft mij in de problemen der experimentele natuurkunde ingewijd. Ik assisteerde hem bij zijn onderzoekingen over magnetische eigenschappen van chroomaluinen en werkte verder mee aan metingen van lineaire en circulaire polarisatie van gammastraling.

De natuurkunde en mechanica colleges voor mijn doctoraal examen, afgelegd in October 1957, volgde ik bij Prof. Dr S. R. DE GROOT, Dr P. MAZÜR en Dr J. VAN KRANENDONK. Sinds 1956 ben ik als assistent verbonden aan het practicum voor praecandidaten.

Het werk waarop dit proefschrift is gebaseerd werd begonnen in 1956 en stond aanvankelijk onder leiding van Dr M. J. STEENLAND, later onder de leiding van Dr W. J. HUISKAMP. Sedert mijn doctoraal examen heb ik nauw samengewerkt met de heer H. POSTMA, die onderzoekingen verricht aan beta en gamma emissie van gerichte atoomkernen.

Behalve van de wetenschappelijke staf ondervond ik veel steun van de technische en administratieve staf van het Kamerlingh Onnes Laboratorium, in het bijzonder van de heren J. VAN WEESEL en A. R. B. GERRITSE die mij steeds met raad en daad ter zijde hebben gestaan bij problemen van experimentele aard.

Bij de voorbereiding, uitvoering en uitwerking van metingen werd ik geassisteerd door mej. N. J. VAN DER VLUGT, mej. M. C. EVERSDIJK SMULDERS en de heren P. KALMIJN, W. TOUTENHOOFD, J. LUBBERS en H. VAN KEMPEN. Ook Dr M. KOLÁČ (Praag) nam enige tijd aan het onderzoek deel.

Met genoegen denk ik aan de talrijke discussies op meteorologisch gebied, die ten huize van de heer H. A. D. MISPELBLOM BEYER plaats vonden en waarbij vooral de opstijgende beweging in cumuluswolken in de belangstelling stond.

De Engelse tekst van dit proefschrift werd gecorrigeerd door de heer C. M. KNOBLER.



## CONTENTS

	Page
INTRODUCTION AND SUMMARY . . . . .	1
CHAPTER I. APPARATUS AND SOME EXPERIMENTAL METHODS . . . . .	5
1. Experimental arrangement . . . . .	5
2. The measuring bridge . . . . .	5
3. Temperature measurements below 1° K . . . . .	7
CHAPTER II. EXPERIMENTS WITH SOLIDIFIED SOLUTIONS OF PARAMAGNETIC SALTS . . . . .	10
1. Cr(NO <sub>3</sub> ) <sub>3</sub> ·9H <sub>2</sub> O in 1-propanol ( $7.5 \times 10^{-4}$ mole/cm <sup>3</sup> ) . . . . .	11
2. Cr(NO <sub>3</sub> ) <sub>3</sub> ·9H <sub>2</sub> O in 1-propanol ( $2.5 \times 10^{-4}$ mole/cm <sup>3</sup> ) . . . . .	13
3. CrCl <sub>3</sub> ·6H <sub>2</sub> O in 1-propanol ( $10 \times 10^{-4}$ mole/cm <sup>3</sup> ) . . . . .	14
4. FeCl <sub>2</sub> ·6H <sub>2</sub> O in 1-propanol ( $17.5 \times 10^{-4}$ and $3.5 \times 10^{-4}$ mole/cm <sup>3</sup> ) . . . . .	15
5. CuCl <sub>2</sub> ·2H <sub>2</sub> O in 1-propanol ( $8.5 \times 10^{-4}$ mole/cm <sup>3</sup> ) . . . . .	17
6. Ce(NO <sub>3</sub> ) <sub>3</sub> ·9H <sub>2</sub> O in ethanol ( $25 \times 10^{-4}$ mole/cm <sup>3</sup> ) . . . . .	19
7. The negative result of an attempt to obtain nuclear polarization . . . . .	19
CHAPTER III. SOME EXPERIMENTS ON HEAT TRANSFER BELOW 1° K . . . . .	20
1. General remarks . . . . .	20
2. Recent Leiden experiments . . . . .	22
3. Experimental data and analysis . . . . .	23
4. Derivation of the value for the thermal conductivity of CrK-alum . . . . .	29
5. Comparison with theory . . . . .	30
6. The thermal resistance of a crystal-glue-copper contact . . . . .	32
7. Conclusions and comparison of different indirect cooling methods . . . . .	34
CHAPTER IV. THE MAGNETIC BEHAVIOUR OF FOUR TUTTON SALTS BELOW 1° K. . . . .	38
1. Manganese ammonium tutton salt . . . . .	40
2. Cobalt ammonium tutton salt . . . . .	46
3. Absorption and dispersion measurements . . . . .	47
4. Copper ammonium tutton salt . . . . .	50
5. Copper potassium tutton salt . . . . .	52
CHAPTER V. THE MAGNETIC STRUCTURE OF THE INVESTIGATED TUTTON SALTS . . . . .	55
1. A molecular field model for CoNH <sub>4</sub> - and MnNH <sub>4</sub> -tutton salt . . . . .	55
2. Calculations of spin angle and zero field susceptibilities . . . . .	57
3. The magnetic structure of CuNH <sub>4</sub> - and CuK-tutton salt . . . . .	67
4. Conclusions . . . . .	70
CHAPTER VI. SOME EXPERIMENTS ON NUCLEAR ORIENTATION IN MAGNETICALLY ORDERED TUTTON SALTS . . . . .	73
1. Experiments . . . . .	73
2. Some theoretical aspects . . . . .	76
3. Comparison with theory . . . . .	78
4. Discussion . . . . .	80
5. Conclusions . . . . .	82
6. The crystal field splitting of manganese ions in a tutton salt . . . . .	82
SAMENVATTING . . . . .	84

Faint, illegible text, possibly bleed-through from the reverse side of the page. The text is arranged in several paragraphs and appears to be a formal document or report.

## INTRODUCTION AND SUMMARY

The experiments which will be reported in this thesis have been performed at temperatures below 1° K. These temperatures can be attained by the method of adiabatic demagnetization of paramagnetic salts. The method was proposed independently by DEBYE [1] and GIAUQUE [2] and the first experimental results were obtained in 1933. A detailed description of the physical principles of the method has been given by many authors; for this the reader is referred to the literature, ref. [3] and [4]. Briefly, use is made of the fact that certain salts retain their paramagnetic properties down to temperatures of about 0.01° K and possess a large entropy at liquid helium temperatures because the electron magnetic moments are nearly free. This entropy may be removed for a greater part by magnetizing at a temperature of about 1° K in magnetic fields of the order of 10<sup>4</sup> oersted. A subsequent adiabatic removal of the field will result in a fall in the temperature of the salt, until the small magnetic interaction between the paramagnetic ions brings about the same degree of order as the strong magnetic field did at 1° K. Increasing the magnetic field and decreasing the starting temperature results in a lower final temperature. For ideal paramagnetic salts the entropy removed is a function of  $H/T$  as can be seen from the formula:

$$(1) \quad S/R = \alpha \coth \alpha - (2J+1) \alpha \coth \alpha(2J+1) + \\ + \log \sinh \alpha(2J+1) - \log \sinh \alpha$$

where  $\alpha = \frac{1}{2} g \mu_B H/kT$ ,  $J$  denotes the total angular momentum,  $\mu_B$  the Bohr magneton and  $g$  the Landé splitting factor. In practice the formula does not hold rigorously since in most cases the lattice entropy still gives a notable contribution to  $S$  at 1° K and the paramagnetic salts are not ideal because of magnetic and electric interactions. However, in many cases the corrections are small.

At the low temperatures reached after adiabatic demagnetization the temperature can not be measured by the methods usual at high temperatures. Indirect procedures must be applied in which use is made of properties of the salt itself; for instance, the magnetic properties. In chapter I a short description of the apparatus for measuring the magnetic properties of a salt will be given. The experimental way to determine the absolute temperatures from magnetic measurements alone will be explained and some properties of salts which can be used as thermometers will be compared.

The thermal and magnetic properties of about 30 paramagnetic materials have been studied in some detail below 1° K. The behaviour at the lowest temperatures that can be reached by demagnetization is

mainly determined by the magnetic interactions between neighbouring paramagnetic ions. Collective magnetic effects, like ferro- or antiferromagnetism may occur at these temperatures. Such magnetic effects can be expected to be anisotropic with respect to the crystal field axes and, if possible, magnetic investigations should therefore be performed with a single crystal. In this thesis the data obtained with single crystals of four magnetic tutton salts will be reported. The magnetic behaviour of cobalt- and manganese ammonium tutton salt and two copper tutton salts is described in chapter IV. A simple model for the structure of the magnetic ordering in the ammonium tutton salts will be given which is in fair agreement with the experimental results. The magnetic interactions in the investigated crystals are considered in more detail in chapter V and a quantitative discussion of the magnetic interaction between a particular ion and its magnetic neighbours is given.

A new type of paramagnetic substances, solidified solutions of paramagnetic ions in alcohols, has been investigated. Using solvents which can readily be supercooled it is possible to experiment on solutions below  $1^{\circ}$  K. In some respects the magnetic behaviour of the solutions does not differ much from that of the normal paramagnetic crystals, but in a few cases rather strange effects such as very long spin-lattice relaxation times or large electric splittings were found. The results obtained with several solutions of chromium, iron and copper ions are reported in chapter II.

It is evident that the method of adiabatic demagnetization can only be used for paramagnetic substances. In order to cool down other materials or paramagnetics which cannot be demagnetized to a sufficiently low temperature, it is necessary to achieve good thermal contact between these materials and a salt which can be demagnetized to low enough a temperature. Since heat transfer takes place by means of thermal vibrations it is clear that the thermal contact problem becomes the more serious the lower the temperature. In chapter III experiments are described concerning heat transfer from a single crystal to a cooling substance which consists of a solution of paramagnetic ions in alcohol. The heat flow has been measured at temperatures between  $0.6$  and  $0.015^{\circ}$  K. With the experimental data covering such a large temperature range, an analysis of the various thermal resistances occurring can be given. The results will be compared with the theory of heat transport by phonons.

The method for indirect cooling developed was applied in experiments on nuclear alignment in antiferromagnetic salts. Nuclear orientation may occur if the interaction energy between a magnetic field and the magnetic moment of a nucleus is not small compared with the thermal energy  $kT$ . Since magnetic moments of nuclei are much smaller than those of electrons the readily obtainable  $H/T$  values of  $10^4$  Oe/deg are not sufficient to remove entropy from the nuclear system. A way to realize

the large  $H/T$  values of about  $10^7$  Oe/deg which are needed, was suggested by GORTER [5] and ROSE [6]. Use is made of the magnetic fields caused by the atomic electrons at the position of the nuclei, which are of the order of  $10^5$ – $10^6$  Oe (the hyperfine structure interaction, h.f.s.). The electron moments can be oriented at a temperature of  $0.01^\circ$  K, which is reached after adiabatic demagnetization, in a field of a few hundred oersted. The nuclei will then be polarized, since  $H/T$  values of  $10^7$ – $10^8$  Oe/deg are reached at their position. The electrons may also be oriented at  $0.01^\circ$  K without external magnetic field if strongly anisotropic magnetic interactions, related to the crystalline fields, occur [7]. In that case the nuclei will be oriented in antiparallel directions, involving a decrease in entropy but no resulting magnetic moment. Such nuclear alignment might also occur in an antiferromagnetic salt, if a preferential direction is present.

Nuclear orientation can be detected when radioactive nuclei are used, the directional distribution of the gamma radiation emitted from oriented nuclei being anisotropic. Expressions for the anisotropy have been derived theoretically for many types of transitions, ref. [8] and [9].

In chapter VI the data on the alignment of radioactive  $^{54}\text{Mn}$  and  $^{60}\text{Co}$  nuclei incorporated in magnetically ordered cobalt ammonium and manganese ammonium tutton salt will be reported. The temperatures reached with these salts after demagnetization are not very low due to the strong magnetic interactions existing in the crystals. In order to attain a larger anisotropy of the gamma radiation the application of an indirect cooling method is essential. For anisotropy effects of the order of magnitude reached in the experiments reported in chapter VI the normalized  $\gamma$ -ray intensity in a direction which makes an angle  $\beta$  with the nuclear alignment axis is given by:

$$(2) \quad W(\beta) = 1 - (15/7)N_2 f_2 P_2$$

where  $N_2 = I/(2I-1)$ ,  $I$  is the nuclear spin quantum number,  $f_2$  is determined by the h.f.s. interaction and the absolute temperature and  $P_2$  stands for  $(3/2)(\cos^2 \beta - 1/3)$ .

Formula (2) shows that by comparing the  $\gamma$ -ray intensities measured in several directions, the position of the axes of nuclear orientation can be derived with respect to the crystal axes. From the  $W$  versus  $T$  relation experimentally found and by comparing the alignment directions of the nuclei with those of the electron magnetic moments as derived from magnetic investigations on the same salts (chap. V), information about the h.f.s. interaction in antiferromagnetic crystals has been obtained.

#### REFERENCES

1. DEBYE, P., Ann. Phys. 81, 1184 (1926).
2. GIAUQUE, W. F., J. Amer. Chem. Soc. 49, 1864 (1927).

3. DE KLERK, D. and M. J. STEENLAND, Progress in Low Temperature Physics, North-Holland Publ. Co., Amsterdam (1955).
4. ———, Handbuch der Physik 15, 38 (1956).
5. GORTER, C. J., Cérémonies Langevin et Perrin, Paris, 77, (1948). Commun. Kamerlingh Onnes Lab., Leiden suppl. 97d; Physica 14, 504 (1948).
6. ROSE, M. E., Phys. Rev. 75, 213 (1949).
7. BLEANEY, B., Phil. Mag. 42, 441 (1951).
8. STEENBERG, N. R., Proc. Phys. Soc. (London) A 66, 391 (1953).
9. TOLHOEK, H. A., Physica 18, 1257 (1952).  
——— and J. A. M. Cox, Physica 19, 101 (1953).

## CHAPTER I

### APPARATUS AND SOME EXPERIMENTAL METHODS

#### 1. *Experimental arrangement*

For the method of adiabatic demagnetization one needs a suitable paramagnetic substance in a cryostat with liquid helium at as low a temperature as possible and mounted in such a way that it can be magnetized in heat contact with the liquid helium (isothermally) and demagnetized under thermal insulation (adiabatically). The equipment used in the Kamerlingh Onnes Laboratory has been described extensively several times, ref. [1], [2] and [3]. A short description will be given here. The cryostat is located between the poles of an 80 kW electromagnet, which gives a field of 22300 oersted in a pole gap of 7.5 cm and which is homogeneous to within 1 % over a region with a diameter of 5 cm.

In order to obtain a low starting temperature for the demagnetization process the liquid helium is evaporated under reduced pressure. By means of a combination of an oil diffusion pump (Booster) and a large capacity mechanical pump the temperature of the liquid helium bath can be reduced to somewhat below 1° K. The heat contact between the salt and the liquid helium bath is made and broken with the help of exchange gas; the sample is mounted in a vacuum space and during isothermal magnetization the space is filled with helium gas at a pressure of about  $10^{-3}$  mm Hg. Thereafter the gas is pumped off with a Hg diffusion pump and then the field is removed. The sample being now thermally isolated from the surrounding helium bath the demagnetization is practically isentropic and the temperature of the salt falls. After demagnetization the sample warms up again slowly. The amount of heat which enters the sample can be reduced to less than 0.1 erg/s, which makes it possible to perform the low temperature measurements nearly isothermally, if the heat capacities of the cooled substances are not too small.

#### 2. *The measuring bridge*

The magnetic properties, such as the static susceptibility  $\chi_0$  and the real and imaginary parts of the oscillating susceptibility  $\chi'$  and  $\chi''$ , have been determined by means of an induction bridge of the Hartshorn type. It can be used for both ballistic and a.c. measurements. A schematic diagram of the bridge method can be seen in fig. 1.1.  $M_1$  represents the paramagnetic salt surrounded by the primary and secondary windings of a mutual inductance. This is connected in series with a variable inductance  $M_2$ , which is a part of the bridge circuit. If the bridge is used for ballistic measurements, the primary circuit is fed from a storage cell;

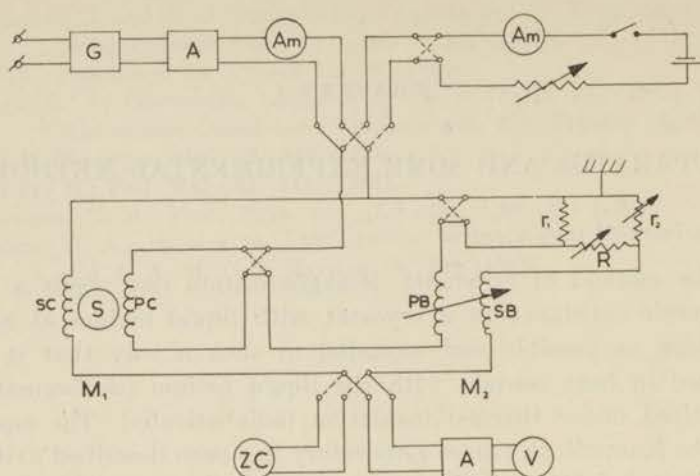


Fig. 1.1 The measuring bridge.

G	generator	PC	primary coil cryostat	SB	secondary bridge
A	amplifier	SC	secondary coils cryostat	ZC	ballistic galvanometer
Am	ammeter	PB	primary bridge	V	vibration galvanometer
S	sample				

for measurements with alternating measuring fields the voltage is taken from a low frequency signal generator (200 Hz), the detecting device being a ballistic galvanometer (Z.C.) or a vibration galvanometer, respectively. The vibration galvanometer is used as a null detector. The secondary voltage of  $M_1$  can be resolved into two components only one of which is in phase with the alternating current and can be compensated by  $M_2$ . The other component, which is due to a.c. losses occurring in the sample can be compensated by tapping off a small voltage from a potentiometer ( $r_1, r_2, R$ ) in the primary circuit. Zero deflection of the vibration galvanometer can only be obtained if both  $M_2$  and  $R_{\text{eff}}$ , which equals  $r_1 r_2 / (r_1 + r_2 + R)$  are set to the correct value. The two components of the susceptibility are found from the experimental values of  $M_2$  and  $R_{\text{eff}}$  by means of

$$(1.1) \quad \chi' = (-M_0 + M_2)/q \quad \text{and} \quad (1.2) \quad \chi'' = R_{\text{eff}}/\omega q$$

where  $\chi_0 = \chi' - i\chi''$ ,  $M_0$  is the value of  $M_2$  when compensating the empty mutual inductance  $M_1$ ,  $q$  is the efficiency factor when measuring the variation of  $M_1$  and  $\omega$  the angular frequency of the measuring field. In our apparatus  $r_1 = 1\Omega$ ,  $R$  is a resistance of  $10^2, 10^3, 10^4$  or  $10^5\Omega$  and  $r_2$  is variable from  $0 - 100\Omega$ . The values of  $M_0$  and  $q$  are found from susceptibility measurements between 4 and  $1^\circ\text{K}$ . In this temperature region most of the investigated paramagnetic substances follow the Curie law

$$(1.3) \quad \chi = C/T$$

The Curie constant  $C$  equals  $NJ(J+1)g^2\mu_B^2/3k$  and its value is known if the value of  $g$  is known from other experiments, which is usually the case. The temperature values are calculated from the measured vapour pressure of the liquid helium bath, using the tables of Van Dijk and Durieux ( $T_{55}$  scale). The differences between the  $T_{58}$  temperature scale and the  $T_{55}$  scale are of no practical importance; the differences between the two scales are smaller than  $0.003^\circ\text{K}$  and the corresponding error in our measurements is less than  $0.5\%$ . From a graph of the relation between  $M_2$  and  $1/T$  the values of  $M_0$  and  $q$  can be derived easily.

### 3. Temperature measurements below $1^\circ\text{K}$

It is easy to determine the temperatures as long as Curie's law is valid, since then the susceptibility is inversely proportional to the temperature. In general, the quantity  $C/\chi$  is denoted by  $T^*$ , called the magnetic temperature and equal to the real temperature when the energy differences caused by the crystalline interactions are low compared to  $T$  and thus Curie's law applies.

The magnitude of a magnetic field inside a magnetized sample differs from the external field due to the demagnetizing field. At high temperatures the deviation from Curie's law caused by the demagnetizing field is described by  $\chi = C/(T - \theta)$  with  $\theta = -NC'$  (where  $N$  is the demagnetizing factor and  $C'$  the Curie constant per  $\text{cm}^3$ ). A second correction occurs because of the interactions between the magnetic ions. If the magnetic ions have a cubic arrangement the interaction gives a contribution to  $\theta$  of  $(4\pi/3)C'$ , if no exchange interaction is taken into account. For a sphere  $N = 4\pi/3$  and thus the resulting value of  $\theta = 0$ .

The  $T^*$  and susceptibility values,  $\chi_0$ ,  $\chi'$  and  $\chi''$ , given in the following correspond to the values of  $dM/dh$  for a spherical sample,  $h$  being the measuring field. When the investigated magnetic material had not a spherical shape, the experimental values of  $dM/dh$  were corrected by means of:

$$(1.4) \quad \chi = \chi_e [1 + (4\pi/3 - N)\chi_v]^{-1}$$

where  $\chi_e$  is the experimental value of the susceptibility and  $\chi_v$  the susceptibility per  $\text{cm}^3$ .

At the lowest attainable temperatures large deviations from Curie's law may occur. In measuring the absolute temperature it will be essential to use the fundamental definition of temperature introduced by Kelvin:

$$(1.5) \quad dQ = T dS$$

Performing a large number of demagnetizations from various initial conditions it is possible to obtain the relation between entropy, calculated from the initial field and temperature values, and a certain quantity which will be called the thermometric parameter  $P_t$  (for instance,  $T^*$ ).

When a known amount of heat is added to the sample the increase of entropy can be derived from the change of  $P_t$ .

During the measurements to be described here, the heat is added by an alternating magnetic field. The heat absorption in the sample is given by:

$$(1.6) \quad dQ/dt = (1/2)h_0^2\omega\chi''$$

$h_0$  being the amplitude of the alternating field. The heat may be added continuously or in short periods. In the first case the absolute temperatures follow from:

$$(1.7) \quad T = (dQ/dt)/(dP_t/dt)(dS/dP_t)$$

In the second case the deduced value of  $T$  is the averaged value during the heating period being found by means of the formula:

$$(1.8) \quad T = \int_{t_1}^{t_2} (1/2)h_0^2\omega\chi'' dt / (S_2 - S_1)$$

When determining absolute temperatures, it is important to use a heat input which is large compared to the heat leak: at least 10 times larger. A correction for the heat leak cannot be accurate, since it may cause a inhomogeneous distribution of the temperature.

The value of  $\chi''$  depends strongly on entropy in most cases and thus the amplitudes of the alternating fields must vary with entropy in order that the required heating be obtained. If the thermometric parameter depends on the amplitude of the measuring field, it may not be convenient to use the first measuring method, an accurate relation between  $P_t$  and entropy for each field value not always being available. If quantities independent of  $h_0$  are measurable, as, for instance,  $\chi'$  and  $\chi''$  in the case of alcoholic solutions of paramagnetic ions, the first method is preferable to the second one.

Another way to add heat to a demagnetized sample in a nearly homogeneous way can be found in the absorption of  $\gamma$ -rays. The  $\gamma$ -rays cause a constant heat input, which can be calibrated, measuring the entropy variation at high temperatures, where Curie's law is valid.

It is clear that if the relation between entropy and temperature has been found, any temperature-sensitive property can be used as a secondary thermometer as its variation as a function of entropy can easily be determined. Magnetic thermometers, such as  $\chi'$  and  $\chi''$ , have the disadvantage that their measured value depends on the shape of the sample and may vary a little for different samples of the same paramagnetic substance. Relatively large quantities of a salt are needed to get a high measuring accuracy.

In some cases a preferable thermometer may be the anisotropy of gamma-rays emitted by oriented radioactive nuclei. The  $\gamma$ -ray intensities emitted in a given direction are dependent on temperature. In several cases the relation between  $\gamma$ -ray anisotropy and temperature has been

thoroughly investigated. A  $\gamma$ -ray thermometer is shape independent in zero field, it does not vary for different samples of the same salt and it can also be used if only small amounts of salt are present. The latter fact means an important advantage for experiments on heat transfer (see chapter III). A  $\gamma$ -ray thermometer can only be used for crystals, not for alcoholic solutions (chapter II) and for many nuclei it is not highly accurate at temperatures above  $0.1^\circ\text{K}$ . There are, however, ions which have such large h.f.s. interactions that an anisotropic  $\gamma$ -ray distribution is found even at  $1^\circ\text{K}$  for radioactive nuclei (for example  $^{166}\text{Ho}$  [4]).

#### REFERENCES

1. DE KLERK, D., Thesis, Leiden (1948).
2. STEENLAND, M. J., Thesis, Leiden (1952).
3. BEUN, J. A., Thesis, Leiden (1957).
4. POSTMA, H., A. R. MIEDEMA and Miss M. C. EVERSDIJK SMULDERS, Commun. Kamerlingh Onnes Lab., Leiden 316a; *Physica* 25, 671 (1959).

## CHAPTER II

## EXPERIMENTS WITH SOLIDIFIED SOLUTIONS OF PARAMAGNETIC SALTS

The possibility of investigating solutions of paramagnetic ions below  $1^{\circ}$  K only exists if solvents are used which do not crystallize. Some liquids are known which can be supercooled if the temperature is lowered below their normal freezing point. These liquids attain a glassy state at very low temperatures instead of crystallizing. Examples of such liquids are ethanol [1], 1-propanol [2] and glycerol [3]. Pure ethanol may crystallize between 110 and  $160^{\circ}$  K if the cooling has not been fast enough, whereas with propanol it is difficult to obtain the crystalline state. Gibson *e.a.* describe 1-propanol at  $125^{\circ}$  K as having a jelly-like consistency which contracts at lower temperatures to a hard, transparent glass.

Solutions of copper chloride in ethanol and propanol have been investigated with X-rays at liquid air temperatures. The X-ray patterns showed that no crystals of copper chloride were present.<sup>1)</sup>

The solubility of inorganic salts in the three above mentioned liquids is rather high due to the large electrical dipole moment in the liquids. Especially nitrates and chlorides can be dissolved in large amounts; sulphates are less soluble in these alcohols. The maximum obtainable concentrations at room temperature are given in table II.I for a few paramagnetic salts. They are compared with the concentrations of magnetic ions in crystals which have been used frequently for adiabatic demagnetization experiments.

TABLE II, I

Concentrations of paramagnetic ions in some solutions and crystals, used for demagnetization experiments, units mole/cm<sup>3</sup>

Salt	Solubility in 1-propanol at $300^{\circ}$ K	Crystal	Concentration
$\text{FeCl}_3 \cdot 6\text{H}_2\text{O}$	$17.5 \times 10^{-4}$	$\text{Ce}_2\text{Mg}_3(\text{NO}_3)_{12} \cdot 24\text{H}_2\text{O}$	$28 \times 10^{-4}$
$\text{Cr}(\text{NO}_3)_3 \cdot 9\text{H}_2\text{O}$	$7.5 \times 10^{-4}$	$\text{CrK}(\text{SO}_4)_2 \cdot 12\text{H}_2\text{O}$	$37 \times 10^{-4}$
$\text{CuCl}_2 \cdot 2\text{H}_2\text{O}$	$8.5 \times 10^{-4}$	$\text{CuK}_2(\text{SO}_4)_2 \cdot 6\text{H}_2\text{O}$	$55 \times 10^{-4}$

The apparatus used during the measurements on alcoholic solutions is shown in fig. 2.1. The solutions are put in a glass sphere with a diameter

<sup>1)</sup> I am much indebted to Prof. C. H. MAC GILLAVRY and her coworkers who performed the X-ray analysis.

of about 3 cm. This sphere is connected to a piece of CrK-alum, which absorbs the heat coming from the bottom of the apparatus. In preliminary experiments it was found that the thermal contact between the sample and the wall of its surrounding sphere could become very bad, due to the contraction of the solidified alcohol. After reducing the temperature of the helium bath to between 4 and 1° K the temperature of the sample decreased only very slowly, and after a demagnetization it could take a long time to get the sample back to 1° K, even when exchange gas was present between the glass sphere and the wall of the apparatus. In order to improve thermal contact, helium gas was put inside the glass sphere before mounting.

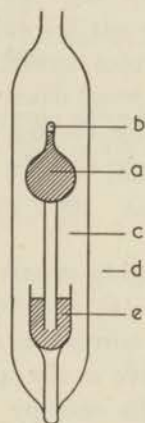


Fig. 2.1  
Apparatus used for experiments with solidified solutions.

- a alcoholic solution
- b filling tube with He gas
- c exchange gas
- d liquid helium bath
- e CrK-alum guard cylinder

1.  $Cr(NO_3)_3 \cdot 9H_2O$  in 1-propanol ( $7.5 \times 10^{-4}$  mole/cm<sup>3</sup>)

Susceptibility measurements were carried out with an a.c. measuring bridge (frequency 225 Hz). In the liquid helium temperature range Curie's law was valid within the experimental accuracy. Demagnetizations were performed starting from a number of fields and an initial temperature of about 1° K. From this the relation between entropy and susceptibility has been derived. The results, which reproduced for several measuring days, are shown in fig. 2.2. The real part of the susceptibility  $\chi'$  increases rapidly at entropies below  $R \ln 2$ . The imaginary part  $\chi''$  becomes important at entropies below  $0.6 R$ . The entropies are calculated from the initial values of the magnetic fields and temperatures with  $g=2$  and are corrected for the entropy of the lattice heat waves and the entropy change due to the electric contributions to the energy splittings. For the first correction a value of  $S_L = 0.05RT^3$  has been derived from demagnetizations from initial temperatures of 1 and 1.5° K. If compared to the values for crystals this correction is rather large, as may be seen from the corresponding value of the Debye constant  $\theta$  which equals 40° K.

At entropies above  $R \ln 2$  the experimental points are in good agreement with Hebb and Purcell's formulae, if for the stark splitting parameter the value  $\delta/k = 0.30^\circ$  K is assumed. The calculated relation is given in

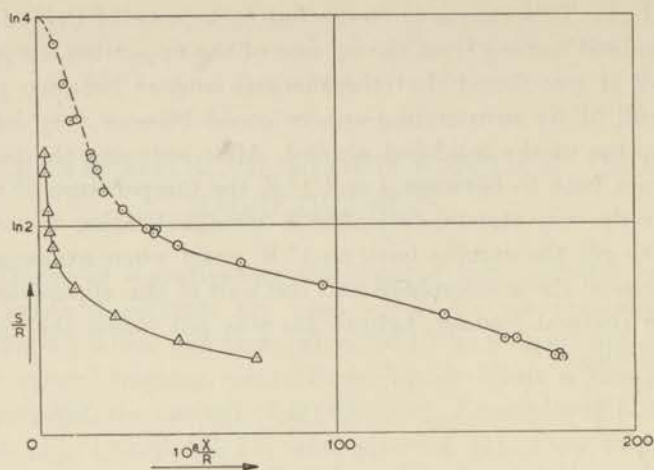


Fig. 2.2 Susceptibility versus entropy for a solution of chromic nitrate in propyl alcohol ( $7.5 \times 10^{-4}$  mole/cm<sup>3</sup>). A curve calculated with  $\delta/k = 0.30^\circ$  K is given in the high entropy region (dashed line).

$$\circ \quad 10^8 \times \chi'/R$$

$$\triangle \quad 10^9 \times \chi''/R$$

fig. 2.2 as a dashed line. The value found for  $\delta$  roughly equals the value obtained with crystalline chromium nitrate, ref. [4] and [5], and it differs only slightly from the values found in the chromium alums [6].

The relatively high values of  $\chi''$  below  $S=0.6 R$  gave us the opportunity to measure the thermodynamic temperature in this entropy region by the a.c. heating method.  $\chi''$  proved to be independent of the amplitude of the alternating field for the values between 0.08 and 8 oersted used. The energy was added continuously (10 erg/s) or in periods of 10 seconds (30 erg/s). Fig. 2.3 shows the relation between entropy and absolute

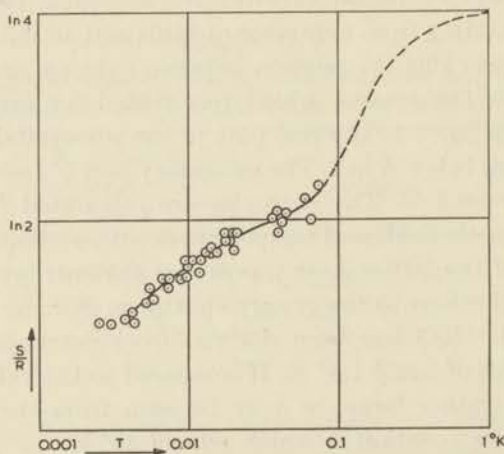


Fig. 2.3 The relation between entropy and absolute temperature of a solution of chromic ions in propyl alcohol ( $7.5 \times 10^{-4}$  mole/cm<sup>3</sup>). The dashed curve is calculated with  $\delta/k = 0.30^\circ$  K.

temperature obtained. The lowest temperature attained was  $0.003^\circ\text{K}$ . The experimental points measured at entropies below  $0.8 R$  are in agreement with the  $S$  versus  $T$  relation for entropies above  $R \ln 2$ , calculated with the electrical field splitting concluded from the  $S$  versus  $\chi'$  relation (dashed line in fig. 2.3).

In fig. 2.3 the temperatures are plotted on a logarithmic scale, hence the derivatives of the  $S$  versus  $T$  curve are proportional to the specific heat. It can be concluded from the figure that the specific heat has a pronounced minimum between  $0.05$  and  $0.02^\circ\text{K}$ . At lower temperatures it rises roughly in proportion to  $1/T$ .

## 2. $\text{Cr}(\text{NO}_3)_3 \cdot 9\text{H}_2\text{O}$ in 1-propanol ( $2.5 \times 10^{-4}$ mole/cm<sup>3</sup>)

The value for the entropy of the heat waves of  $S_L = 0.05 RT^3$  found with the former solution suggested that the lattice entropy was small enough to reach lower temperatures when demagnetizing less concentrated chromium nitrate solutions. Experimentally, however, it was found to be hardly possible to reach temperatures below  $0.1^\circ\text{K}$ . Figure 2.4 shows

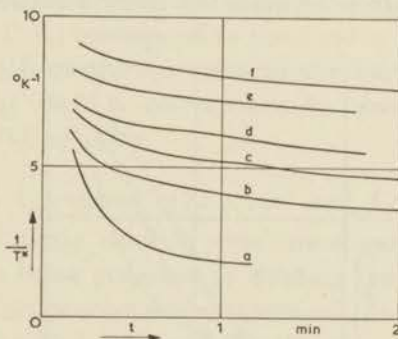


Fig. 2.4 Warming up curves obtained with a  $\text{Cr}(\text{NO}_3)_3 \cdot 9\text{H}_2\text{O}$  solution ( $2.5 \times 10^{-4}$  mole/cm<sup>3</sup>) after demagnetization from  $H = 2 \times 10^4$  Oe,  $T = 1^\circ\text{K}$ . The sample was kept at  $H = 1 \times 10^4$  Oe,  $T = 0.5^\circ\text{K}$  for a time increasing from curve a to curve f.

a	0 min.	d	6 min.
b	1 min.	e	15 min.
c	3 min.	f	31 min.

a number of warming-up curves obtained after demagnetization from the same initial field and temperature ratio ( $H/T = 2 \times 10^4$  Oe/deg). For the curves b–f the magnetic field was reduced to half its initial value at first and after a waiting time, varying from 1 minute for curve b to 31 minutes for curve f, the magnetic field was removed completely. The figure shows that after a longer waiting period the warming-up rate is significantly smaller.

The results indicate that irreversible processes occur during demagnetization, which may be ascribed, for instance, to a temperature difference between heat waves and electron spins. Demagnetizing to  $0.5^\circ\text{K}$  at first has the result that a large part of the entropy of the heat waves is removed

before the complete demagnetization takes place. The relatively large difference existing between the curves e and f (waiting times 15 and 31 minutes, respectively), suggests that a relaxation time between the electron spin system and the heat waves at  $0.5^\circ\text{K}$  in a field of  $10^4$  Oe is of the order of 10 minutes, at least.

In earlier experiments with a more diluted chromium nitrate solution ( $1 \times 10^{-4}$  mole/cm<sup>3</sup>) no temperatures lower than  $0.5^\circ\text{K}$  could be reached after demagnetization ( $H/T = 2 \times 10^4$  Oe/deg). The longest time during which the magnetic field was kept at half its initial value was 10 minutes in this case. With more concentrated solutions of chromium nitrate, ferric chloride and copper chloride no indications for the occurrence of irreversible processes have been found in the warming-up curves.

### 3. $\text{CrCl}_3 \cdot 6\text{H}_2\text{O}$ in 1-propanol ( $10 \times 10^{-4}$ mole/cm<sup>3</sup>)

Two, freshly prepared solutions of chromium chloride of the same concentration have been investigated, one solution being prepared at room temperature, the other one being warmed to  $70^\circ\text{C}$  when dissolving the chromium salt. Figure 2.5 gives the relation between entropy and the

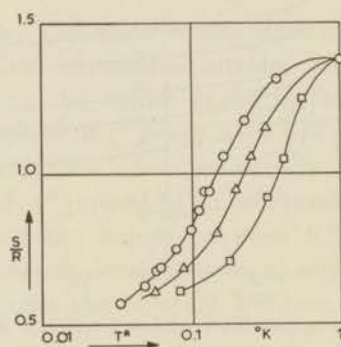


Fig. 2.5 The relation between entropy and magnetic temperature for three solutions of chromic ions in 1-propanol.

- $\text{Cr}(\text{NO}_3)_3 \cdot 9\text{H}_2\text{O}$  conc.  $7.5 \times 10^{-4}$  mole/cm<sup>3</sup>, prepared at  $20^\circ\text{C}$
- △  $\text{CrCl}_3 \cdot 6\text{H}_2\text{O}$  conc.  $10 \times 10^{-4}$  mole/cm<sup>3</sup>, prepared at  $70^\circ\text{C}$
- $\text{CrCl}_3 \cdot 6\text{H}_2\text{O}$  conc.  $10 \times 10^{-4}$  mole/cm<sup>3</sup>, prepared at  $20^\circ\text{C}$

magnetic temperature in the high entropy region for both chromium chloride solutions and for the chromium nitrate solution mentioned before. The curves can be characterized by the value of the Stark splitting parameter  $\delta$ , which, as a matter of fact, will be an average value for ions in a solution. For the solution prepared at  $70^\circ\text{C}$  we derived a value for  $\delta/k$  of about  $0.5^\circ\text{K}$ , for the solution prepared at room temperature the mean value of  $\delta/k$  is  $1.0^\circ\text{K}$ . The  $S$  versus  $T^*$  relation for chromium nitrate is in agreement with  $\delta/k = 0.30^\circ\text{K}$ .

An explanation for the different  $\delta$  values can be found in the chemical behaviour of chromic ions. Two complexes of chromic ions occur in

chromium chloride, a violet and a green one, their formulae being  $[\text{Cr}(\text{H}_2\text{O})_6]^{3+}$  and  $[\text{Cr}(\text{H}_2\text{O})_4\text{Cl}_2]^+$ , respectively. According to OLIE [7] the number of each type of ions present in a solution of chromium chloride depends on temperature and concentration. In crystalline chromium chloride only the green modification is present. Upon dissolving the salt  $[\text{Cr}(\text{H}_2\text{O})_4\text{Cl}_2]^+$  ions will be transformed to  $[\text{Cr}(\text{H}_2\text{O})_6]^{3+}$  ions, the equilibrium time varying from many days at room temperature to several minutes at  $70^\circ\text{C}$ .

When preparing a solution at room temperature it may be expected that mainly  $[\text{Cr}(\text{H}_2\text{O})_4\text{Cl}_2]^+$  ions are present, whereas when preparing a chromium chloride solution at  $70^\circ\text{C}$  part of the green modification will be transformed into the violet one. In the chromium nitrate solutions which were always prepared at room temperature, only  $[\text{Cr}(\text{H}_2\text{O})_6]^{3+}$  ions occur. The magnetic measurements with this solution thus represent the magnetic behaviour of chromic ions surrounded by six water molecules and it is not surprising that the derived value for the crystal field splitting ( $\delta/k=0.3^\circ\text{K}$ ) equals the value found for chromium nitrate crystals.

If the results obtained with the chloride solution prepared at room temperature ( $\delta/k=1^\circ\text{K}$ ) correspond to the  $\delta$  value of  $[\text{Cr}(\text{H}_2\text{O})_4\text{Cl}_2]^+$  ions, one might evaluate from the  $\delta/k$  value of the warmly prepared solution its composition;  $\delta/k=0.5^\circ\text{K}$  corresponds to about 70 %  $[\text{Cr}(\text{H}_2\text{O})_6]^{3+}$  and 30 %  $[\text{Cr}(\text{H}_2\text{O})_4\text{Cl}_2]^+$  ions.

#### 4. $\text{FeCl}_3 \cdot 6\text{H}_2\text{O}$ in 1-propanol ( $17.5 \times 10^{-4}$ and $3.5 \times 10^{-4}$ mole/cm<sup>3</sup>)

Two solutions of ferric chloride were investigated, the one with the lower concentration being prepared by diluting the concentrated solution a factor 5 with a propanol-water mixture of the same composition as present in the  $17.5 \times 10^{-4}$  mole/cm<sup>3</sup> solution.

Susceptibility measurements showed that in the temperature range between 4 and  $1^\circ\text{K}$  Curie's law was not obeyed. The  $\chi$  versus  $1/T$  plot was not a straight line but the slope of the curve decreased about 15 % between 4 and  $1^\circ\text{K}$ .

From measurements performed with the same apparatus on a spherical sample of CrK-alum with the same volume and nearly the same susceptibility per cm<sup>3</sup> as the  $17.5 \times 10^{-4}$  mole/cm<sup>3</sup> ferric chloride solution, it was derived that at  $2^\circ\text{K}$  the  $\chi$  value of the ferric ions was not more than 66 % of the value calculated from the theoretical Curie constant. This suggests that the electrical crystal field at the position of a ferric ion due to the surrounding water and alcohol molecules, causes splittings of the  $S=5/2$  ground level which are of the order of several degrees Kelvin. These splittings are much larger than those known for hydrated crystals containing ferric ions.

Figure 2.6 shows the relation between both  $T$  and  $T^*$  and entropy. The  $T^*$  values are calculated with the mean slope of the  $\chi$  versus  $1/T$  curve between 4 and  $1^\circ\text{K}$  and the entropy values, which are calculated from

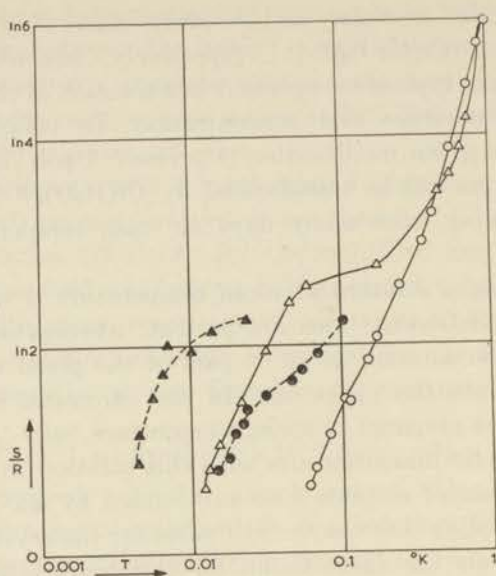


Fig. 2.6 The relation between entropy and  $T, T^*$  obtained with solutions of  $\text{FeCl}_3 \cdot 6\text{H}_2\text{O}$  in 1-propanol.

- $T^*$  conc.  $17.5 \times 10^{-4}$  mole/cm<sup>3</sup>      △  $T^*$  conc.  $3.5 \times 10^{-4}$  mole/cm<sup>3</sup>  
 ●  $T$  conc.  $17.5 \times 10^{-4}$  mole/cm<sup>3</sup>      ▲  $T$  conc.  $3.5 \times 10^{-4}$  mole/cm<sup>3</sup>

$S = 5/2$  and  $g = 2$ , have been corrected for the entropy of the heat waves, as found with solution 1. The  $T$  values have been measured with the relaxation heating method. It is clear that the  $T, T^*$  and entropy values given in fig. 2.6 have no absolute meaning; they can be used, however, when comparing the two solutions with different iron concentrations. The figure shows that in the low entropy region the values of  $T$  and  $T^*$  derived for the two solutions differ by practically the same factor as the concentrations do (a factor 5).

The  $T$  and  $T^*$  values which are reached at entropies smaller than  $R \ln 2$  can be expected to be determined by the magnetic dipolar interactions between different magnetic ions. VAN VLECK [8] has shown that to a first approximation this interaction is characterized by the so-called internal magnetic field  $H_1$ , which can be found from the formula

$$(2.1) \quad (H_1)^2 = 2\mu^2 \sum_{p+q} r_{pq}^{-6}$$

$\mu^2$  is the average square of the magnetic moment of one ion,  $q$  indicates an arbitrary ion and the summation over  $p$  has to be extended over all other ions in the whole crystal (solution). Our experimental results are in agreement with this formula since in a 5 times less concentrated solution the distances  $r_{pq}$  are altered by a factor  $3^{1/5}$  and hence  $H_1$  decreases a factor 5.

The result differs from the relation between  $H_1$  and concentration

measured in crystals diluted by replacing magnetic ions by diamagnetic ions. In this case, (see, for instance, ref. [9] for measurements with cobalt ammonium tutton salt)  $H_1^2$  and not  $H_1$  depends linearly on concentration, in agreement with formula (2.1), since now the distances  $r_{pq}$  remain unchanged but the number of ions over which the summation should be extended decreases proportionally with the dilution factor.

#### 5. $\text{CuCl}_2 \cdot 2\text{H}_2\text{O}$ in 1-propanol ( $8.5 \times 10^{-4}$ mole/cm<sup>3</sup>)

In the liquid helium temperature range the susceptibility of a copper chloride solution followed Curie's law within the experimental accuracy. Demagnetizations have been performed from a number of fields and the resulting relation between  $S$  and  $T, T^*$  can be seen in figure 2.7. The entropy values are calculated from the conditions before demagnetization with  $g=2.2$  and  $S=1/2$  and are corrected for the entropy of the heat waves with  $S_L=0.05 RT^3$ .

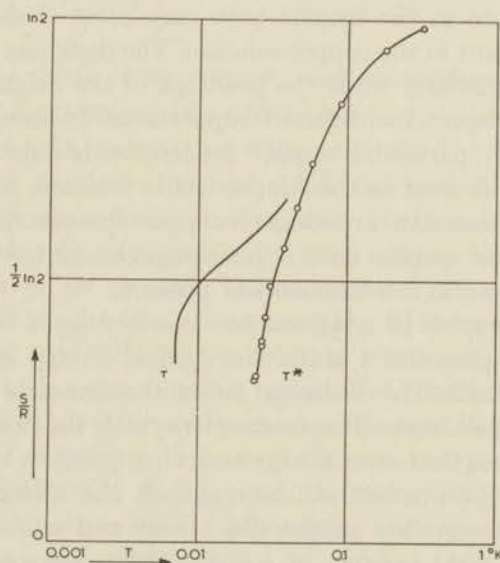


Fig. 2.7  $\text{CuCl}_2 \cdot 2\text{H}_2\text{O}$  in 1-propanol ( $8.5 \times 10^{-4}$  mole/cm<sup>3</sup>).  $T$  and  $T^*$  as functions of entropy.

The imaginary component of the susceptibility becomes measurable below  $S=0.5 R$  and reaches its highest value,  $\chi''/\chi'=0.03$ , at the lowest entropy.  $\chi''$  proved to be independent of the amplitude of the alternating field between 0.08 and 0.8 oersted. Below  $S=0.45 R$  the absolute temperature has been measured with the relaxation heating method. The lowest temperature reached is  $0.008^\circ \text{K}$ .

Assuming that  $T$  equals  $T^*$  in the high entropy region, the specific heat can be derived from the slope of the curve in fig. 2.7, the temperature scale being logarithmic. The specific heat at relatively high temperatures

is found to be proportional to  $1/T^2$  and can be written as  $C_v = 0.0020 R/T^2$ . At lower temperatures the specific heat has a minimum at an entropy of  $S = 0.4 R$  (fig. 2.8).

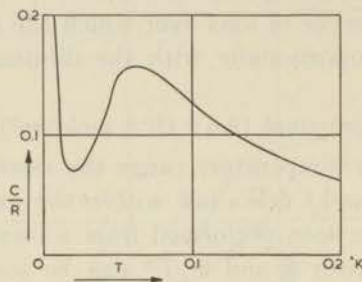


Fig. 2.8 The specific heat of a solution of  $\text{CuCl}_2 \cdot 2\text{H}_2\text{O}$  in 1-propanol ( $8.5 \times 10^{-4}$  mole/cm<sup>3</sup>) as a function of temperature.

Such a minimum in the specific heat may occur if short range order effects are important in the copper solution. The distances between copper ions will vary irregularly while the positions of the neighbouring oxygen atoms will be different for different copper ions. It seems reasonable to suppose that one particular copper ion has only one nearest copper neighbour, being defined as the copper ion to which it has the strongest magnetic interaction. An ordering of copper spins in pairs may cause a minimum in the specific heat if ferromagnetic or both ferromagnetic and antiferromagnetic interactions are present.

A system of 2 spins ( $S = 1/2$ ) can be described by 4 basic states. For completely free spins the 4 states have equal energy and the entropy per ion will be  $k \ln 2$ . The exchange interaction causes a splitting into a singlet and a triplet state. For interactions with the ferromagnetic sign the triplet state has the lowest energy and when going to low temperatures an entropy of  $k(\ln 4 - \ln 3)/2$  will be removed. For interactions with the antiferromagnetic sign the singlet lies lowest and when decreasing the temperature the total entropy of  $k \ln 2$  will be removed.

Strictly, the splitting into a singlet and a triplet state is only true for isotropic  $g$  values. In our case the assumption of an isotropic  $g$  value will be roughly justified since  $g - 2$  is small. The value of  $g$  has been found by comparing the magnetization in a field of  $2 \times 10^4$  Oe with the value of the zero field susceptibility at  $1^\circ \text{K}$ . Since we are not able to measure the magnetization directly in such a large field it was derived from the magnetization curve in a longitudinal field after the sample was demagnetized from  $H/T = 2 \times 10^4$  Oe/deg. At low temperatures the magnetization is practically saturated in a field of 600 Oe and without much difficulty it was possible to extrapolate the isentropic magnetization curve to  $H = 2 \times 10^4$  Oe.

The zero field susceptibility at  $1^\circ \text{K}$  is proportional to  $g^2$  whereas the

magnetization in a field of  $2 \times 10^4$  Oe is roughly proportional to  $g$  as it equals

$$(2.2) \quad M = Ng\mu_B(e^\alpha - e^{-\alpha})/2(e^\alpha + e^{-\alpha})$$

where  $\alpha = g\mu_B H/2kT$ . As a result a  $g$  value of  $2.20 \pm 0.10$  has been derived which nearly equals the mean value for copper ions in several paramagnetic crystals (chapter IV).

6. *Ce(NO<sub>3</sub>)<sub>3</sub> · 9H<sub>2</sub>O in ethanol ( $25 \times 10^{-4}$  mole/cm<sup>3</sup>)*

Preliminary measurements have been performed with an alcoholic solution of cerium nitrate. Between 4 and 1° K Curie's law was valid. After demagnetization from  $H/T = 2 \times 10^4$  Oe/deg a value for  $T^*$  of  $0.004^\circ$  K was measured. In a second experiment with the same sample the magnetic properties were completely different. The slope of the calibration curve was much smaller and no low temperatures were reached after demagnetization. We ascribed this effect to the crystallization of ethanol, when the sample warmed up very slowly between the two measuring days.

7. *The negative result of an attempt to obtain nuclear polarization*

A solution of ferric chloride ( $5 \times 10^{-4}$  mole/cm<sup>3</sup>) in propanol, containing about 10  $\mu$ C of both radioactive <sup>52</sup>Mn and <sup>60</sup>Co has been investigated. Polarizing fields between 100 and 1000 Oe were used but no  $\gamma$ -ray anisotropy larger than 0.5 % was present. The temperatures being low enough, the lack of  $\gamma$ -ray anisotropy may suggest that for cobalt and manganese ions in an alcoholic solution the h.f.s. interaction is very anisotropic. This results in a strong coupling of the nuclear spins to the electrical crystal field, which in a solution will cause nuclear alignment in a direction which varies from ion to ion. For cobalt ions an anisotropic h.f.s. interaction exists in several paramagnetic crystals but for manganese ions it is rather surprising. Apparently it was not possible, even in an external field of 1000 Oe, to magnetize the manganese electron magnetic moments in a direction which differs from their preferential direction, as determined by the crystal field.

REFERENCES

1. KELLEY, K. K., J. Amer. Chem. Soc. 51, 779 (1929).
2. GIBSON, G. E., G. S. SPARKS and W. M. LATIMER, J. Amer. Chem. Soc. 42, 1542 (1920).
3. SIMON, F., Ann. Phys. 68, 241 (1922).
4. TEUNISSEN, P., Thesis, Groningen (1939).
5. CASIMIR, H. B. G., D. DE KLERK and D. POLDER, Commun. Kamerlingh Onnes Lab. Leiden 261a; Physica 7, 737 (1940).
6. BEUN, J. A., A. R. MIEDEMA and M. J. STEENLAND, Commun. 315a; Physica 25, 399 (1959).
7. OLIE, J., Z. Anorg. Chem. 51, 29 (1906).
8. VAN VLECK, J. H., J. Chem. Phys. 5, 320 (1937).
9. BROEK, J. VAN DEN, L. C. VAN DER MAREL and C. J. GORTER, Commun. 314c; Physica 25, 371 (1959).

## SOME EXPERIMENTS ON HEAT TRANSFER BELOW 1° K

1. *General remarks*

One of the main purposes of demagnetization work is, besides investigating the thermal and magnetic properties of paramagnetic materials, to cool down other substances. In this kind of experiment it is necessary to achieve good thermal contact between a material which can be cooled by the method of adiabatic demagnetization (the cooling salt) and the material under investigation. In such experiments, where heat transfer is essential, the following thermal "resistances" may be important.

- a.* The inverse heat transmission coefficient between the electron spins of the cooling salt and its heat waves.
- b.* The inverse thermal conductivity of the cooling salt.
- c.* The contact resistance at the surface between the cooling salt and the transfer medium.
- d.* The thermal resistance of the transfer medium, which, in case a certain distance exists between the cooling salt and the substance under investigation, will be called the heat-link.
- e.* The boundary resistance between the transfer medium and the substance under investigation.
- f.* The inverse thermal conductivity of the substance itself.

The cooling salt consists of a magnetically concentrated material in which the "resistance" *a* is expected to be of no importance. For example, according to the data of BÖLGER [1] the energy transfer between the electronic spin system and lattice heat waves in a crystal of CrK-alum is in the liquid helium region given by  $\dot{Q} = 3 \times 10^6 T^{-0.9}$  erg/s cm<sup>3</sup>, the extrapolated value of this heat flow being much higher than the flow permitted by other resistances, as will be shown later.

The thermal conductivity of a lattice is known to be proportional to its specific heat and therefore to  $T^3$  at very low temperatures. In the case of a non-superconducting metal, the heat conduction will be mainly due to the free electrons, which results in its proportionality to  $T$ . For this reason if a copper wire is used for the heat-link, its diameter being chosen not too small, the thermal resistance *d* will be less important than *b* at the lowest temperatures.

A number of physicists have performed experiments on thermal contact below 1° K. In order to know the cooling rate of the investigated substance, one must measure its temperature. Thus in the first instance, materials having properties known as functions of temperature, are to

be used. These materials will be referred to as the thermometer in the following.

The first metal-to-cooling-salt contact was constructed by MENDOZA [2]. Thin copper sheets were soldered to a copper rod. The spaces between the copper sheets were filled with powdered CrK-alum crystals and a binding agent of plastic cement. The sample was pressed under a pressure of 2000 atmospheres. The cooling salt and the thermometer were prepared in the same way, the contact area being 30 cm<sup>2</sup>. Mendoza obtained data on the heat transport between 1 and 0.2° K, the latter temperature being the equilibrium temperature when the cooling salt was demagnetized from  $H/T = 12 \times 10^3$  Oe/deg, the thermometer being not demagnetized at all. The results for the heat flow between the two salt pills could be represented by the empirical formula:

$$(3.1) \quad \dot{Q} = \beta A (T_1^3 - T_2^3)$$

$A$  represents the contact area,  $T_1$  is the temperature of the thermometer,  $T_2$  the temperature of the copper and  $\beta$  a constant. The experimental value of  $\beta$  was about 10<sup>2</sup> erg/s cm<sup>2</sup> deg<sup>3</sup>. Mendoza's basic idea was developed and modified by several investigators [3], [4]. The copper vanes were replaced by copper wires and the contact area was largely increased. In an unpublished Leiden experiment by Wheatley, 500 wires with a total contact area of 100 cm<sup>2</sup> were used. In order to cool 10 grms of CrK-alum to 0.06° K with this apparatus a time of three quarters of an hour was needed.

Better results were obtained by ROBINSON in Oxford [5]. The sample was not compressed at all in his experiments, glycerol being used as a binding agent. With a very large contact area it was possible to cool a pill of cerium magnesium nitrate to 0.025° K within one hour. A cooling salt of this type was used in the experiments on nuclear demagnetization of KURTI *et al.* [6]. A mixture of CrK-alum, glycerol and water cooled the metal nuclear sample, the total area of contact being 400 cm<sup>2</sup>. In an experiment, where instead of the nuclear sample a CeMg-nitrate mixture was cooled, which was prepared in the same way as the cooling substance, a temperature of 0.011° K was measured 10 minutes after demagnetization, the heat-leak at the place of the thermometer being 1 erg/min. The heat transport between the cerium salt and the CrK-alum mixture could be described by formula (3.1) when  $\beta$  is about 10<sup>3</sup> erg/s cm<sup>2</sup> deg<sup>3</sup>.

Experiments on the cooling of single crystals have been reported by WHEATLEY *et al.* [7]. Single crystals of ferric ammonium alum were glued to a thermal link of copper or crystalline quartz. The experimental data for the heat-flow, obtained at temperatures between 0.2 and 0.16° K gave much larger values than that measured in earlier experiments. Also, in this case formula (3.1) was in good agreement with the experiments,  $\beta$  having a value of about 10<sup>4</sup> erg/s cm<sup>2</sup> deg<sup>3</sup>.

All authors ascribe the thermal resistance found in the heat flow experiments to a contact resistance at the boundary between different materials.

## 2. *Recent Leiden experiments*

In 1956 experiments on heat transfer were started, making use of solidified solutions of paramagnetic ions in alcohol as a cooling salt. 1-propanol was chosen for the solvent because of its low freezing point (146° K). The low freezing point is an advantage in experiments on thermal contact, the contact being made at a temperature below the normal freezing point and the shrinking of materials at lower temperatures being of no importance. As stated in the foregoing chapter, ethyl alcohol has the disadvantage that it may crystallize when passing slowly through the liquid-air temperature region. Nearly all nitrates and chlorides can be dissolved in alcohols. High values for the concentration of paramagnetic ions and hence large thermal capacities at low temperatures can be obtained with ferric chloride, chromic chloride and chromic nitrate (Table II, I). A solution of ferric chloride has not been used in the heat transfer experiments because it reacts chemically with copper. With a chromic nitrate solution, in combination with enamelled copper wires, a chemical reaction takes place only after the sample had been cooled down and warmed up again to room-temperature a few times. In principle the reactions might have been avoided if use was made of a copper chloride solution for the cooling salt or of gold wires instead of copper wires.

In a first experiment both the cooling salt and the thermometer consisted of a solidified solution of chromium chloride in propanol. The solutions were contained in glass spheres, their volumes being 11 and 3.5 cm<sup>3</sup>, respectively. Thermal contact was attained by means of a string of 1000 copper wires 0.05 mm in diameter. The area of contact between this heat-link and the alcoholic solutions was 30 cm<sup>2</sup> on each side, the average distance between the two samples being 7 cm. Data about the heat transfer between 0.07 and 0.10° K have been obtained.

The other experiments concern heat transport from paramagnetic single crystals to a solution of paramagnetic ions in 1-propanol. Fig. 3.1 shows the apparatus. The cooling agent had a volume of 12 cm<sup>3</sup> and consisted of a solution of chromium nitrate [Cr(NO<sub>3</sub>)<sub>3</sub>·9H<sub>2</sub>O] in propyl alcohol, the concentration being  $7.5 \times 10^{-4}$  mole/cm<sup>3</sup>. Thermal contact between the cooling solution and the copper heat-link was achieved by means of 130 copper wires 0.07 cm in diameter and with a total area of 70 cm<sup>2</sup> in contact with the solution. The wires were soldered in a copper vase, which was connected to a wire of electrolytically pure copper with a diameter which was varied for several measuring days between 0.02 and 0.09 cm. On the upper end the heat link ended in a circular copper plate 0.02 cm thick and 1.2 cm in diameter. Two sets of experiments with single

crystals were performed. In the first one two halves of a spherical single crystal of CrK-alum were glued to each side of the copper plate with Apiezon N grease. The crystals, which had a total volume of  $0.75 \text{ cm}^3$ , were pressed against the copper plate by two german silver pinches (contact area  $2 \text{ cm}^2$ ). The heat flow from the CrK-alum crystals was measured between  $0.6$  and  $0.04^\circ \text{ K}$ . The susceptibilities of the alum and of the cooling solution were used as thermometers.

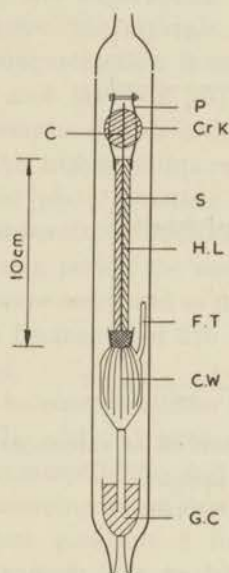


Fig. 3.1  
Apparatus used for indirect cooling experiments.

CrK	CrK-alum thermometer
P	pinches
C	copper plate
S	supports
H.L.	heat-link
C.W.	contact wires
F.T.	filling tube
G.C.	guard cylinder

In a second set of experiments the CrK-alum was replaced by small CeMg-nitrate crystals containing some radioactive  $^{60}\text{Co}$ . The surface area in contact with the copper was about  $1 \text{ cm}^2$  and the total volume of the crystals about  $0.15 \text{ cm}^3$ . In this case the temperature was deduced from the  $\gamma$ -ray anisotropy.

### 3. Experimental data and analysis

During the first experiments on 2 chromium chloride samples a temperature difference was created by demagnetizing the two pills from different fields. The magnetic temperatures of both solutions were measured as functions of time with the a.c. bridge. A typical run which shows that it is possible to perform a temperature measurement, in less than five seconds, can be seen in fig. 3.2. During the first five minutes, when the temperature difference is large, it decreases rapidly, but it takes a long time before thermal equilibrium is reached. The temperatures have been evaluated from the magnetic temperatures making use of  $\delta/k = 0.5^\circ \text{ K}$  as found for a chromium chloride solution prepared at  $70^\circ \text{ C}$ .

The  $3.5 \text{ cm}^3$  sample (thermometer) was demagnetized from the lower field and thus it has the higher temperature in fig. 3.2. During an

experimental run it was possible to reverse the sign of the temperature difference by means of a magnetic field of 500 oersted, which was placed at the position of the smaller sample. Upon removing this field after several minutes, the smaller sample reached the lowest temperature, warming up rather quickly afterwards.

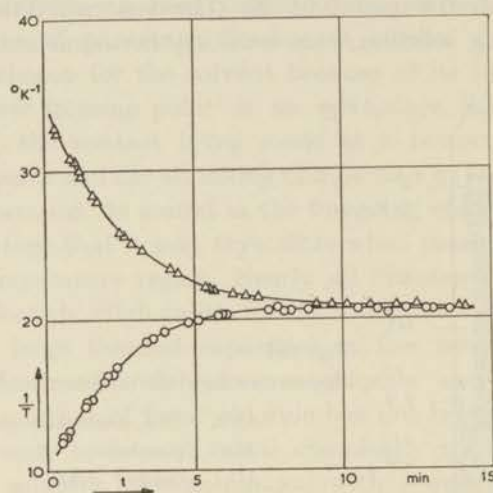


Fig. 3.2 Heat transfer between two alcoholic solutions of chromium chloride.

- $1/T$  versus time 3.5 cm<sup>3</sup> sample  
 △  $1/T$  versus time 11 cm<sup>3</sup> sample

Values of the heat-flow have been derived at the moments when relatively large temperature differences were present, the higher temperature varying between 0.10 and 0.07° K. Assuming that the heat-flow could be described by:

$$(3.2) \quad \dot{Q} = B(T_h^n - T_c^n)$$

where  $T_h$  and  $T_c$  are the temperatures of the "hot" and the cold sample, it was not possible to find an accurate value for  $n$  from the measurements. Agreement between formula and experiment could be obtained for  $n$  values between 2 and 3, the coefficient  $B$  being  $54 \times 10^2$  erg/s deg<sup>2</sup> in the case where  $n=2$  and  $6.5 \times 10^4$  erg/s deg<sup>3</sup> for  $n=3$ .

If the contact resistance between copper wires and paramagnetic solution dominates and if it corresponds to formula (3.2) with  $n=3$  as suggested by Mendoza, Wheatley *e.a.* and Kurti *e.a.* the value of  $\beta$  equals  $0.5 \times 10^4$  erg/s cm<sup>2</sup> deg<sup>3</sup> since  $B = A\beta/2$  and  $A = 30$  cm<sup>2</sup>. In fact, this relatively high value for  $\beta$  will be still larger, because the thermal resistance of the copper heat-link is not negligible in this case. If alternatively the total thermal resistance found is ascribed to the heat-link, a value for the thermal conductivity of the copper wires at 0.1° K of  $K = 0.4 T$  watt/cm deg is derived. This value is of the order of magnitude of the value estimated from the electrical conductivity of

electrolytically pure copper using Wiedemann-Franz law which roughly equals the value for the thermal conductivity of copper reported by several investigators (average value  $1.8 T$  watt/cm deg, ref. [8]). The experiment with two alcoholic samples indicates that the thermal contact between an alcoholic solution and copper wires is good, the values of  $\beta$  being not smaller than the values reported by Wheatley *e.a.* for a single crystal, glued very carefully to a copper plate.

During the experiment in which CrK-alum crystals were used as a thermometer, the crystals were heated up by a 2 MHz oscillating field after demagnetization from fields between 5 and 22 kOe. According to AMBLER and HUDSON [9] chromium alums have a strong absorption for frequencies of this order of magnitude up to temperatures of about  $0.1^\circ\text{K}$ . At higher temperatures the heat will mainly be generated in the copper plate. Starting from  $0.01\text{K}^\circ$  it was found to be possible to reach temperatures between  $0.05$  and  $0.5^\circ\text{K}$  in a few seconds. After each heating period the susceptibilities of the CrK-alum and the cooling solution were measured as functions of time by means of an a.c. measuring bridge. A frequency of 225 Hz and a field amplitude of about 0.1 oersted were used.

From the susceptibilities the temperatures of the "hot" and the "cold" sample ( $T_h$  and  $T_c$ ) were obtained as functions of time. The relation between susceptibility and temperature for CrK-alum has been taken from measurements of BEUN *e.a.* [10], a correction for the value of the Curie-Weiss constant  $\theta$  found in the helium temperature range by VAN DIJK and DURIEUX [11], being applied. Table III, I shows the relation between temperature, entropy and susceptibility. For the chromium solution this relation has been given in the foregoing chapter.

TABLE III, I  
Thermal and magnetic properties of CrK-alum

$T^\circ\text{K}$	$S/R$	$\chi/R \times 10^8$
0.40	1.335	5.23
0.30	1.321	6.87
0.25	1.271	8.10
0.20	1.233	10.0
0.15	1.145	12.8
0.10	1.017	17.1
0.08	0.949	19.3
0.06	0.866	21.1
0.05	0.821	23.9
0.04	0.774	25.9

A typical run is shown in fig. 3.3.

Using the known specific heat of CrK-alum the heat flow can easily be calculated. The heat flow at various values of  $T_h$  and  $T_c$  is given in

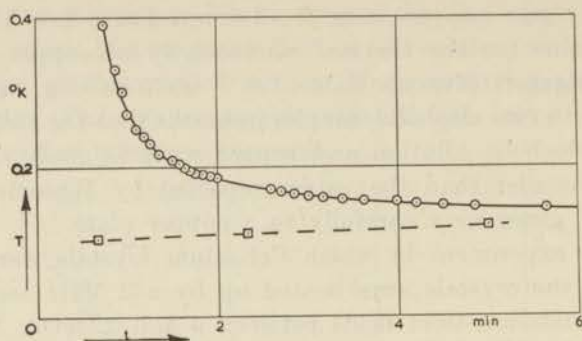


Fig. 3.3 A typical run. Temperatures of CrK-alum crystal and cooling solution as functions of time.

- $T_h$  temperature upper salt  
 □  $T_c$  temperature cooling agent

TABLE III, II

The heat flow between a CrK-crystal and the cooling agent at several temperatures

$T_h$ °K	$T_c$ °K	$\dot{Q}$ erg/s	$\dot{Q}$ calculated erg/s	$T_h$ °K	$T_c$ °K	$\dot{Q}$ erg/s	$\dot{Q}$ calculated erg/s
0.55	0.25	580	600	0.17	0.06	43	46
0.55	0.35	450	440	0.10	0.06	6.7	7.2
0.48	0.26	370	390	0.10	0.06	6.9	7.2
0.40	0.17	320	321	0.10	0.04	10.2	9.0
0.35	0.18	200	206	0.09	0.06 <sup>5</sup>	2.8	4.4
0.35	0.11	220	252	0.08	0.05 <sup>5</sup>	2.7	2.9
0.30	0.11 <sup>5</sup>	230	177	0.08	0.04 <sup>5</sup>	3.2	3.2
0.30	0.11 <sup>5</sup>	160	177	0.07	0.04	2.0	1.8
0.29	0.10	165	174	0.06	0.04 <sup>9</sup>	1.0	1.0
0.26	0.07	126	119	0.06	0.04 <sup>4</sup>	0.7 <sup>5</sup>	0.7
0.26	0.07	108	119	0.05 <sup>4</sup>	0.04	0.4 <sup>4</sup>	0.49
0.25	0.07	130	127	0.04 <sup>6</sup>	0.02 <sup>5</sup>	0.4 <sup>4</sup>	0.46
0.21	0.07 <sup>5</sup>	69	80	0.04	0.02	0.2 <sup>9</sup>	0.28
0.18	0.08	56	50	0.04	0.02	0.2 <sup>5</sup>	0.28
0.17	0.08 <sup>5</sup>	34	40				

table III, II. It varies from 580 erg/s for a  $T_h = 0.55^\circ \text{K}$  to 0.25 erg/s for  $T_h = 0.04^\circ \text{K}$ .

In principle, in this experiment five thermal "resistances" occur. They are: the thermal resistance of the cooling solution, the contact resistance between the heat-link and alcohol, the resistance of the heat-link, the contact resistance between the crystal and copper and the thermal resistance of the CrK-alum crystal. The first two may be neglected since the contact resistance at the position of the cooling salt is much smaller than at the position of the single crystals, as can be concluded from the two alcoholic pill experiments and also from an experiment in which the number of contact wires present in the alcohol was decreased by a

factor of 20. It is only after absorption of considerable amounts of heat that the thermal resistance of the alcohol may become a limiting factor for the heat flow.

Let us assume that the heat flow through each of the other 3 resistances can be described by a formula like formula (3.2)  $\dot{Q} = B(T_h^n - T_c^n)$  in which  $T_h$  and  $T_c$  are now the temperatures on both sides of the resistance.

On the basis of earlier data on thermal contact experiments one would expect that a resistance with  $n=3$  is the most important. For this reason we analysed our measurements by comparing the values obtained for  $\dot{Q}/(T_h^3 - T_c^3)$  at different values of  $T_h$ . If a formula with  $n=3$  could describe the heat flow  $\dot{Q}/(T_h^3 - T_c^3)$  would be independent of  $T_h$ . Figure 3.4 shows that this is not at all the case.  $\dot{Q}/(T_h^3 - T_c^3)$  has a maximum for  $T_h = 0.2^\circ \text{K}$  and thus a thermal resistance with  $n > 3$  has to be present

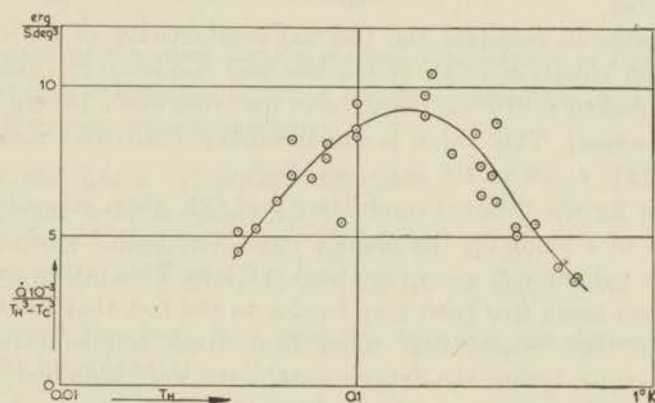


Fig. 3.4 Check of the formula  $\dot{Q} = B(T_h^3 - T_c^3)$ . If the formula were valid the  $\dot{Q}/(T_h^3 - T_c^3)$  versus  $T_h$  curve should be a horizontal line.

at temperatures lower than  $0.2^\circ \text{K}$  and a resistance with a corresponding  $n < 3$  is present at temperatures higher than  $0.2^\circ \text{K}$ . It was found to be possible to describe the heat flow by a combination of two thermal resistances, with the values  $n=2$  and  $n=4$ , respectively. In table III, II the experimental values of  $\dot{Q}$  are compared with values calculated by means of:

$$(3.3) \quad \dot{Q} = 12 \times 10^4 (T_h^4 - T_b^4) \text{ erg/s}$$

$$(3.4) \quad \dot{Q} = 26 \times 10^2 (T_b^2 - T_c^2) \text{ erg/s}$$

In these equations  $T_b$  represents a temperature between  $T_h$  and  $T_c$ . Within the experimental accuracy agreement has been obtained. A thermal resistance with  $n=3$  may be present, but its coefficient  $B$  has to be larger than  $5 \times 10^4 \text{ erg/s deg}^3$ , which means that if we ascribe such a term to a boundary resistance between the alum and the copper  $\beta > 2.5 \times 10^4 \text{ erg/s deg}^3 \text{ cm}^2$ .

The thermal resistance corresponding to formula (3.4) was obviously

due to the heat-link, since its coefficient varies from  $40 \times 10^2$  to  $2.7 \times 10^2$  erg/s deg<sup>2</sup> when the diameter of the copper was varied from 0.9 to 0.2 mm. The corresponding values for the thermal conductivity of copper were  $K = 0.32 T$  and  $K = 0.64 T$  watt/cm deg. These relatively low values [8] are not surprising as two solder joints were present in the heat-link.

MENDOZA [2], WHEATLEY *e.a.* [7] and KURTI *e.a.* [6] conclude from their experiments that a boundary resistance is described by  $\dot{Q}/A = \beta(T_h^3 - T_c^3)$ . If the contact resistance is described by such a formula in our experiments, we must ascribe the resistance with  $n=4$  to the CrK-alum crystals. This agrees with the fact that the coefficient of the thermal resistance with  $n=4$  was a constant for four successive measuring days, while the crystal-glue-copper contact was renewed before each measuring day.

It is possible to estimate the thermal conductivity of the CrK-alum crystals from equation (3.3). If the thermal conductivity follows a  $T^3$  law, the coefficient  $\lambda_1$  of  $\lambda = \lambda_1 T^3$  will be of the order of  $4 \times 10^4$  erg/s cm deg<sup>4</sup> (see next section). This value is much smaller than that measured by GARRETT [12]:  $\lambda_1 = 5.3 \times 10^5$  erg/s cm deg<sup>4</sup>.

The value for the thermal conductivity of CrK-alum given by Garrett corresponds to a value for the phonon mean free path  $l$  of about 2 mm, whereas our value for  $\lambda_1$  gives  $l$  is about 0.2 mm. This rather small value of the phonon mean free path may be due to the fact that the CrK-alum crystals had been cooled four times from room temperature to very low temperatures before the experimental data were obtained. A similar discrepancy exists between the values of the thermal conductivity measured at higher temperatures by BIJL [13] and by VAN DEN BROEK *e.a.* [14]. Van den Broek's values are a factor 10 smaller than those

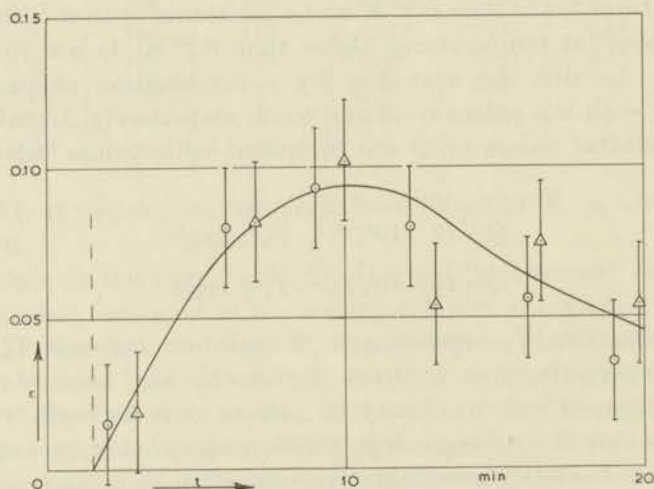


Fig. 3.5  $\gamma$ -anisotropy of  $^{60}\text{Co}$  in CeMg-nitrate as a function of time. The crystals were heated up at  $t = 1'30''$ .  $\varepsilon = 0.08$  corresponds to  $T = 0.015^\circ \text{K}$ .

of Bijl, but he also made measurements on a sample which had been cooled from room temperature to helium temperatures many times.

In the experiments with CeMg-nitrate the crystals were heated up immediately after demagnetization in the same way as described for the CrK-alum crystals. The temperatures were derived from the normalized  $\gamma$ -ray intensities,  $W$ , measured in the direction of the alignment axis and in the direction perpendicular to it. The relation between the anisotropy  $\varepsilon$ , defined as  $[W(\pi/2) - W(0)]/W(\pi/2)$ , and the temperature has been taken from data of AMBLER *et al.* [15]. Figure 3.5 shows the results of two identical runs taken together. After 6 minutes  $\varepsilon$  reached a value of about 0.08, which corresponds to a temperature of  $0.015 \pm 0.002^\circ \text{K}$ . In this experiment the contact area between the CeMg-nitrate crystals and the copper plate was about  $1 \text{ cm}^2$  and the radioactive heat input was about  $0.06 \text{ erg/s}$ .

#### 4. Derivation of the value for the thermal conductivity of CrK-alum

The heat flow differential equation has been solved for the CrK-crystals with the following approximations:

- a) The crystal has a cylindrical shape.
- b) The specific heat is constant.
- c) The thermal conductivity can be written as  $\lambda_1 T^3$ .
- d) The temperature of the cold side of the crystal  $T_b = 0$ .

In this case the heat flow problem becomes one-dimensional. The equation to be solved is:

$$(3.5) \quad \frac{\partial^2 T^4}{\partial x^2} = \frac{4C_v}{\lambda_1} \frac{\partial T}{\partial t}$$

Assuming  $t > 0$ , the solution can be found by the method of separating variables, as the relative temperature distribution will become independent of its actual (unknown) initial conditions. Hence we write  $T$  in the form:

$$(3.6) \quad T(x, t) = f(x) g(t)$$

$f(x)$  is found by solving numerically the equation:

$$(3.7) \quad \frac{\partial^2 f^4}{\partial x^2} = \frac{4C_v}{\lambda_1} g'(t) f/g^4$$

The relative temperature distribution  $f(x)$  is shown by fig. 3.6 in terms of  $T^4$  as a function of  $x$ . The solution will also hold for values of  $T_b \neq 0$  as long as  $T_b^4 < \bar{T}^4$ . It is possible to calculate from fig. 3.6 the relation between the heat transport through  $1 \text{ cm}^2$  cross-section of the crystal and the average temperature.

$$(3.8) \quad \dot{Q}/A = 0.85 \lambda_1 (\bar{T}^4 - T_b^4)/L$$

In our case approximations  $b$  and  $c$  will be roughly justified. The specific heat of CrK-alum is nearly constant in the temperature region

between 0.1 and 0.04° K where the conductivity of the crystal limits the heat flow in our experiments. The  $T^3$  dependence of the thermal conductivity has been measured by GARRETT [12] and is confirmed by our formula (3.3).

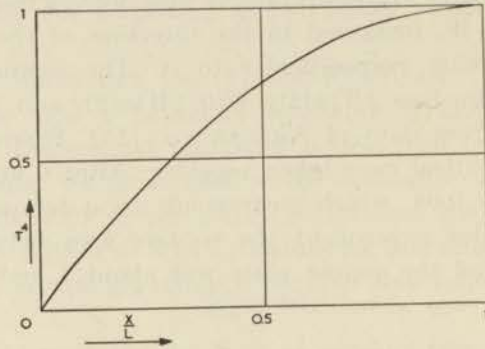


Fig. 3.6 Temperature distribution in a cylindrical CrK-alum crystal of length  $L$ , which is cooled at  $x = 0$ . The heat flow through each  $\text{cm}^2$  cross-section of the crystal is given in arbitrary units by the derivatives of the curve.

When approximating formula (3.8) in the case of the two spherical crystals by taking  $L = 0.6$  cm, the result is:

$$(3.9) \quad \dot{Q} = 2.8 \lambda_1 (\bar{T}^4 - T_b^4)$$

The coefficient will increase if a correction is applied for the fact that the average susceptibility has been measured instead of the average temperature. The magnitude of this correction depends mainly on the actual value of the temperature of the cold side of the crystal and hence varies throughout the experiments. Assuming (3.9) to be valid, formula (3.3) gives a thermal conductivity of a CrK-alum crystal not higher than  $\lambda = 4 \times 10^4 T^3$  erg/s cm deg.

##### 5. Comparison with theory

Debye's theory gives the following formulae for the thermal conductivity and lattice specific heat of non-metals at very low temperatures

$$(3.10) \quad \lambda = (1/3) l c C_v = \lambda_1 T^3$$

$$(3.11) \quad C_v = 0.4 k^4 \pi^2 T^3 / \hbar^3 c^3$$

in which

- $l$  = phonon mean free path,
- $C_v$  = lattice specific heat per unit volume,
- $c$  = velocity of sound.

The heat flow through a unit area of a cylindrical crystal with length  $L$  is given by:

$$(3.12) \quad \dot{Q}/A = \lambda_1 (T_h^4 - T_c^4) / 4L = k^4 \pi^2 l (T_h^4 - T_c^4) / 30 \hbar^3 c^2 L$$

The maximum possible heat flow at a given value of  $T_h$  is obtained with  $l=L$  and  $T_c=0$ .

Thus:

$$(3.13) \quad \dot{Q}/A < k^4 \pi^2 T_h^4 / 30 \hbar^3 c^2 = 1 \times 10^{17} T_h^4 / c^2 \text{ erg/s cm}^2$$

In the case of CeMg-nitrate equation (3.13) gives  $\dot{Q}/A < 2 \times 10^6 T_h^4 \text{ erg/s cm}^2$  the value of  $c$  being deduced from the lattice specific heat at  $1^\circ \text{K}$  [16]. In our experiments we approached this maximum value of  $\dot{Q}/A$  rather closely. The heat transport of  $0.06 \text{ erg/s}$  with  $T_h = 0.015^\circ \text{K}$  corresponds to  $\dot{Q}/A$  is about  $10^6 T_h^4 \text{ erg/s cm}^2$ .

The question arises why the theoretical value calculated for ideal thermal contact between a crystal and copper should not surpass the experimental value many times, two reflecting surfaces and a glue layer being present at the contact surface. There is a possibility to explain this, discussed hereafter.

It may be expected that in the small CeMg-nitrate crystals the phonon mean free path is of the order of the crystal thickness (1 mm). In this case one may doubt whether it is justified to relate the flow of energy and the temperature, as derived from the observed  $\gamma$ -anisotropy, by means of Debye's theory. The temperature of the system of  $^{60}\text{Co}$  nuclei only depends on the frequency distribution in that part of the phonon spectrum with which the cobalt nuclear spins interact and not on that of other frequencies. It cannot be expected that in such small crystals, the thermal vibrations into which the kinetic energy of the emitted  $\beta$  particles is transformed attain a Boltzmann distribution. Since the kinetic energy of the  $\beta$  particles is extremely high if compared to the energy of thermal vibrations, one may expect that a relatively large number of high frequency phonons be generated. If these phonons leave the crystal immediately the energy thus transported adds itself to energy transported in accordance with Debye's theory, in which the temperature of the cobalt nuclear spins and the part of the phonon spectrum that interacts with them, is used. This offers a possibility to explain the fact that the observed energy transport almost equals the value to be expected for ideal thermal contact.

Other data on the heat flow from radioactive crystals come from experiments on the asymmetry of  $\beta$ -rays. In these experiments one uses radioactive layers on a directly demagnetized crystal. In experiments on the  $\beta$ -asymmetry of  $^{58}\text{Co}$  and  $^{52}\text{Mn}$  nuclei of POSTMA *et al.* [17], where the radioactive heat input was of the order of  $0.1 \text{ erg/s cm}^2$ , the layer warmed up quickly to a temperature which varied between  $0.013$  and  $0.020^\circ \text{K}$  for different experiments, as has been derived from the observed  $\gamma$ -anisotropies. The energy transport was extremely large if compared to Debye's theory which may suggest that also in these experiments there is no thermal equilibrium in the phonon system.

### 6. The thermal resistance of a crystal-glue-copper contact

It may be expected that apart from the radioactive heat input there is a heat leak in the CeMg-nitrate crystals of the order of 0.01 erg/s. This indicates that the resistance of a crystal-glue-copper contact is rather small. It will be shown in this section that the resistance of a glue layer may not be so important and that it is in principle even possible to have better thermal contact using a glue than in case of perfect mechanical contact without a glue layer.

We shall first neglect the presence of the glue layer and consider the transmission coefficient for phonons at the surface between a crystal and copper. The transmission coefficient  $\Gamma_{ik}$  is determined by the following formula given by RAYLEIGH [18], phonons being in principle acoustical waves of extremely high frequencies.

$$(3.14) \quad \Gamma_{ik} = 4\rho_1\rho_2c_1c_2 \cos \theta_1 \cos \theta_2 / (\rho_1c_1 \cos \theta_2 + \rho_2c_2 \cos \theta_1)^2$$

$\theta_2$  is the angle with the normal on the reflecting surface at which a phonon with an angle of incidence  $\theta_1$  will be refracted. The angles  $\theta_1$  and  $\theta_2$  are related by Snellius' law of acoustic refraction.

In order to know the total amount of refracted energy it will be necessary to integrate over all incident angles  $\theta_1$ . Calculations have been made by LITTLE [19], who described the thermal resistance at a surface between two different materials by

$$(3.15) \quad \dot{Q}/A = 5 \times 10^{16} [\Gamma_1/c_1^2 + 2\Gamma_t/c_t^2] (T_h^4 - T_c^4) \text{ erg/s cm}^2$$

$\Gamma_1$  and  $\Gamma_t$  are the transmission coefficients and  $c_1$  and  $c_t$  the propagation velocities of longitudinal and transverse phonons, respectively. The evaluation of  $\Gamma_1$  and  $\Gamma_t$  is difficult because each wave, whether longitudinal or transverse, in general, breaks up into four waves, reflected transverse and longitudinal waves and refracted transverse and longitudinal waves as has been stated by KOLSKY [20]. Little calculated the transmission coefficients by numerical integration, using an electronic computer. In his paper the results are given in the form of parametric plots, where the values of  $\Gamma_1$  and  $\Gamma_t$  can be derived from the ratios of the densities and the velocities of sound in the two media.

Using the values of  $\rho$  and  $c$  as known from measurements at room temperature, Little derived that the reflection of phonons at a contact surface between a crystal (CrK-alum) and copper will correspond to a boundary thermal resistance of the kind given by formula (3.2) with  $n=4$  and  $B/A = 0.5 \times 10^6 \text{ erg/s cm}^2 \text{ deg}^4$ . The values of  $\rho$  and  $c$  of CeMg-nitrate crystals are slightly different from the ones in CrK-alum; the calculated value of  $B$  will be somewhat higher but it remains of the same order of magnitude,  $10^6 \text{ erg/s cm}^2 \text{ deg}^4$ .

If a glue layer is present there are two reflecting surfaces between the crystal and the copper plate. The heat flow from a crystal at temperature  $T_h$ , of density  $\rho_1$ , and in which the velocity of sound is  $c_1$ , through a glue

layer of thickness  $L$ , density  $\rho_2$  and velocity of sound  $c_2$  to a metal at temperature zero with quantities  $\rho_3$  and  $c_3$  will be determined by the following equations:

$$(3.16) \quad (\dot{Q}/A)_{gl} = 1 \times 10^{17} (T_h^4 - T_1^4) \Gamma_{12} / c_1^2 = 1 \times 10^{17} l (T_1^4 - T_3^4) / c_2^2 L = 1 \times 10^{17} \Gamma_{23} T_3^4 / c_2^2 \text{ erg/s cm}^2$$

where  $T_1$  and  $T_3$  are the temperatures of the glue at the crystal-glue surface and the glue-copper surface, respectively, and  $l$  is the mean free path of the phonons in the glue. By eliminating  $T_1$  and  $T_3$  from the equations the ratio of the heat flow values using glue and without glue can be derived. The result is:

$$(3.17) \quad \dot{Q}_{gl}/\dot{Q} = [\Gamma_{12}\Gamma_{23}/\Gamma_{13}] [\Gamma_{23} + c_2^2(\Gamma_{23} + l/L)\Gamma_{12}/c_1^2(l/L)]^{-1}$$

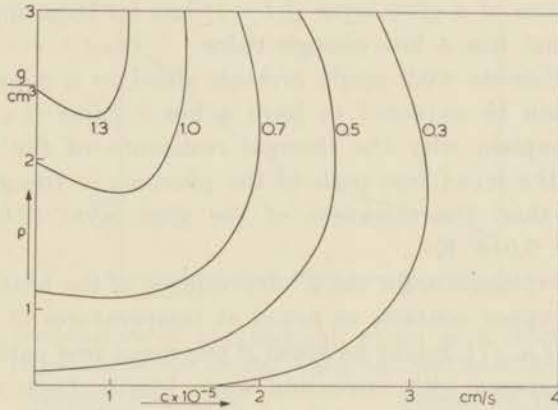


Fig. 3.7 The ratio of the heat flow from a perfect CeMg-nitrate crystal to copper, using a glue and without it, as a function of the density and the velocity of sound in the glue. The thermal resistance of the glue layer itself is neglected ( $l/L = 1$ ).

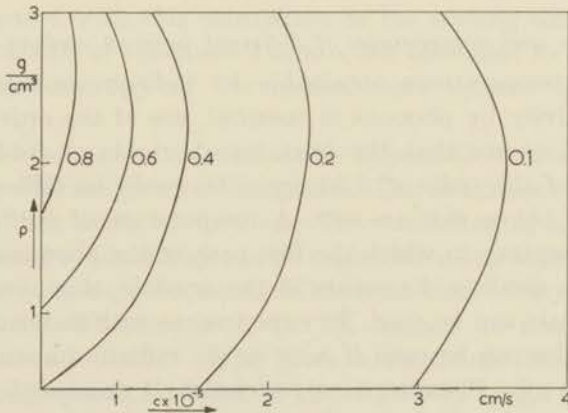


Fig. 3.8 The ratio of the energy transport from a CeMg-nitrate crystal to copper, using a glue and without it, as a function of the properties of the glue. The thermal resistance of the glue layer is described by  $l/L = 0.1$ .

As an approximation formula (3.14) with  $\theta_1 = \theta_2 = \pi/2$ , will be used for the calculation of the transmission coefficient. The approximation gives reliable results as can be seen from the comparison of values of the transmission coefficients calculated by Little with the approximate ones. In figs. 3.7 and 3.8 the values of  $\dot{Q}_{g1}/\dot{Q}$  are given as a function of the density and the velocity of sound in the glue, using the following values for the other quantities:  $\rho_1 = 2 \text{ g/cm}^3$ ,  $\rho_3 = 9 \text{ g/cm}^3$ ,  $c_1 = 2.3 \times 10^5 \text{ cm/s}$ ,  $c_3 = 3.5 \times 10^5 \text{ cm/s}$ . When calculating the curves of fig. 3.7 the thermal resistance of the glue layer has been neglected ( $l/L = 1$ ). Fig. 3.8 is constructed using  $l/L = 0.1$ . Fig. 3.7 shows that in principle there is a possibility of increasing the transfer of heat when using a glue, if the glue has an acoustical impedance ( $\rho c$ ) which does not differ much from the acoustical impedance of the crystal, but while it has a much lower velocity of sound. Comparison of the figures 3.7 and 3.8 shows that the thermal resistance of a glue layer ( $l/L < 1$ ) has no large influence if the velocity of sound has a low enough value.

In our experiments with single crystals glued to a copper plate, the Apiezon glue can be expected to have a low  $c$  value ( $c < 1 \times 10^5 \text{ cm/s}$ ) which might explain why the thermal resistance of the glue layer is small, even if the mean free path of the phonons in the glue is several times smaller than the thickness of the glue layer (0.05 mm) at a temperature of  $0.015^\circ \text{ K}$ .

A tentative explanation for the  $T^3$  dependence of the heat flow through a crystal-glue-copper contact, as found at temperatures of about  $0.2^\circ \text{ K}$  by WHEATLEY *et al.* [7], might be given if the mean free path of a phonon in the glue increases with increasing wave length. Such a dependence often has been found experimentally in the attenuation of normal acoustic waves in high polymers [20].

If the thermal resistance measured by Wheatley *et al.* is only due to the resistance of the glue layer, we obtain  $l/L = 0.02$  at  $0.2^\circ \text{ K}$ . ( $l \approx 10^{-3} \text{ mm}$ ).

### 7. Conclusions and comparison of different indirect cooling methods

The lowest temperatures obtainable by indirect cooling methods in which conductivity by phonons is essential, are of the order of  $0.01^\circ \text{ K}$ . Formula (3.13) shows that the heat transportable at  $0.01^\circ \text{ K}$  through  $1 \text{ cm}^2$  area is of the order of  $0.01 \text{ erg/s}$ . It would be difficult to reduce the heat leaks below this amount. A temperature of  $0.01^\circ \text{ K}$  can only be reached in crystals in which the free path of the phonons is not much larger than the smallest dimension of the crystals, thus, only perfect or very thin crystals can be used. In experiments with radioactive crystals no high activities can be used if  $\alpha$ ,  $\beta^-$  or  $\beta^+$  radiation is emitted. For a decay starting with K-capture no restriction is necessary.

In experiments on, for example, two stage demagnetization, nuclear orientation in external magnetic fields or nuclear alignment in anti-ferromagnetics, where materials with large heat capacities are to be

cooled, the time needed to obtain a considerable decrease in temperature will also be an important factor. For the cases where thermal conductivity by phonons is essential, the time factor can be estimated. Fig. 3.9 gives the temperature of a particular crystal as a function of time, the properties of the crystal being assumed as follows: the entropy of the crystal per mole can be written as  $10^{-4}R/T^2$ , the thickness of the crystal is 1 mm, the molecular weight is 500 and the density is 2. The heat transport is assumed to be described by  $10^6T^4$  erg/s cm<sup>2</sup>. Fig. 3.9 shows that it takes 3 hours in this case to reach a temperature of 0.01° K. For other values of the parameters the corresponding curve can be found easily, the times in fig. 3.9 being plotted on a logarithmic scale and a change of the parameters resulting in a constant shift of the whole curve.

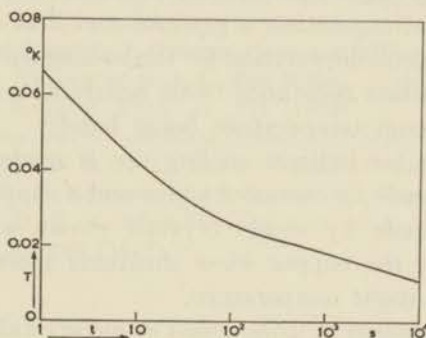


Fig. 3.9 The temperature of a cylindrical crystal as a function of time, the properties of the crystal being assumed as follows.

density = 2 g/cm<sup>3</sup>                      entropy =  $10^{-4}R/T^2$   
 molar weight = 500                      thickness = 1 mm  
 The cooling rate is given by  $10^6T^4$  erg/s cm<sup>2</sup>

The results obtained when cooling antiferromagnetics (chapter VI) can be compared with this calculation of the cooling time. A crystal of CoNH<sub>4</sub>-tutton salt of thickness 3 mm could be cooled to about 0.035° K in 1000 s, the entropy of the nuclear spin system being given by  $8 \times 10^{-4} R/T^2$ .

Surface resistances are not necessarily important at the lowest temperatures if crystals are glued to flat plates. The thickness of the glue layer has to be of the order of 0.01 cm. The resistance of a heat-link with electron thermal conductivity can be neglected at the lowest temperatures if the diameter is not too small. With heat-links of crystalline quartz, as are used by Wheatley *e.a.*, 0.01° K cannot be reached. The high velocity of sound ( $5 \times 10^5$  cm/s) gives a maximum heat flow through a unit area of a quartz heat-link of about  $3 \times 10^5 T^4$  erg/s cm<sup>2</sup>. In practice this number will be reduced if the heat-link is longer than a few times the phonon mean free path.

The cooling salts which have been used successfully by several inves-

tigators can be divided into two groups. One group consists of the kind of cooling substances containing large numbers of copper wires in a paramagnetic salt and a binding agent, the latter being glycerol [6], Apiezon oil [21] or alcohol. The results have shown that the thermal contact using propanol is very good, the freezing point of the alcohol corresponding to a temperature below which the shrinking of materials is not so important. However, not only the thermal contact but also the heat capacity of the cooling salt present in the intimate surroundings of the copper wires should be taken into account. Magnetically more concentrated crystals can be added to an alcoholic solution to increase the heat capacity, but experimentally it turns out that not more than 30 percent crystals (CrK-alum) can be allowed, the heat contact being reduced when using larger amounts of crystals. It appears that, when cooling large thermal capacities, a glycerol and CrK-alum mixture may be preferable to an alcoholic solution for the cooling salt, the heat capacity being larger, the contact resistance being nearly as good and its method of preparation at room temperature being handy.

In other methods for indirect cooling use is made of single crystals. A thermal contact made by means of a glue and a copper plate is preferred above a contact made by single crystals grown around metal wires (ref. [22] and [23]), the copper wires shrinking more than the crystals when cooled below room temperature.

A difficulty encountered in using glued single crystals is the preparation of the crystals and the establishment of a large contact area. The thermal conductivity of crystals can be expected to be much better than that of mixtures, which means that if a large enough contact area can be attained a single crystal cooling salt can give the best results, especially if a large amount of heat must be absorbed by the cooling salt. Such apparatus has been used in the investigations on nuclear alignment (chapter VI), a contact area of about 60 cm<sup>2</sup> being obtained by using 16 flat cylindrical plates 2 cm<sup>2</sup> in cross-section and 3 mm thick cut from a large CrK-alum crystal. All crystal plates were glued to copper on both sides. In fact this cooling salt can be represented by one large cylinder 1.5 mm long with a cross-sectional area of 60 cm<sup>2</sup>. The heat flow through such a CrK-alum cylinder calculated by means of formula (3.8) and the experimentally derived thermal conductivity is  $12 \times 10^6 (T_h^4 - T_c^4)$  erg/s, which consequently indicates that its resistance can be neglected if the substance to be cooled has a contact area of only a few cm<sup>2</sup>.

#### REFERENCES

1. BÖLGER, B., Thesis, Leiden (1959).
2. MENDOZA, E., *Cérémonies Langevin et Perrin*, Paris, 62 (1958).
3. GOODMAN, B. B., *Proc. Phys. Soc. (London) A* 66, 217 (1953).
4. DAUNT, J. C., *Proc. Int. Conf. Low Temp. Phys. Oxford*, 157 (1951).
5. ROBINSON, F. N. H., Thesis, Oxford (1954).

6. KURTI, N., F. N. H. ROBINSON, F. SIMON and D. A. SPOHR, *Nature* 178, 450 (1956).
7. WHEATLEY, J. C., D. T. GRIFFING and T. L., ESTLE, *Rev. Sci. Instrum.* 27, 1070 (1956).
8. NICOL, J. and T. P. TSENG, *Phys. Rev.* 92, 1062 (1953).
9. AMBLER, E. and R. P. HUDSON, *Phys. Rev.* 104, 1500 (1956).
10. BEUN, J. A., A. R. MIEDEMA and M. J. STEENLAND, *Commun. Kamerlingh Onnes Lab., Leiden* 305d; *Physica* 23, 1 (1957).
11. DIJK, H. VAN, and M. DURIEUX, *Commun. Suppl.* 115a; *Physica* 24, 20 (1958).
12. GARRETT, C. G. B., *Phil. Mag.* 41, 621 (1950).
13. BIJL, D., *Commun.* 276b; *Physica* 14, 684 (1948).
14. BROEK, J. VAN DEN, L. C. VAN DER MAREL and C. J. GORTER, to be published *Physica*.
15. AMBLER, E., M. A. GRACE, H. HALBAN, N. KURTI, N. DURAND, C. E. JOHNSON and H. R. LEMMER, *Phil. Mag.* 44, 216 (1953).
16. DANIELS, J. M. and F. N. H. ROBINSON, *Phil. Mag.* 44, 630 (1953).
17. POSTMA, H., W. J. HUISKAMP, A. R. MIEDEMA, M. J. STEENLAND, H. A. TOLHOEK and C. J. GORTER, *Commun.* 310b; *Physica* 24, 157 (1958).
18. LORD RAYLEIGH, *Theory of Sound*, Mac Millan, London (1894).
19. LITTLE, W. A., *Canad. J. Phys.* 37, 334 (1959).
20. KOLSKY, H., *Stress waves in Solids*, Oxford University Press, London (1953).
21. DANIELS, J. M. and M. A. R. LE BLANC, *Canad. J. Phys.* 36, 638 (1958).
22. DABBS, J. W. T., L. D. ROBERTS and S. BERNSTEIN, *Phys. Rev.* 98, 1512 (1955).
23. DUGDALE, J. S., D. K. C. MAC DONALD and A. A. M. CROXON, *Canad. J. Phys.* 35, 502 (1957).

THE MAGNETIC BEHAVIOUR OF FOUR TUTTON SALTS  
BELOW 1° K

The investigated tutton salts have the general formula  $M^{++}M_2^+(SO_4)_2 \cdot 6H_2O$  where  $M^{++}$  is a divalent ion and  $M^+$  a monovalent ion. The crystals are monoclinic, their structure having been investigated by HOFFMAN [1]. The angle between the crystalline  $a$  and  $c$  axes was found to be  $106^\circ$ , the  $b$  axis being perpendicular to the  $ac$  plane. The dimensions of the unit cell in the directions of the crystalline  $a$ ,  $b$  and  $c$  axes are 9.2, 12.4 and 6.2 Å, respectively.

There are two lattice positions for the magnetic ions,  $[0, 0, 0]$  and  $[\frac{1}{2}, \frac{1}{2}, 0]$ , the environment of the one in the  $ac$  plane being the mirror image of that of the other. The crystal field acting on the magnetic ions has roughly tetragonal symmetry and has the same character for the two lattice positions. Only the directions in space of the symmetry axes of the crystal field are different. Fig. 4.1 gives the positions of the tetragonal axes ( $T$ ) and of the principal axes of magnetization ( $K_1, K_2, K_3$ ). The parameters  $\psi$  and  $\alpha$ , in the figure shown for the case of  $CoNH_4$ -tutton salt, are different for different tutton salts as can be seen in table IV, I. The data have been found by paramagnetic resonance methods. For Co and Mn ions the parameters have been derived from measurements on a crystal which was magnetically diluted with Zn ions. Susceptibility measurements have shown that the parameters are roughly the same for concentrated  $CoNH_4$ -tutton salt [2], but for the concentrated

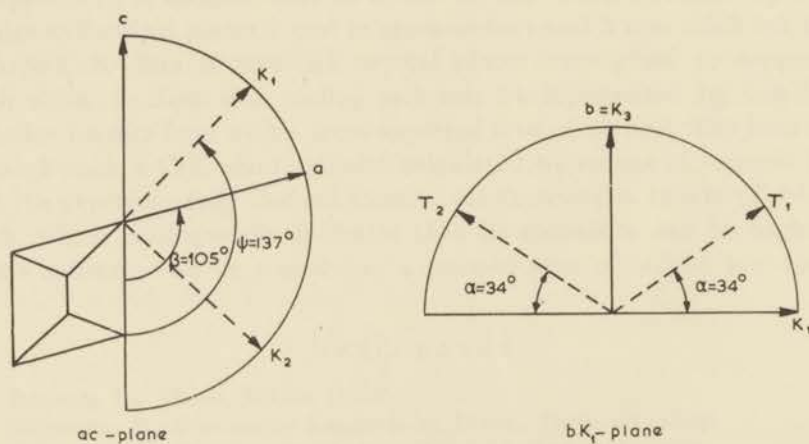


Fig. 4.1 Positions of magnetic susceptibility axes ( $K$ ) and tetragonal field axes ( $T$ ) with respect to the crystallographic axes in cobalt ammonium sulphate.

TABLE IV, I

Parameters of the magnetic ions in four tutton salts. The values for Co and Mn ions are obtained on a  $\text{ZnNH}_4$ -tutton salt crystal

Tutton salt	$S$	$\psi$	$\alpha$	$g_{  }$	$g_2$	$g_{\perp}$ ( $\text{K}_1\text{K}_2$ )	Ref.
CuK	$\frac{1}{2}$	105	42	2.36	2.04	2.14	BLEANEY <i>e.a.</i> [10]
$\text{CuNH}_4$	$\frac{1}{2}$	65	39	2.45	2.06	2.12	BLEANEY <i>e.a.</i> [10]
$\text{CoNH}_4$	$\frac{1}{2}$	137	34	6.45	3.06	3.06	VAN DEN BROEK <i>e.a.</i> [11]
$\text{MnNH}_4$	$\frac{5}{2}$	58	32	$D/k = 0.038^\circ \text{K}$		$g = 2$	BLEANEY <i>e.a.</i> [12]

manganese salt  $\psi$  apparently is about  $150^\circ$ , as will be discussed in chap. VI, section 6.

Experiments performed with single crystals of  $\text{MnNH}_4$ -,  $\text{CoNH}_4$ -,  $\text{CuNH}_4$ - and CuK-tutton salt will be reported. The samples were used in the shapes in which they had been grown in order to prevent confusion as to the directions of the axes. The susceptibilities were corrected to the values for a spherical sample, although the investigated crystals did not have an ellipsoidal shape. Though a demagnetizing factor has only a well defined meaning for an ellipsoidally shaped crystal it is assumed that the susceptibilities can be corrected in first approximation by means of an average  $N$  value. This  $N$  has been determined experimentally by measuring the susceptibility of a piece of Armco iron modelled to the shape of the crystal, as compared with that of an Armco iron sphere (see HUISKAMP *e.a.* [3]). The magnetic induction  $B$  in such a ferromagnetic sample is inversely proportional to  $1/N$  for magnetic fields which are considerably smaller than the saturation value and considerably higher than the coercive field. The estimated  $N$  values are given in table IV, II.

TABLE IV, II

Weights and demagnetizing factors (units  $4\pi/3$ ) of the investigated tutton salt crystals

Tutton salt	Weight g	$N_1$	$N_2$	$N_3$
CuK	2.9	0.56	1.79	0.90
$\text{CuNH}_4$	3.4	1.02	1.45	0.70
$\text{CoNH}_4$	9	1.02	1.20	0.79
$\text{MnNH}_4$	11	1.12	0.96	0.83

The ballistically measured susceptibilities have been corrected to the value for a spherical sample by means of:

$$(4.1) \quad \chi = \chi_e / (1 + \varepsilon \chi_e)$$

in which  $\chi_e$  is the experimental value of the susceptibility,  $\varepsilon = (4\pi/3 - N)\rho/M_0$ ,  $\rho$  is the density and  $M_0$  the molecular weight. If strong relaxation effects occur the formula can not be used for susceptibilities measured with an

alternating field. In that case the following formulae have been used:

$$(4.2) \quad \chi'' = \frac{\chi_e''}{1 + \varepsilon^2(\chi_e'^2 + \chi_e''^2) + 2\varepsilon\chi_e'}$$

and

$$(4.3) \quad \chi' = \frac{\chi_e' + \varepsilon(\chi_e'^2 + \chi_e''^2)}{1 + \varepsilon^2(\chi_e'^2 + \chi_e''^2) + 2\varepsilon\chi_e'}$$

where  $\chi_e'$  and  $\chi_e''$  are the experimental values of the susceptibility per mole.

### 1. Manganese ammonium tutton salt

Previously measurements on powdered crystals of  $\text{MnNH}_4$ -tutton salt have been performed by COOKE [4] and by STEENLAND *e.a.* [5], who found a pronounced maximum in the susceptibility versus entropy curve. Cooke measured the relation between temperature and entropy above the Néel temperature; Steenland *e.a.* did the same below that temperature.

The present experiments were performed with a single crystal, the different magnetic axes being placed in the direction of the vertical measuring field on different measuring days. Fig. 4.2 shows the adiabatic susceptibilities in zero field. The measurements in the  $K_3$  direction were performed ballistically, while for the  $K_1$  and  $K_2$  directions an a.c. bridge was used as the values of  $\chi''$  proved to be negligible in these directions. At entropies above  $\ln 4$  the susceptibilities are not very different for the three directions, the largest value being found in the  $K_1$  and the lowest value in the  $K_2$  direction. At an entropy of about  $R \ln 4$  the  $K_3$  suscepti-

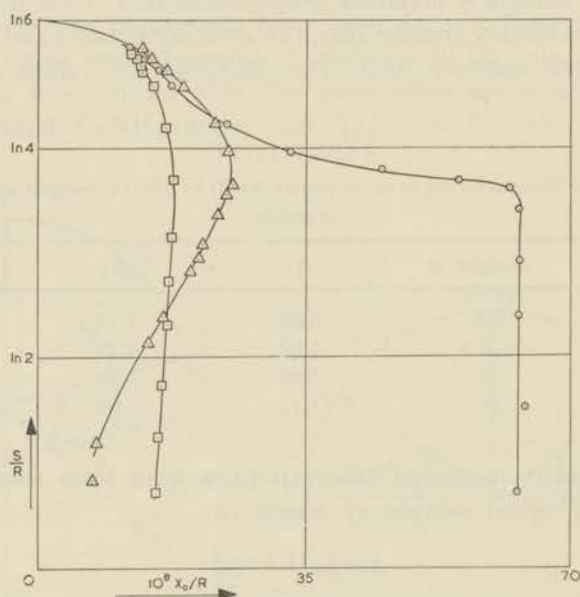


Fig. 4.2  $\text{MnNH}_4$ -tutton salt. The susceptibility measured in zero field as a function of entropy for the three magnetic axes.

△  $K_1$  direction      □  $K_2$  direction      ○  $K_3$  direction

bility increases sharply with decreasing entropy to a maximum value which if calculated per  $\text{cm}^3$  equals the value  $3/4\pi$  within the experimental accuracy of 2 %. At the entropy  $S=1.25 R$  the  $K_1$  susceptibility passes through a pronounced maximum, whereas the  $K_2$  susceptibility becomes independent of entropy. This entropy of  $1.25 R$  will be considered as the entropy at the Néel temperature ( $S_N$ ). At the lowest entropy reached ( $S=0.29 R$ ), the  $K_1$  susceptibility has decreased to  $\chi=7 \times 10^{-8} R$  the  $K_2$  and  $K_3$  susceptibilities being  $15 \times 10^{-8} R$  and  $63 \times 10^{-8} R$ , respectively.

Relaxation effects only occur in the  $K_3$  direction. The values of  $\chi'$  and  $\chi''$  have been measured as functions of entropy. Both are strongly dependent on the amplitude and the frequency of the measuring field. Fig. 4.3 shows the susceptibilities ( $\chi_0$ ,  $\chi'$  and  $\chi''$ ) in the  $K_3$  direction measured with an alternating field of 0.05 Oe amplitude at a frequency of 225 Hz. At relatively high entropies, above  $S_N$ ,  $\chi''$  is negligibly small and  $\chi'$  equals  $\chi_0$ . Below  $S_N$  the value of  $\chi'$  decreases with decreasing entropy, whereas  $\chi''$  reaches a maximum at  $S$  is about  $0.8 R$ . The maximum value of  $\chi''$  corresponds to  $\chi''/\chi_0=0.22$ . The susceptibilities in fig. 4.3 are corrected for the demagnetizing factor using formulae (4.2) and (4.3).

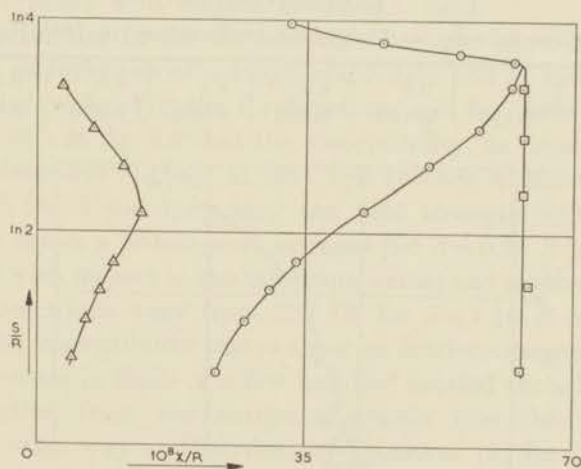


Fig. 4.3  $\text{MnNH}_4$ -tutton salt.  $\chi_0$ ,  $\chi'$  and  $\chi''$  measured in the direction of the  $K_3$  axis as functions of entropy. The alternating field has an amplitude of 0.05 Oe and a frequency of 225 Hz.

□  $\chi_0$                       ○  $\chi'$                       △  $\chi''$

No remanences have been observed in the three directions in which the susceptibility measurements were performed, using a measuring field of 1 oersted. By means of the relaxation heating method temperature determinations were carried out. As thermometric parameters the values of  $\chi'$  in the  $K_3$  direction in primary fields of 0.05 and 0.7 Oe were used. The amount of heat supplied was determined from the measured values of  $\chi''$ . Using the field of 0.7 Oe amplitude for heating the sample, the heat supply was of the order of 1000 erg/s. The amplitude of the field

was chosen large enough that the  $\chi''$  versus  $S$  curve did not show a maximum (see section 3). Thus  $\chi''$  decreases with rising temperature which keeps the temperature distribution in the salt more homogeneous. After a heating period of 100 seconds the field was reduced to 0.05 Oe and  $\chi'$  was measured. Three such heating periods were performed after each demagnetization. The average temperature in one heating period could be calculated using the value of  $\Delta S$  derived from the 0.05 Oe measurements. From the values of  $d\chi'/dt$  measured during a heating period absolute temperatures have also been derived with the aid of the relation  $T = (dQ/dt)/(dS/d\chi') (d\chi'/dt)$ . The results are given in fig. 4.4 and in table IV, III. They can be compared with the relation between entropy and absolute temperature obtained by Cooke, which was obtained using  $\gamma$ -ray heating at entropies above  $S_N$  (solid line in fig. 4.4). The agreement is good and connecting our experimental curve with that of Cooke, a value of  $0.14^\circ \text{K}$  for  $T_N$  is found. Measurements of Steenland *e.a.* gave temperatures of the same order of magnitude but their measurements may have been less accurate, since in powdered crystals the relaxation

TABLE IV, III  
Relation between entropy and absolute temperature in  $\text{MnNH}_4$ -tutton salt

$S/R$	1.1	1.0	0.9	0.8	0.7	0.6	0.5	0.4
$T(^{\circ}\text{K})$	0.124	0.117	0.109	0.102	0.093	0.086	0.080	0.074

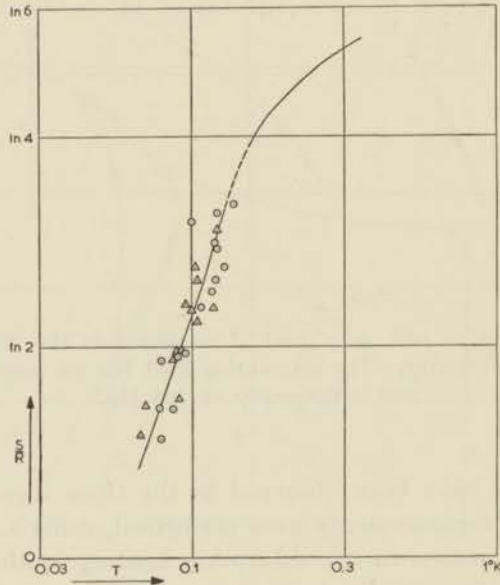


Fig. 4.4  $\text{MnNH}_4$ -tutton salt. The relation between absolute temperature and entropy. The solid line in the high entropy region has been derived from measurements of Cooke. The  $\chi'$  versus  $S$  relations with two different field amplitudes  $h_0$  are used as a thermometer.

○  $h_0 = 0.05$  Oe

△  $h_0 = 0.7$  Oe

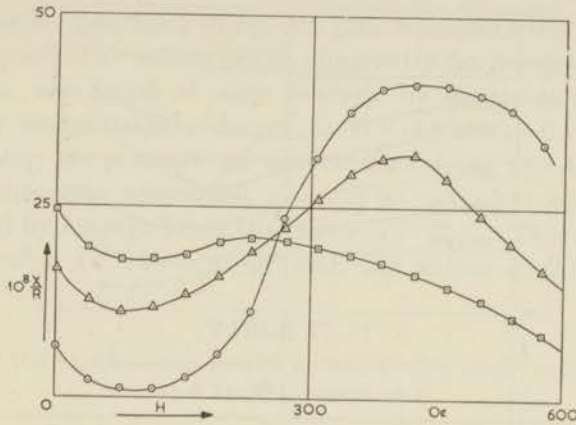


Fig. 4.5  $\text{MnNH}_4$ -tutton salt. The susceptibility in the  $K_1$  direction as a function of a longitudinal field.

○  $S = 0.29 R$       △  $S = 0.83 R$       □  $S = 1.16 R$

heating is very inhomogeneous due to the different orientations of the  $K_3$  axes of the crystals with respect to the a.c. field.

The susceptibilities in the  $K_1$  and  $K_3$  directions have been measured adiabatically as functions of a longitudinal field and at several values of the entropy below  $S_N$ . For the  $K_1$  directions and for three values of the entropy it is seen in fig. 4.5 that the susceptibility, as measured with the a.c. bridge, decreases slightly at first and reaches a minimum in fields of about 100 Oe. Upon increasing the field strength still further, the susceptibility shows a pronounced increase (for  $S = 0.29 R$  it increases by a factor of 40 with respect to the minimum value) and reaches a maximum for field values which vary from 250 Oe for  $S = 1.16 R$  to 460 Oe for  $S = 0.29 R$ . The susceptibility curves show an antiferromagnetic character, the strong increase in fields of a few hundred oersted probably being due to the transition from the antiferromagnetic into the paramagnetic state. In the same way as described by GARRETT [2] for  $\text{CoNH}_4$ -tutton salt the changes in temperature produced on isentropic magnetization have been derived for  $\text{MnNH}_4$ -tutton salt. From the  $\chi_{||}$  versus  $H$  curves the adiabatic magnetization curves were deduced by graphical integration. Using the formula  $\Delta T = -\int_0^H (\partial M / \partial S)_H dH$  the temperature during isentropic magnetization has been calculated. The temperature reaches a minimum at a certain field strength and thereafter rises again. It will be assumed here, which may not be strictly correct, that the locus of the minima of the  $T$  versus  $H$  curves (fig. 4.6) corresponds to the boundary of the antiferromagnetic region. The dashed line connects these minima and the extrapolated value at zero temperature gives 540 Oe for the critical field in the  $K_1$  direction. The  $K_3$  susceptibility was measured ballistically. It can be seen in fig. 4.7 that the magnetic behaviour in this direction is very different from that in the  $K_1$  direction. The

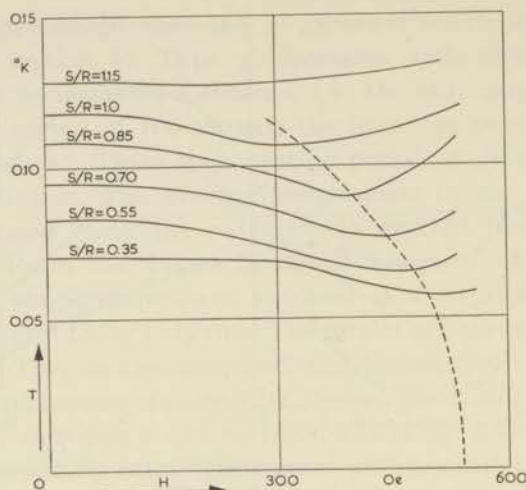


Fig. 4.6 The temperature variation during isentropic magnetization in antiferromagnetic  $\text{MnNH}_4$ -tutton salt. The dashed line represents the boundary of the magnetically ordered region.

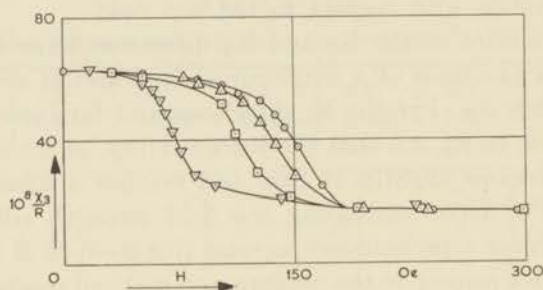


Fig. 4.7  $\text{MnNH}_4$ -tutton salt. The susceptibility in the  $K_3$  direction as a function of a longitudinal field.

- |                |                |
|----------------|----------------|
| ○ $S = 0.29 R$ | □ $S = 0.83 R$ |
| △ $S = 0.57 R$ | ▽ $S = 1.07 R$ |

susceptibility retains the very high value which it had at zero field up to fields which vary from 50 Oe for  $S=1.07 R$  to about 100 Oe for  $S=0.29 R$ . At higher field values the susceptibility drops to about 30 % of its initial value and becomes nearly independent of the magnetic field.

The  $\chi_3$  versus  $H$  curves show a ferromagnetic character. The values of  $3/4\pi$  per  $\text{cm}^3$  for the susceptibilities correspond to an infinite value if reduced to an infinitely long cylinder. The susceptibility of  $1/N$  means, in fact, that the  $\chi$  value of the  $\text{MnNH}_4$ -tutton salt crystal was equal to the susceptibility of the Armco iron sample of the same shape and volume which was used when determining the approximate demagnetizing factor.

In order to derive a value for the ferromagnetic moment from the isentropic magnetization measurements, the experimental  $M$  values are

plotted *versus*  $H - (4\pi/3)M_v$  in fig. 4.8 ( $M_v$  represents the magnetization moment per  $\text{cm}^3$ ). The values of the apparently ferromagnetic saturation moment,  $M_{fe}$ , are found at each entropy by extrapolating the linear parts of the magnetization curves to  $H - (4\pi/3)M_v = 0$ .  $M_{fe}$  increases with decreasing temperature as can be seen from fig. 4.9. The value of the ferromagnetic saturation moment at complete ordering of the spins is found by extrapolating the curve to  $T \ll T_N$ . This magnetization is given in table IV, IV together with the values of  $T_N, S_N$  and the

TABLE IV, IV

Comparison of the experimental results obtained with single crystals of  $\text{CoNH}_4$ - and  $\text{MnNH}_4$ -tutton salt

	$T_N$ (°K)	$\frac{S_N}{R}$	$\frac{M_{fe}}{R} \times 10^6$	$H_{er}$ (Oe)	$\theta_M$ (degree)
$\text{CoNH}_4$	0.084	0.43	85	400	10
$\text{MnNH}_4$	0.14	1.25	94	540	16

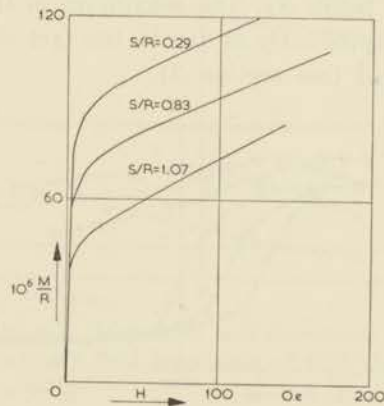


Fig. 4.8  $\text{MnNH}_4$ -tutton salt. Isentropic magnetization curves for a field in the  $K_3$  direction. The external fields have been corrected with  $H = H_e - (4\pi/3)M_v$ .

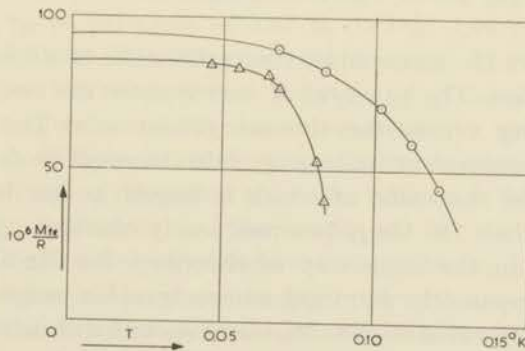


Fig. 4.9 The experimental values of the ferromagnetic saturation moment,  $M_{fe}$ , plotted *versus* temperature.

○  $\text{MnNH}_4$ -tutton salt

△  $\text{CoNH}_4$ -tutton salt

critical field in the  $K_1$  direction. The extrapolated value of  $M_{Te}$  equals 31 % of the total saturation moment, the latter being calculated with  $S=5/2$  and  $g=2$ .

## 2. Cobalt ammonium tutton salt

A single crystal of  $\text{CoNH}_4$ -tutton salt has been already investigated by GARRETT [2] who measured pronounced anisotropies in the zero field susceptibilities. The  $K_1$  susceptibility, which is the highest in the liquid helium temperature range, shows a pronounced maximum as a function of entropy. At the entropy corresponding to this maximum the  $K_3$  susceptibility increases sharply and reaches a value of about  $3/4\pi$  per  $\text{cm}^3$ . Garrett also determined the relation between entropy and temperature and derived a value of 400 Oe for the critical field in the  $K_1$  direction.

New experiments on a  $\text{CoNH}_4$ -tutton salt crystal were performed in order to make a complete comparison between  $\text{CoNH}_4$ - and  $\text{MnNH}_4$ -tutton salt possible. The ballistic measurements showed a constant susceptibility equal to  $3/4\pi$  per  $\text{cm}^3$  within the experimental accuracy (2 %) in the  $K_3$  direction at entropies below  $S_N$ . The maximum in the  $\chi_3$  versus  $S$  curve reported by Garrett, apparently is due to the fact that  $\chi_3$  was measured with a 40 Hz a.c. field (see section 3).

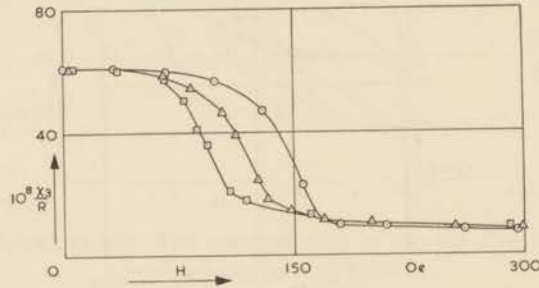


Fig. 4.10  $\text{CoNH}_4$ -tutton salt. The  $K_3$  susceptibility as a function of a longitudinal field.

$$\circ \quad S = 0.050 R \quad \triangle \quad S = 0.262 R \quad \square \quad S = 0.365 R$$

Fig. 4.10 shows the susceptibility as a function of a longitudinal field in the  $K_3$  direction. The  $\chi_3$  versus  $H$  curves show the same character as the corresponding curves for the manganese salt. The susceptibility remains nearly constant at its large  $\chi_0$  value in small fields and decreases sharply at a field the value of which is largest at the lowest entropy. In fields larger than 150 Oe  $\chi_3$  becomes nearly constant again at a value of  $10 \times 10^{-8} R$ . In the same way as described for  $\text{MnNH}_4$ -tutton salt values of the apparently ferromagnetic saturation magnetization have been derived at several entropies.  $M_{Te}$  increases with decreasing temperature as may be seen in fig. 4.9. The value of  $M_{Te}$  at complete ordering of the spins is given in table IV, IV. It equals 65 % of the saturation magnetization calculated with  $g_3=4.40$  and  $S=1/2$ .

### 3. Absorption and dispersion measurements

The large specific heats of  $\text{MnNH}_4$ - and  $\text{CoNH}_4$ -tutton salt below their Néel temperatures gave the opportunity of observing the relaxation effects occurring in the  $K_3$  direction at nearly constant temperatures. Using a primary field amplitude of 0.05 Oe and frequencies between 3 and 1100  $\text{Hz}^1$ ) the relaxation curves were measured at four values of the entropy. Fig. 4.11 shows the results for  $\text{MnNH}_4$ -tutton salt. The scale factor of  $\chi''$  is twice that for  $\chi'$ . The measured  $\chi''$  values show a maximum within the range of applied frequencies for three of the entropies. From the shape of the curves, which is not a Debye shape, it may be seen that a well defined single relaxation time does not describe

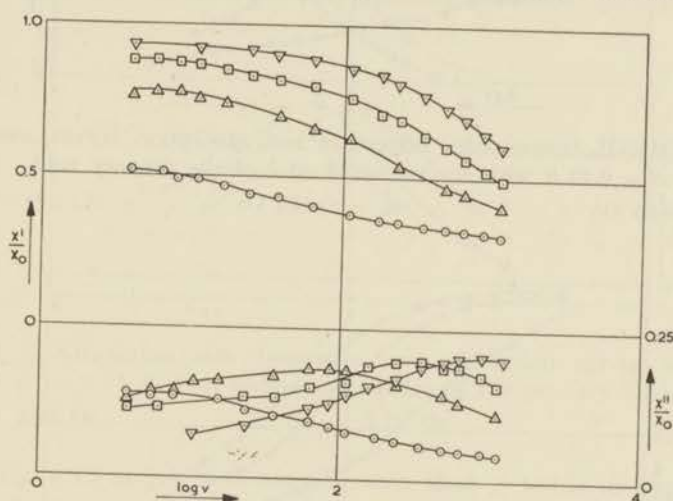


Fig. 4.11  $\text{MnNH}_4$ -tutton salt. Dispersion and absorption curves measured with a primary field amplitude of 0.05 Oe.

○	$S = 0.29 R$	□	$S = 0.83 R$
△	$S = 0.66 R$	▽	$S = 0.95 R$

the phenomena satisfactorily, but an average value,  $\tau_{av}$ , may be derived. The values of  $\tau_{av}$  at entropies of 0.95  $R$ , 0.83  $R$ , 0.66  $R$  and 0.29  $R$  are 0.2, 0.5, 2, and about 60 millisecond, respectively. The character of the relations between the entropy and both  $\chi'$  and  $\chi''$  measured for 225  $\text{Hz}$  (fig. 4.3) are in agreement with these measurements, as the former may be considered as a dispersion and absorption curve measured at constant frequency with varying relaxation time. The relaxation time values proved to be strongly dependent on the amplitude of the measuring field (fig. 4.12). With increasing amplitude the relaxation time becomes shorter and the maximum in the  $\chi''$  versus  $\log v$  curve becomes higher, which indicates that the distribution of the relaxation times becomes narrower.

<sup>1)</sup> The Hartshorn bridge is the one used by VAN DER MAREL and VAN DEN BROEK in paramagnetic relaxation experiments. The cooperation of Mr J. v. D. BROEK during these experiments is gratefully acknowledged.

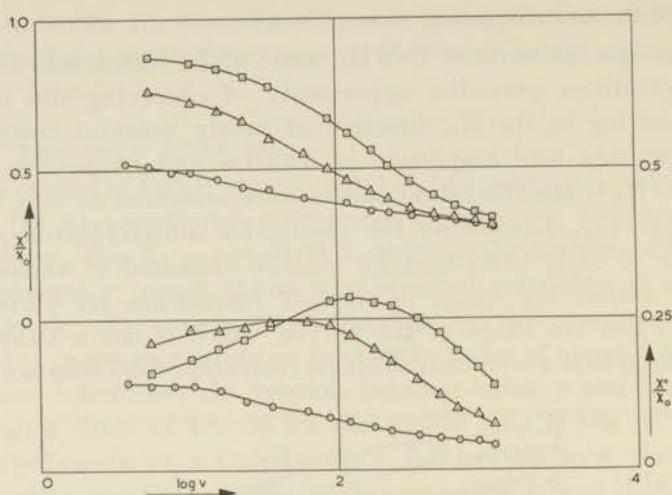


Fig. 4.12  $\text{MnNH}_4$ -tutton salt. Dispersion and absorption curves measured at  $S = 0.29 R$  with several amplitudes of the primary field.

○  $h_0 = 0.05$  Oe      △  $h_0 = 0.125$  Oe      □  $h_0 = 0.25$  Oe

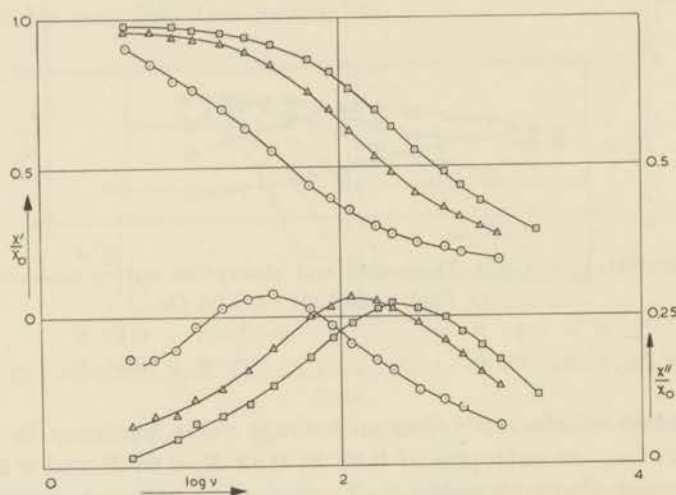


Fig. 4.13  $\text{CoNH}_4$ -tutton salt. Dispersion and absorption curves measured with a primary field amplitude of 0.05 Oe.

○  $S = 0.01 R$       △  $S = 0.20 R$       □  $S = 0.26 R$

The derived values of  $\tau_{av}$  at  $S = 0.29 R$  are 60, 4 and 1.2 millisecond for a field amplitude of 0.05, 0.125 and 0.25 Oe, respectively. In fig. 4.12 it may be seen that at the high frequency side  $\chi'$  approaches a constant value which corresponds to  $\chi'/\chi_0 \approx 0.30$ .

The absorption and dispersion for  $\text{CoNH}_4$ -tutton salt have been measured at three entropies using a measuring field amplitude of 0.05 Oe. The maxima in the  $\chi''$  versus  $\log \nu$  curves are more pronounced (fig. 4.13)

than in the case of manganese and the relaxation times are better defined. From fig. 4.13 we derive  $\tau_{av} = 4, 1.3$  and  $0.6$  millisecond for  $S = 0.01 R, 0.19 R$  and  $0.25 R$ , respectively. At the lowest attainable entropy  $\tau_{av}$  has been measured for three values of the measuring field amplitude, (0.05 Oe, 0.10 Oe and 0.24 Oe) giving for  $\tau_{av}$  4.0, 3.0, and 1.5 millisecond, respectively (fig. 4.14).

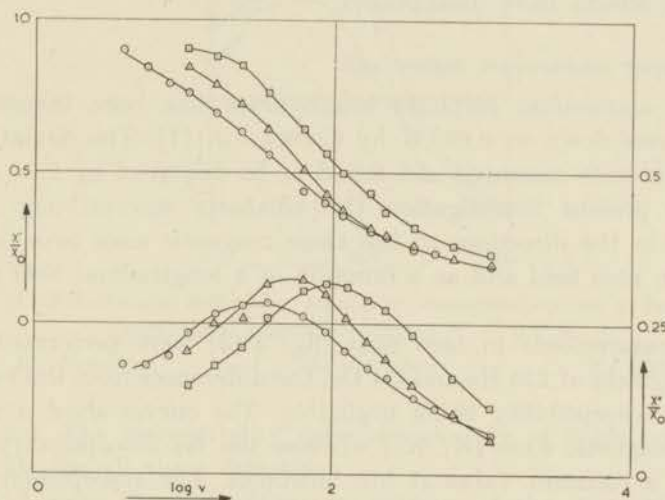


Fig. 4.14  $\text{CoNH}_4$ -tutton salt. Dispersion and absorption curves measured at  $S = 0.01 R$  with several amplitudes of the primary field.

○  $h_0 = 0.05$  Oe      △  $h_0 = 0.10$  Oe      □  $h_0 = 0.25$  Oe

From fig. 4.13 and 4.14 it may be seen that  $\chi'$  tends to approach the same constant value of  $\chi'/\chi_0$  which is nearly equal to 0.15 for all measured curves at the high frequency side.

At an entropy of  $0.19 R$  the influence of a magnetic field on the value of  $\tau_{av}$  has been studied. In small fields the values of  $\tau_{av}$  were independent of the field within the measuring accuracy. At the field value where the ballistic susceptibility (fig. 4.10) drops, the relaxation effects vanish. The absorption and dispersion measurements for  $\text{CoNH}_4$ -tutton salt are satisfactorily described by one rather well defined relaxation time. For the manganese salt the absorption maximum is less pronounced and a broad interval of relaxation times seems to be present. The  $\chi'/\chi_0$  value does not approach  $\chi'/\chi_0 = 1$  at low frequencies. Combined with the dependence of the relaxation curves on the amplitude of the alternating field this suggests that some kind of a coercive field may be present. Such a coercive field would be of the order of a few hundredths of an oersted and therefore there is no disagreement with the absence of a remanence, measured ballistically with a measuring field of 1 Oe. STEENLAND *et al.* [5] reported a small remanence of  $0.10 \pm 0.05$  gauss  $\text{cm}^3/\text{mole}$ , whereas KURTI [6] measured much higher values on a powdered sample of  $\text{MnNH}_4$ -tutton salt.

The differential susceptibility in a magnetic field, in which the ferromagnetic saturation is reached, and the zero field susceptibility in alternating fields of about 1000 Hz are nearly equal for both salts. This suggests that the susceptibility in a longitudinal field in the  $K_3$  direction can be divided into two parts, a ferromagnetic part where the spin system shows long relaxation times and a quasi-paramagnetic part, where the relaxation effects have disappeared.

#### 4. Copper ammonium tutton salt

Copper ammonium sulphate hexahydrate has been investigated at temperatures down to  $0.05^\circ \text{K}$  by COOKE *et al.* [7]. The deviations from Curie's law were measured and found to be described by  $\theta = 0.010^\circ \text{K}$ .

In the present investigation the adiabatic susceptibility has been measured in the directions of the three magnetic axes as a function of entropy in zero field and as a function of a longitudinal field at several entropies.

The measurements in zero field (fig. 4.15) were performed with an alternating field of 225 Hz and 0.1 Oe, the differences from the ballistically measured susceptibility being negligible. The curves show a maximum for two magnetic axes ( $K_1, K_3$ ) whereas the  $K_2$  susceptibility tends to approach a constant value at low entropies. The susceptibility maxima occur at entropies of  $0.42 R$  and  $0.36 R$  for the  $K_1$  and the  $K_3$  curve, respectively. The  $K_1$  susceptibility, which is largest at high entropies due to the fact that for this direction the  $g$  factor has the largest value, becomes the smallest of the three susceptibilities at low entropies.

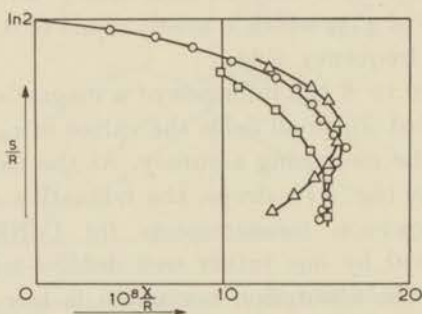


Fig. 4.15  $\text{CuNH}_4$ -tutton salt. The relation between susceptibility and entropy.  $\triangle$   $K_1$  direction  $\square$   $K_2$  direction  $\circ$   $K_3$  direction

$\chi''$  was smaller than  $1 \times 10^{-9} R$  for all three measuring directions. The dependence of the adiabatically measured susceptibility on a longitudinal field can be seen in fig. 4.16 for the lowest entropy,  $S = 0.2 R$ . The curves show a pronounced maximum in two cases ( $K_1, K_3$ ) in fields of about 150 Oe, the increase of the susceptibility being more than a factor two for the  $K_1$  curve. The  $K_2$  curve shows an increase of only 7% in the

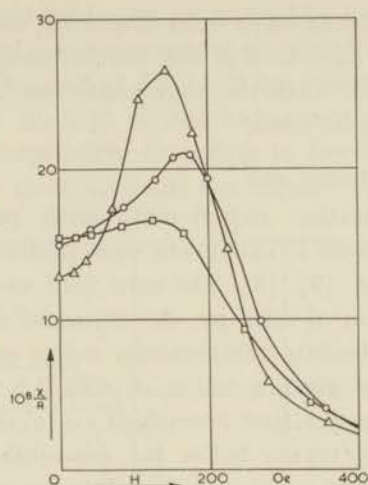


Fig. 4.16  $\text{CuNH}_4$ -tutton salt. The adiabatic susceptibility as a function of a longitudinal magnetic field at  $S = 0.2 R$ .

$\triangle$   $K_1$  direction       $\square$   $K_2$  direction       $\circ$   $K_3$  direction

same region. The susceptibility decreases sharply at fields between 150 and 180 Oe for all three directions.

Fig. 4.17 gives the dependence on entropy of the susceptibility in a longitudinal field for the  $K_1$  direction. The maximum in the  $\chi_{\parallel}$  versus  $H$  curve becomes less pronounced at higher entropies but it is still present at an entropy of  $0.38 R$ . The results obtained with  $\text{CuNH}_4$ -tutton salt suggest the occurrence of antiferromagnetism. Maxima in the  $\chi$  versus  $S$

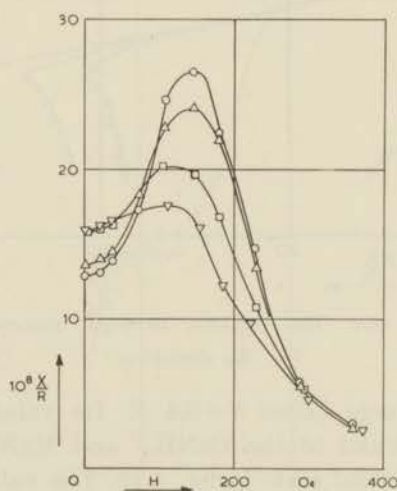


Fig. 4.17  $\text{CuNH}_4$ -tutton salt. The  $K_1$  susceptibility as a function of a longitudinal field for several entropies.

$\circ$   $S = 0.19 R$        $\square$   $S = 0.32 R$   
 $\triangle$   $S = 0.24 R$        $\nabla$   $S = 0.38 R$

and the  $\chi$  versus  $H$  curves have been found for two magnetic axes  $K_1$  and  $K_3$ . This may be explained if the antiferromagnetic ordering takes place in the  $K_1K_3$  plane, while the alignment direction(s) do not coincide with one of the magnetic axes.

#### 5. Copper potassium tutton salt

Previous demagnetization experiments with powdered crystals of copper potassium sulphate hexahydrate were performed by GARRETT [8] and by STEENLAND *e.a.* [9], [5]. The zero field susceptibility showed a maximum as a function of entropy. At entropies above this maximum Garrett derived the absolute temperature versus entropy relation from his magnetic data. He gives a value of  $0.034^\circ$  K for the Curie-Weiss constant, the sign being positive. Steenland *e.a.* evaluated the  $T$  versus  $S$  relation in the entropy region below the susceptibility maximum. The temperature of the Curie point was found to be about  $0.04^\circ$  K.

The present investigation of a single crystal has been performed in the directions of the 3 magnetic axes. From fig. 4.18 it can be seen that the zero field susceptibility, measured with an alternating field of 225 Hz and 0.1 Oe, has a maximum for the  $K_1$  and  $K_3$  directions. Its values are much larger than those found for the  $\text{CuNH}_4$ -salt, the  $\chi$  scale of fig. 4.15 being two times larger. The  $K_2$  susceptibility becomes nearly constant at entropies below  $0.4 R$  at a value which differs not more than 5 % from  $3/4\pi$  per  $\text{cm}^3$ . The anisotropy of the susceptibility at low entropies differs completely from the one in the high entropy region where the  $K_1$  susceptibility is largest, corresponding to the large  $g$  value in that direction.

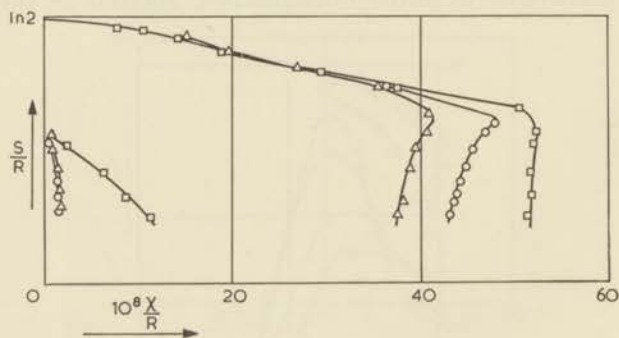


Fig. 4.18 CuK-tutton salt. The relation between susceptibility and entropy.  
 $\triangle$   $K_1$  direction       $\square$   $K_2$  direction       $\circ$   $K_3$  direction

$\chi''$  is measurably large below  $S=0.4 R$ . Its values are considerably smaller than those found in the  $\text{CoNH}_4$ - and  $\text{MnNH}_4$ -tutton salts,  $\chi''$  being plotted on a tenfold scale in fig. 4.18. The values of  $\chi''$  in the  $K_2$  direction are higher than those found in the other two directions. In agreement with the small values of  $\chi''$  present in CuK-tutton salt the ballistically measured susceptibility differs only slightly from the  $\chi'$  values given in fig. 4.18 ( $< 2\%$ ).

In small longitudinal fields the susceptibility keeps its high value but it decreases sharply to a few percent of its initial value in fields of about 100 Oe. The curves obtained at  $S=0.2 R$  are shown in fig. 4.19. At higher entropies, but below  $S=0.35 R$ , the behaviour remains the same, the steep fall of the susceptibility occurring in lower magnetic fields. The remarkable fact that in small fields the highest susceptibility is reached

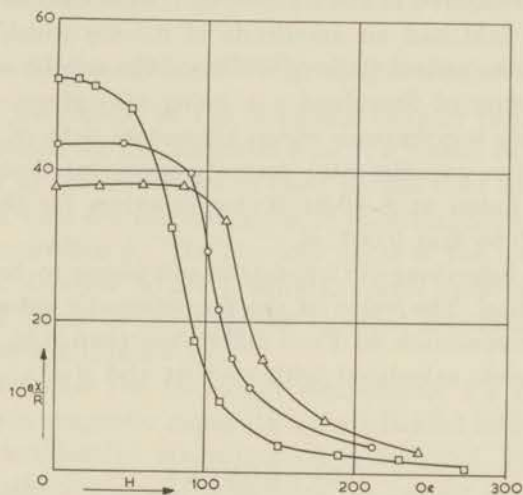


Fig. 4.19 CuK-tutton salt. The susceptibility as a function of a longitudinal field at  $S = 0.2 R$ .

△  $K_1$  direction      □  $K_2$  direction      ○  $K_3$  direction

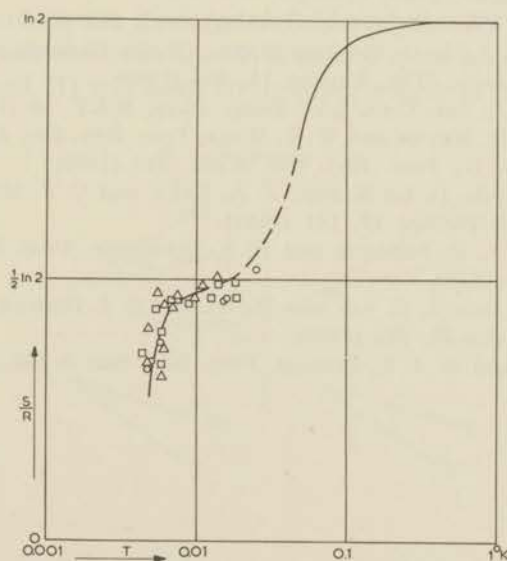


Fig. 4.20 CuK-tutton salt. The relation between absolute temperature and entropy. The solid line, given in the high temperature region, is derived from data of Garrett.

○ Steenland *e.a.*      △  $\chi'$  thermometer      □  $\chi''$  thermometer

in the direction with the smallest  $g$  value can be checked easily. It is possible to derive the magnetization as a function of the magnetic field by graphical integration of the curves in fig. 4.19. In agreement with the anisotropy of the  $g$  values the magnetization in a field of 250 Oe is largest in the  $K_1$  direction and smallest in the  $K_2$  direction.

Using the  $\chi''$  heating method, absolute temperatures have been derived. Both  $\chi'$  and  $\chi''$ , measured in the  $K_3$  direction, were used as thermometers. The alternating field had an amplitude of 0.5 Oe which supplied heat to the sample of the order of 10 erg/s. The results can be seen in fig. 4.20, experimental points of Steenland *et al.* being also given. The solid line drawn in the high temperature region represents data of Garrett. When connecting the two experimental curves a pronounced minimum of the specific heat is found at  $S=0.34 R$ , two maxima for the specific heat occurring near 0.05 and 0.007° K.

The magnetic behaviour of CuK-tutton salt seems to be ferromagnetic in the  $K_2$  direction. The value of the ferromagnetic saturation moment obtained by extrapolation to  $T=0$  differs less than 8 % from the total saturation moment, calculated with  $g=2.04$  and  $S=1/2$ .

#### REFERENCES

1. HOFFMANN, W., Z. Kristallogr. 78, 279 (1931).
2. GARRETT, C. G. B., Proc. Roy. Soc. A 206, 242 (1951).
3. HUISKAMP, W. J., A. N. DIDDENS, J. C. SEVERIENS, A. R. MIEDEMA and M. J. STEENLAND, Commun. Kamerlingh Onnes Lab., Leiden 308b; Physica 23, 605 (1957).
4. COOKE, A. H., Proc. Phys. Soc. (London) A 62, 269 (1949).
5. STEENLAND, M. J., L. C. VAN DER MAREL, D. DE KLERK and C. J. GORTER, Commun. 279c; Physica 15, 906 (1949).
6. KURTI, N., Proc. Int. Conf. Low Temp. Phys. M.I.T. 59 (1949).
7. COOKE, A. H., H. MEYER and W. P. WOLF, Proc. Roy. Soc. A 233, 536 (1956).
8. GARRETT, C. G. B., Proc. Roy. Soc. A 203, 375 (1950).
9. STEENLAND, M. J., D. DE KLERK, J. A. BEUN and C. J. GORTER, Commun. 284d; Physica 17, 161 (1951).
10. BLEANEY, B., R. P. PENROSE and B. I. PLUMPTON, Proc. Roy. Soc. A 198, 406 (1949).
11. BROEK, J. VAN DEN, L. C. VAN DER MAREL and C. J. GORTER, Commun. 314c; Physica 25, 371 (1959).
12. BLEANEY, B. and D. J. E. INGRAM, Proc. Roy. Soc. A 205, 336 (1951).

THE MAGNETIC STRUCTURE OF THE INVESTIGATED  
TUTTON SALTS

1. *A molecular field model for  $\text{CoNH}_4$ - and  $\text{MnNH}_4$ -tutton salt*

As has been mentioned in the foregoing chapter (fig. 4.1), there are two lattice positions for the magnetic ions in a tutton salt crystal, which are different as to the directions of their crystal field axes. For Co ions the crystal field axes are the directions of easy magnetization since  $g_{\parallel}$  is considerably larger than  $g_{\perp}$ . The absolute value of the magnetic moment of a cobalt ion depends on its orientation with respect to the crystal field axis and is largest if the magnetic moment is parallel to the crystal field axis (section 2, formula 5.30).

Suppose that below the transition temperature  $T_N$  the situation in which the electron magnetic moments are subdivided into two sublattices with mutually antiparallel magnetization is favoured. It will be shown that if these antiferromagnetic sublattices are present in a  $\text{CoNH}_4$ -tutton salt crystal and coincide with the two systems of ions mentioned before, the magnetic behaviour can be explained. It may be expected that at temperatures lower than  $T_N$  the resulting directions of the magnetic moments are not fully antiparallel to each other in the  $K_1$  direction, but somewhere between the crystal field and the  $K_1$  axes. The corresponding picture is shown in fig. 5.1. A pair of spins belonging to different sublattices (I and II) will have no resulting magnetic moment in the  $K_1$

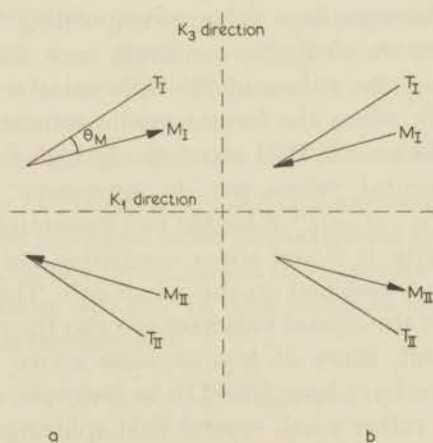


Fig. 5.1 Directions of the electron magnetic moments in  $\text{CoNH}_4$ -tutton salt in the magnetically ordered state.  $T_I$  and  $T_{II}$  represent the tetragonal field axes. There are two possibilities, *a* and *b*, for the antiferromagnetic structure.

direction, but they do have a net magnetization in the  $K_3$  direction. There are two equally probable possibilities for this magnetization in the  $K_3$  direction ( $a$  and  $b$  in fig. 5.1). Using this model it may be expected that below  $T_N$  and in zero external field there will be regions in the crystal which have a structure  $a$  and regions with a magnetic structure  $b$ , which domains have opposite magnetization with respect to the  $K_3$  direction. The ferromagnetic behaviour in this direction can be explained since in a magnetic field the domains with magnetization of the wrong direction with respect to the field may be transformed into domains with the right direction of the magnetization. The two possibilities for the magnetic structure have equal energies and thus the magnetization of a domain may change its direction in a very small magnetic field. If this field is zero, the volume susceptibility reaches  $3/4\pi$  for a spherical sample, i.e.  $\chi_0$  is infinitely large if reduced to an infinitely long cylinder. In small external fields the susceptibility keeps this high value but a saturation effect in larger fields occurs due to the fact that in high fields mainly domains of one type are left, the whole crystal becoming one large domain. The value of the ferromagnetic saturation magnetization,  $M_{te}$ , depends on the angle between the orientation direction of the magnetic moments and their tetragonal axes ( $\theta_M$ ). Since the angle between the T axes and  $K_1$  axis is  $34^\circ$  in  $\text{CoNH}_4$ -tutton salt, the ferromagnetic magnetization at zero temperature equals  $N\langle\mu\rangle \sin(34 - \theta_M)$ . The expectation value of the magnetic moment,  $\langle\mu\rangle$ , depends slightly on the value of  $\theta_M$  and both have been derived from the observations of the ferromagnetic saturation magnetization (see section 2).  $M_{te}$  is  $85 \times 10^{-6} R$  which corresponds to  $\theta_M = 10^\circ$  and  $\langle\mu\rangle = 3.1 \mu_B$ .

It is suggested that the transformation of domains  $a$  into domains  $b$  may be responsible for the relaxation effects occurring in small magnetic fields. At high frequencies the domains can not be reversed and the susceptibility will decrease to a value corresponding to a small periodic rotation of the electron magnetic moments into the direction of the magnetic field. Hence the values of the differential susceptibility in the  $K_3$  direction in fields where the ferromagnetic saturation is reached and the ones measured in an a.c. field of relatively high frequency should be equal. The experimental values are, in agreement with this picture,  $\chi_3 = 10 \times 10^{-8} R$  and  $\chi' = 9 \times 10^{-8} R$  for the two susceptibilities, respectively.

A striking similarity is found when comparing the data on  $\text{MnNH}_4$ -tutton salt with those obtained on the cobalt salt. The analogy indicates that the directions of the crystal field axes are also the preferred directions in the manganese salt. Since at temperatures above  $1^\circ \text{K}$  the  $g$  values of the manganese ions have been found to be isotropic, such an anisotropy must be due to the rather small crystal field splittings of the  $^6S$  ground state. These splittings are due to the combined action of the crystal field and the spin-spin interactions between the electrons of one manganese ion, which results in a predominantly axial symmetry [1] and thus the

dominant term in the Hamiltonian is given by  $D(S_z^2 - 35/12)$ . This has been confirmed in paramagnetic resonance experiments by BLEANEY *et al.* [2]; the values of the parameter  $E$ , which describes the deviations from axial symmetry, and of the parameter  $a$ , which describes the terms in the Hamiltonian due to the cubic portion of the crystal field, are found to be much smaller than  $D$ . The sixfold degenerate spin  $5/2$  level is split into three twofold degenerate levels, corresponding to values of the angular momentum in the direction of quantization  $S_z = \pm 1/2$ ,  $S_z = \pm 3/2$  and  $S_z = \pm 5/2$ , respectively. Fig. 5.1 may describe the magnetic ordering in  $\text{MnNH}_4$ -tutton salt if the energy levels with  $S_z = \pm 5/2$  have the lowest energy ( $z$  axis = T axis). The magnetic interactions cause energy splittings which are of the same order of magnitude as the crystal field splittings and the orientation direction of the spins in this case also will be appreciably different from both the  $K_1$  and the crystal field axis. The value of the ferromagnetic magnetization in  $\text{MnNH}_4$ -tutton salt equals  $(5/2)Ng\mu_B \sin(32 - \theta_M)$  and thus the angle between the T axes and the direction of the electron spins can be derived from the observed value for  $M_{1c}$  of  $94 \times 10^{-8} R$ . Using  $g = 2$  the result is  $\theta_M = 16^\circ$ . Just as was found for the cobalt salt, the differential susceptibility in a magnetic field where the ferromagnetism is saturated and  $\chi'$  in an alternating field of 1000 Hz are nearly equal,  $18 \times 10^{-8} R$ . For both  $\text{CoNH}_4$ - and  $\text{MnNH}_4$ -tutton salt the susceptibility in the  $K_1$  direction is rather small in agreement with the fact that a pair of spins has no net magnetization in this direction, the angle between the magnetic moments being small.

Starting from the present model for the magnetic structure of cobalt and manganese ammonium tutton salt below their transition temperature URYU [3] gives a quantitative discussion of the magnetic behaviour of these salts. He calculates the zero field susceptibilities and the angle between crystal field axis and magnetic moments at zero temperature, taking into account both dipolar and exchange interactions between magnetic ions. In the next section we shall follow the discussion given in Uryu's paper, but there will be differences in many details.

## 2. Calculations of spin angle and zero field susceptibilities

The contributions of magnetic dipolar and exchange interactions may be expected to be of the same order of magnitude in both  $\text{CoNH}_4$ - and  $\text{MnNH}_4$ -tutton salt, as can be concluded from specific heat data obtained at helium temperatures (see ref. 4). The terms in the Hamiltonian due to the magnetic interactions are:

$$(5.1) \quad \mathcal{H}_{\text{ex}} = - \sum_{i>k} J_{ik} \boldsymbol{\mu}_i \cdot \boldsymbol{\mu}_k$$

and

$$(5.2) \quad \mathcal{H}_{\text{dip}} = \sum_{i>k} r_{ik}^{-3} [\boldsymbol{\mu}_i \cdot \boldsymbol{\mu}_k - 3(\boldsymbol{\mu}_i \cdot \mathbf{r}_{ik})(\boldsymbol{\mu}_k \cdot \mathbf{r}_{ik})/r_{ik}^2]$$

where  $\mu_i$  is the magnetic moment vector of an ion  $i$  and  $r_{ik}$  the vector connecting two ions  $i$  and  $k$ .

To the magnetic exchange interaction only the interaction between ions placed at short distances will contribute. According to X-ray data of HOFFMANN [5] the first neighbours of a particular ion are two ions of the same kind (direction  $c$  axis, distance 6.2 Å) and the second neighbours are four ions of the dissimilar type ( $ab$  plane, 7.7 Å) while the next near neighbours are more than 9 Å away. According to the model of fig. 5.1 the magnetic moments of ions with the same direction of their crystal field axis are parallelly aligned and the exchange interaction may be described by:

$$(5.3) \quad \mathcal{H}_{\text{ex}} = - \sum_i (2J_1 \mu_{1i} \mu_{1i} + 4J_2 \mu_{1i} \mu_{2i}) \quad i = x, y, z.$$

The indices 1 or 2 correspond to the two sublattices. For the constants we take  $2J_1$  and  $4J_2$ , respectively, since now the values of  $J_1$  and  $J_2$  may give the exchange interaction for a pair of similar or dissimilar ions if the magnetic neighbours more than 9 Å away do not contribute to the exchange interaction.

When calculating the dipolar interactions the dipole sum is usually divided into two parts. The first part is the sum over the magnetic ions inside a small sphere and the other over magnetic ions outside it. In a homogeneously magnetized spherical sample the latter part vanishes because the field due to the magnetic polarization of the surface of the small sphere and the demagnetizing field due to the polarization of the outside of the sample are equal in magnitude and have opposite sign. The dipole sum for magnetic moments inside the sphere equals zero if the magnetic ions are placed on a cubic lattice. Since the lattice structure of the tutton salts is not cubic there may be a net contribution. Uryu gives the terms in the Hamiltonian due to dipolar interaction by means of 9 constants  $G_{1i}$ ,  $G_{2i}$  and  $G_{3i}$  which are the coefficients of  $\mu_{1i}\mu_{1i}$ ,  $\mu_{1i}\mu_{2i}$  and  $\mu_{2i}\mu_{2i}$ , respectively. The coefficients  $G_{1i} = G_{3i}$  and  $G_{2i}$  were calculated by NAKAMURA and URYU [6] and are given in table V, I. They obtained the same results when calculating the dipole sum for a sphere with a radius of 17 Å and for a sphere with a radius of 40 Å.

The  $x$  axis coincides with the  $K_1$  axis, the  $z$  axis is the  $K_3$  axis and the  $y$  axis the  $K_2$  axis.  $G_{1i} = G_{3i}$  because of the symmetry towards the three

TABLE V, I

The numerical values of the constants  $G_{1i}$  and  $G_{2i}$ , which describe the dipolar interactions in  $\text{CoNH}_4$ -tutton salt

$i$	$G_{1i}$	$G_{2i} \times 10^{-22} \text{ cm}^{-3}$
$x$	- 0.41	+ 0.37
$y$	- 0.74	+ 0.50
$z$	+ 1.16	- 0.87

magnetic axes. In fact the entries in the table were calculated for cobalt ammonium tutton salt ( $\psi = 137^\circ$ ) but they also can be used for the manganese salt since the difference in lattice constants is negligibly small and the  $\psi$  values are nearly equal.

Table V, I shows that the dipolar interactions are very anisotropic, the Lorentz field corresponding to 0.60 in the same units. The dipolar interactions may be considered as favouring parallel orientation for similar ions and favouring antiparallel orientation for dissimilar ions in the  $x$  and  $y$  directions, while in the  $z$  direction the dipolar interactions have the other sign. The constants  $G_{1i}$  and  $G_{2i}$  describe the dipolar interactions in the ordered states if there is no resultant magnetic moment in any direction. However, in the present case there is a net magnetization in the  $z$  direction. Then the constants  $G_{1z}$  and  $G_{2z}$  only may be used if the whole crystal is one spherical domain. If the domains are ellipsoidal with their long axis in the  $z$  direction the demagnetizing field becomes smaller and thus the total energy is lower. We assume that the demagnetizing field is zero, corresponding to domains which are infinitely long in the  $K_3$  direction.

In fact we already used this assumption when deriving the value of  $\theta_M$  from the ferromagnetic moment in the  $K_3$  direction. This ferromagnetic moment was found experimentally from the magnetization in a field in which the susceptibility drops down from its value of  $3/4\pi$  per  $\text{cm}^3$  to a much lower value. In this magnetic field the whole crystal is supposed to have one of the two possible domain structures. The external field cancels the demagnetizing field and the remaining magnetic energy is given by the terms  $G_{1i}$  and  $G_{2i}$  mentioned and the field corresponding to the polarization of the inside of the 40 Å sphere. This field equals  $4\pi/3 M_V$  ( $M_V$  is the magnetization per  $\text{cm}^3$ ) and the corresponding term in  $H_{\text{dip}}$  is:

$$(5.4) \quad -4\pi\varrho N\mu_{1z}(\mu_{1z} + \mu_{2z})/6M_0 = \sum_i (K_{1i}\mu_{1i}\mu_{1i} + K_{2i}\mu_{1i}\mu_{2i})$$

where  $K_{1z} = K_{2z} = -0.60 \times 10^{22} \text{ cm}^3$ ,  $K_{1i} = K_{2i} = 0$  for  $i \neq z$ ,  $\varrho$  is the density and  $M_0$  the molecular weight.

When deriving the direction of the magnetic moments and the values for the zero field susceptibilities at zero temperature we must find the minimum of the energy of the whole crystal. Denoting the interaction energy per ion by  $E(I, I)$  and  $E(II, II)$  for similar ions and by  $E(I, II)$  for dissimilar ions we have:

$$(5.5) \quad E(I, I) = E(II, II) = 1/4 [\sum_i (G_{1i} - 2J_1 + K_{1i})\mu_{1i}\mu_{1i}] = 1/4 [\sum_i A_{1i}\mu_{1i}\mu_{1i}]$$

$$(5.6) \quad E(I, II) = 1/2 [\sum_i (G_{2i} - 4J_2 + K_{2i})\mu_{1i}\mu_{2i}] = 1/2 [\sum_i A_{2i}\mu_{1i}\mu_{2i}]$$

## 2a. $MnNH_4$ -tutton salt

In a manganese ion five 3d electrons fill one half of the 3d shell and according to Hund's rule the ground state is an S state with  $S = 5/2$ .

Neglecting the deviations from axial symmetry and the terms due to the cubic portion of the crystalline field the Hamiltonian which describes the energy levels of a manganese ion of sublattice I in zero external field is given by:

$$(5.7) \quad \mathcal{H} = \mu_B^2 g^2 [\sum_i A_{1i} S_{1i} \langle S_{1i} \rangle + \sum_i A_{2i} S_{1i} \langle S_{2i} \rangle] + D(S_{11}^2 - 35/12)$$

$S_{11}$  is the spin component in the direction of the crystal field axis. The problem of finding the positions of the magnetic moments at  $T=0$  is reduced to minimizing the value of:

$$(5.8) \quad E = 1/2 \mu_B^2 g^2 [\sum_i A_{1i} \langle S_{1i} \rangle^2 + \sum_i A_{2i} \langle S_{1i} \rangle \langle S_{2i} \rangle] + D[\langle S_{11} \rangle^2 - 35/12]$$

According to our model (fig. 5.1)  $\langle S_{1x} \rangle = -\langle S_{2x} \rangle = \langle S \rangle \cos(\alpha - \theta_M)$ ,

$$\langle S_{1z} \rangle = \langle S_{2z} \rangle = \langle S \rangle \sin(\alpha - \theta_M) \text{ and } \langle S_{1y} \rangle = \langle S_{2y} \rangle = 0.$$

$\theta_M$  is the angle between the magnetic moments and their crystal field axis.

$$(5.9) \quad E = 1/2 \mu_B^2 g^2 [(A_{1x} - A_{2x}) \langle S \rangle^2 \cos^2(\alpha - \theta_M) + (A_{1z} + A_{2z}) \langle S \rangle^2 \sin^2(\alpha - \theta_M)] + D[\langle S \rangle^2 \cos^2 \theta_M - 35/12]$$

The value of  $\theta_M$  for which the energy has its minimum is determined by:

$$(5.10) \quad \sin(2\theta_M) / \sin 2(\alpha - \theta_M) = \mu_B^2 g^2 (A_{1x} - A_{2x} - A_{1z} - A_{2z}) / 2D = \mu_B^2 g^2 (G_{1x} - G_{2x} - G_{1z} - G_{2z} - 2K_{1z} + 8J_2) / 2D$$

Using  $\theta_M = 16^\circ$ , as observed experimentally, and the values for  $G_{1i}$  and  $G_{2i}$ , as given in table V, I, we obtain a relation between  $J_2$  and  $D'$ , where  $D' = D / (g\mu_B)^2$ :

$$(5.11) \quad J_2 - 0.25D' = -0.02 \times 10^{22} \text{ cm}^{-3}$$

Thus the orientation of the magnetic moments at zero temperature is independent of the exchange interaction between similar ions. This might be expected, since the expectation value of each magnetic moment is independent of its orientation and thus the interaction energy for parallelly ordered magnetic moments is always the same.

Other relations between  $J_2$  and  $D'$  may be obtained from the susceptibilities at zero temperature. These susceptibilities are due to a rotation of the magnetic moments over a small angle  $\varphi$  towards the direction of the measuring field  $h$ . Evaluating the energy in this magnetic field in a Taylor series the result neglecting terms of higher order than  $\varphi^2$  is:

$$(5.12) \quad E = E_0 + E_2 \varphi^2 - E_1 \varphi$$

$E_0$  is the energy in zero field, determined by (5.9) with  $\theta_M = 16^\circ$  and since this energy was a minimum the linear term in  $\varphi$  corresponds to the Zeeman energy. When the measuring field is applied in the  $K_2$  direction  $E_1$  and  $E_2$  are given by:

$$(5.13) \quad E_1 = g\mu_B \langle S \rangle h = \langle \mu \rangle h$$

$$(5.14) \quad E_2 = -\frac{1}{2}\langle\mu\rangle^2[(A_{1x}-A_{2x})\cos^2(\alpha-\theta_M^\circ) + (A_{1z}+A_{2z})\sin^2(\alpha-\theta_M^\circ) - A_{1y} - A_{2y} + 2D'\cos^2\theta_M^\circ]$$

with  $\theta_M^\circ = 16^\circ$  and  $\alpha = 32^\circ$ .

The angle  $\varphi_m$  which corresponds to the minimum energy equals

$$(5.15) \quad \varphi_m = E_1/2E_2$$

The  $K_2$  susceptibility equals

$$(5.16) \quad \chi_2 = N\langle\mu\rangle\varphi_m/h$$

Using the experimental value  $\chi_2 = 14 \times 10^{-8} R$  we obtain:

$$(5.17) \quad J_2 + 0.25 D' = -0.64 \times 10^{22} \text{ cm}^{-3}$$

The  $K_1$  and  $K_3$  susceptibilities can be derived in the same way. When the measuring field is applied in the direction of the  $K_3$  axis  $E_1$  and  $E_2$  are equal to:

$$(5.18) \quad E_1 = \langle\mu\rangle h \cos(\alpha - \theta_M^\circ)$$

$$(5.19) \quad E_2 = -\frac{1}{2}\langle\mu\rangle^2[(A_{1x}-A_{2x}-A_{1z}-A_{2z})\cos 2(\alpha - \theta_M^\circ) + 2D'\cos 2\theta_M^\circ]$$

The  $K_3$  susceptibility is given by:

$$(5.20) \quad \chi_3 = \langle\mu\rangle \cos(\alpha - \theta_M^\circ) E_1/2E_2 h$$

From the experimental value of  $\chi_3 = 18 \times 10^{-8} R$  we derive

$$(5.21) \quad J_2 + 0.25 D' = -0.57 \times 10^{22} \text{ cm}^{-3}$$

The susceptibility in the  $K_1$  direction corresponds to an asymmetrical twisting of the magnetic moments of the two sublattices.  $E_1$ ,  $E_2$  and  $\chi_1$  are in this case given by:

$$(5.22) \quad E_1 = \langle\mu\rangle h \sin(\alpha - \theta_M^\circ)$$

$$(5.23) \quad E_2 = -\frac{1}{2}\langle\mu\rangle^2[(A_{1x}-A_{1z})\cos 2(\alpha - \theta_M^\circ) - A_{2x} + A_{2z} + 2D'\cos 2\theta_M^\circ]$$

$$(5.24) \quad \chi_1 = \langle\mu\rangle \sin(\alpha - \theta_M^\circ) E_1/2E_2 h$$

The experimental values of the susceptibilities have been obtained by extrapolating the  $\chi$  versus  $T$  curves given in fig. 5.2 to zero temperature. The  $K_3$  susceptibility is the one measured in a magnetic field of 150 Oe which equals the susceptibility in a 1000 Hz alternating field. Since the extrapolated value of the  $K_1$  susceptibility is less accurate than the derived values of  $\chi_2$ ,  $\chi_3$  and  $\theta_M^\circ$  we shall use equations (5.11), (5.17) and (5.21) to determine  $J_2$  and  $D'$ . The values which give the best fit are:

$$J_2 = -0.31 \times 10^{22} \text{ cm}^{-3}$$

$$D' = -1.18 \times 10^{22} \text{ cm}^{-3} \rightarrow D/k = -0.029^\circ \text{ K}$$

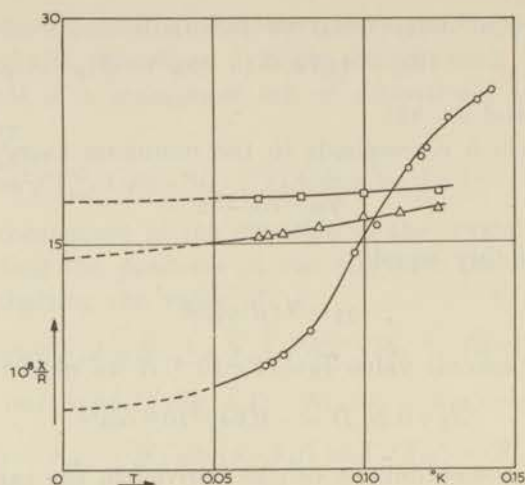


Fig. 5.2 MnNH<sub>4</sub>-tutton salt. The zero field susceptibilities as functions of temperature.

○ K<sub>1</sub> direction      △ K<sub>2</sub> direction      □ K<sub>3</sub> direction

This absolute value of  $D$  is 23 percent smaller than that measured in the diluted salt [2]. Assuming that the absolute values of  $D$  in concentrated and diluted MnNH<sub>4</sub>-tutton salt are equal the best fit is obtained with  $J_2 = -0.31 \times 10^{22} \text{ cm}^{-3}$ , which equals the value given above.

The values of  $\chi_1, \chi_2, \chi_3$  and  $\theta_M^\circ$  calculated with  $J_2 = -0.31 \times 10^{22} \text{ cm}^{-3}$  and  $D/k = -0.029^\circ \text{ K}$  and  $D/k = -0.038^\circ \text{ K}$ , respectively, are given in table V, II together with the experimental results.

The exchange interaction between similar ions does not occur in the foregoing considerations. We may, however, estimate a value of  $J_1$  from the deviations from Curie's law, measured at temperatures much higher than the transition temperature. Between 1 and 4° K a Curie-Weiss constant  $\theta = -0.003^\circ \text{ K}$  was measured for MnNH<sub>4</sub>-tutton salt powder by ERICSON *et al.* [7]. This small  $\theta$  corresponds to a small value of  $J_1 + 2J_2$ . By means of:

$$(5.25) \quad \theta = g^2 \mu_B^2 S(S+1)(2J_1 + 4J_2)/3k$$

we obtain  $J_1 + 2J_2 = -0.02 \times 10^{22} \text{ cm}^{-3}$  and thus  $J_1 = +0.60 \times 10^{22} \text{ cm}^{-3}$ . It may be seen that the exchange interaction is positive, favouring parallel orientation, for similar ions and negative, favouring antiparallel orientation, for dissimilar ions.

TABLE V, II

Observed and calculated values of  $10^8 \times \chi/R$  and  $\theta_M^\circ$  for MnNH<sub>4</sub>-tutton salt

K <sub>1</sub>	K <sub>2</sub>	K <sub>3</sub>	$\theta_M^\circ$	
$4 \pm 2$	$14 \pm 1$	$18 \pm 1$	16	experiment fig. 5.2
1.2	14.5	17.1	16	calc. $J_2 = -0.31 \times 10^{22} \text{ cm}^{-3}$ , $D/k = -0.029^\circ \text{ K}$
1.4	12.8	14.2	13	calc. $J_2 = -0.31 \times 10^{22} \text{ cm}^{-3}$ , $D/k = -0.038^\circ \text{ K}$

In the foregoing calculations the expectation value of the magnetic moment of a manganese ion was assumed to be independent of its angle with the crystal field axis. This is justified if the magnetic interaction may be replaced by a molecular magnetic field. When calculating the expectation value of a manganese spin in magnetic fields by means of the eigenfunctions corresponding to the lowest energy eigenvalue the result was equal to  $(5/2) g\mu_B$  within 1% for fields up to 1000 Oe and angles between magnetic field and crystal field axis of up to  $60^\circ$ .

For manganese ions the h.f.s. interaction is isotropic and at  $T = 0$  the nuclear moments are oriented parallel to the electron magnetic moments. Since the expectation value of the electron moments is independent of the direction of orientation, the h.f.s. interaction will have no influence on the direction of the electron spins and thus it has no influence on the susceptibilities at  $T = 0$ .

## 2b. Application to $\text{CoNH}_4$ -tutton salt

The ground state of a free cobalt ions is, according to Hund's rule,  $4F_{9/2}$ . This ground state is split by the cubic part of the electrical crystal field into a singlet and two triplet states. One of the triplet states has the lowest energy and is split by the joint action of the tetragonal component of the crystal field and the spin-orbit coupling into six Kramers' doublets, the separation being of the order of 400 degrees. At low temperatures only the lowest doublet is populated. It may be characterized by a fictitious spin  $S = 1/2$  with anisotropic  $g$  values. Since in  $\text{CoNH}_4$ -tutton salt there is axial symmetry with respect to the crystal field axis (see ref. 8) the energy levels in a magnetic field  $H$  can be derived from:

$$(5.26) \quad \mathcal{H} = g_{\parallel}\mu_B H_{\parallel} S_{\parallel} + g_{\perp}\mu_B H_{\perp} S_{\perp}$$

The indices  $\parallel$  and  $\perp$  correspond to parallel and perpendicular to the crystal field axis. The energy eigenvalues are:

$$(5.27) \quad E = \pm \frac{1}{2}\mu_B \sqrt{g_{\parallel}^2 H_{\parallel}^2 + g_{\perp}^2 H_{\perp}^2} = \frac{1}{2}g\mu_B H$$

The expectation value of the magnetic moment in the lowest state follows from the corresponding eigenfunctions.

$$(5.28) \quad \langle \mu \rangle = \mu_B \sqrt{(g_{\parallel}^4 \cos^2 \theta_H + g_{\perp}^4 \sin^2 \theta_H)} / 2g$$

$$(5.29) \quad \text{tg } \theta_M = \langle \mu_{\perp} \rangle / \langle \mu_{\parallel} \rangle = g_{\perp}^2 \text{tg } \theta_H / g_{\parallel}^2$$

where  $\theta_H$  is the angle between crystal field axis and magnetic field. From (5.28) and (5.29) it is clear that the magnitude of the magnetic moment of a cobalt ion depends on its angle with the crystal field axis. This makes the exchange interaction given by (5.1) anisotropic.

One may remark that is not justified to use the total magnetic moment  $\mu_i$  in equation (5.1) since both orbital angular momentum and spin moments contribute to the fictitious spin  $S = 1/2$  of a cobalt ion. Semi-empirically ABRAGRAM and PRYCE [9] have found that for Co ions in  $\text{CoNH}_4$ -tutton salt the contribution of the orbital angular momentum is described by  $g_{\parallel}^L = 1.8$  and  $g_{\perp}^L = 0.78$  whereas the contribution of the

electron spins is given by  $g_{\parallel}^S = 4.7$  and  $g_{\perp}^S = 2.5$ . Since the ratio  $g_{\perp}^S/g_{\parallel}^S$  differs only slightly from the ratio of the total  $g$  values,  $g_{\perp}/g_{\parallel}$ , the anisotropy of the intrinsic spin part of the magnetic moment practically equals the anisotropy of the total magnetic moment and thus we use formula (5.1) multiplying  $J_{ik}$  by  $(g^S/g)^2$  which equals about 0.59.

For the range of  $\theta_M$  values in which we are interested in the dependence of  $\langle\mu\rangle$  on  $\theta_M$  for the lowest energy state is described by the following approximate formula, which is derived from (5.28) and (5.29) using  $g_{\parallel} = 6.45$  and  $g_{\perp} = 3.06$ . The formula agrees within 0.2 % with (5.28) and (5.29) for values of  $\theta_M$  up to  $13^\circ$ .

$$(5.30) \quad \langle\mu\rangle = \frac{1}{2}g_{\parallel}\mu_B(1 + P\theta_M^2)$$

with  $P = -1.5$ .

The problem of finding the position of the magnetic moments at zero temperature is reduced to finding the minimum of the energy:

$$(5.31) \quad E = \frac{1}{2}[\sum_i A_{1i}\langle\mu_{1i}\rangle^2 + \sum_i A_{2i}\langle\mu_{1i}\rangle\langle\mu_{2i}\rangle]$$

or

$$(5.32) \quad E = \frac{1}{8}g_{\parallel}^2\mu_B^2(1 + P\theta_M^2)^2[(A_{1x} - A_{2x})\cos^2(\alpha - \theta_M) + (A_{1z} + A_{2z})\sin^2(\alpha - \theta_M)]$$

The constants  $A_{1i}$  and  $A_{2i}$  depend on the two exchange constants  $J_1$  and  $J_2$ . In the same way as described for  $\text{MnNH}_4$ -tutton salt three relations between  $J_1$  and  $J_2$  are obtained from the extrapolated values to zero temperature of  $\chi_2$ ,  $\chi_3$ , and  $\theta_M^\circ$ . The best fit is obtained with:

$$J_2 = -0.80 \times 10^{22} \text{ cm}^{-3}$$

$$J_1 = +0.43 \times 10^{22} \text{ cm}^{-3}$$

The exchange interaction is positive between similar and negative between dissimilar ions, as was derived for  $\text{MnNH}_4$ -tutton salt. The corresponding values of  $\theta_M^\circ$  and the three susceptibilities are compared with the observed data in table V, III.

TABLE V, III

Observed and calculated values of  $10^8 \times \chi/R$  and  $\theta_M^\circ$  for  $\text{CoNH}_4$ -tutton salt at zero temperature

$K_1$	$K_2$	$K_3$	$\theta_M^\circ$	
$2 \pm 2$	$7 \pm 1$	$9 \pm 1$	10	experiment
0.5	7.0	9.6	10	calc. $\left\{ \begin{array}{l} J_1 = +0.43 \times 10^{22} \text{ cm}^{-3} \\ J_2 = -0.80 \times 10^{22} \text{ cm}^{-3} \end{array} \right.$

NAKAMURA and URYU [6] determined the exchange parameters from the Curie-Weiss constants measured by GARRETT [10] in the directions of the three magnetic axes between 0.2 and  $1^\circ$  K. In our notation their results are  $J_2 \approx -0.8 \times 10^{22} \text{ cm}^{-3}$  and  $J_1 \approx +0.9 \times 10^{22} \text{ cm}^{-3}$ .

In cobalt ammonium tutton salt the h.f.s. interaction may influence  $\theta_M$  and the susceptibilities. One expects a strong anisotropy of the h.f.s. interaction from resonance measurements in the diluted salts, which results in a strong coupling of the nuclear spins to the crystal field axis. In this case the h.f.s. interaction may be taken into account formally as a magnetic field with the direction of the crystal field axis and equal to  $AI/g_{II}\mu_B$  at zero temperature. The best fit is obtained with

$$J_2 = -0.8 \times 10^{22} \text{ cm}^{-3} \text{ and } J_1 \approx 0,$$

the corresponding calculated values of  $\chi$  and  $\theta_M^\circ$  being only slightly different from the values given in the table. However, experiments with radioactive nuclei reported in the next chapter have shown that the coupling of the Co nuclei to the crystal field axis is much weaker than expected from the anisotropy of the h.f.s. constants as measured in the diluted salt. For this reason we neglected the influence of the h.f.s. interaction in the foregoing.

From the numerical values of the exchange constants we may estimate a value for the transition temperature. In order to do this we describe the interactions by an effective magnetic field, a so-called molecular field. This description was introduced by Weiss for ferromagnetic materials and for antiferromagnetism by Néel. For the latter case the model has been extended by several physicists (Néel, Van Vleck, Anderson, Gorter).

A simple situation occurs if the crystal can be divided into two sublattices, magnetized in opposite directions. The field acting on magnetic ions belonging to sublattice I may consist of two components, one component parallel and proportional to the magnetization of sublattice I and another part parallel and proportional to the magnetization of sublattice II.

$$(5.33) \quad H_{\text{mol}} = q_1 \mathbf{M}_1 - q_2 \mathbf{M}_2$$

According to Néel the corresponding transition temperature equals:

$$(5.34) \quad T_N = (q_2 + q_1)C/2$$

where  $C$  is the Curie constant.

In our case the situation is somewhat more complicated. The magnetizations of the two sublattices are not antiparallel and since the dipolar interactions are very anisotropic the two components of the molecular field must not be expected to have the directions of the two magnetizations. However, we may use formulae very similar to (5.33) and (5.34) if we consider instead of  $H_{\text{mol}}$  itself, the projection  $H'$  of the molecular field on the magnetization of sublattice I. If we define  $q_1'$  and  $q_2'$  by:

$$(5.35) \quad H' = q_1' |M_1| + q_2' |M_2|$$

the result for  $T_N$  is:

$$(5.36) \quad T_N = (q_2' + q_1')C/2$$

We assume that the angle between the two sublattices is equal just below the Néel temperature and at zero temperature. This may not be strictly correct but a small difference between the two angles has only minor influence on the following calculations.

$q_1'$  and  $q_2'$  are given by, compare (5.7), (5.9) and (5.35):

$$(5.37) \quad Nq_1' = -A_{1x} \cos^2(\alpha - \theta_M^\circ) - A_{1z} \sin^2(\alpha - \theta_M^\circ) - D' \cos^2 \theta_M^\circ$$

$$(5.38) \quad Nq_2' = +A_{2x} \cos^2(\alpha - \theta_M^\circ) - A_{2z} \sin^2(\alpha - \theta_M^\circ)$$

with  $D' = D/g^2\mu_B^2$  and  $D' = 0$  for  $\text{CoNH}_4$ -tutton salt.

Using the values of  $\theta_M^\circ$ ,  $J_1$ ,  $J_2$ ,  $G_{1t}$  and  $G_{2t}$  given before the result for  $\text{CoNH}_4$ -tutton salt is  $T_N = 0.074^\circ \text{K}$ , while the experimental value given by GARRETT [10] is  $T_N = 0.084^\circ \text{K}$ . If we use  $D/k = 0.038^\circ \text{K}$  as found in the diluted  $\text{MnNH}_4$ -tutton salt we obtain  $T_N = 0.153^\circ \text{K}$ , with the 23 % smaller value of  $D$  introduced in this section we obtain  $T_N = 0.135^\circ \text{K}$  for  $\text{MnNH}_4$ -tutton salt (experimental value  $T_N = 0.14^\circ \text{K}$ ).

An evaluation for the critical field may be made on the basis of the dependence of the magnetization on a magnetic field in the  $K_1$  direction at the lowest temperature (chapter IV). At zero temperature the magnetic field in which the antiferromagnetic state goes over into the paramagnetic state is suggested to be 400 Oe in  $\text{CoNH}_4$ -tutton salt and 540 Oe in  $\text{MnNH}_4$ -tutton salt. When magnetizing in the  $K_1$  direction the interaction between similar ions remains practically the same and it may be expected that the derived values for the critical field roughly correspond to the interactions between dissimilar ions, i.e. the values of  $q_2'|M_2|$  must be roughly equal to the values of the critical field in the  $K_1$  direction. From formula (5.38) we obtain  $q_2'|M_2|$  is 510 Oe and 670 Oe in  $\text{CoNH}_4$ - and  $\text{MnNH}_4$ -tutton salt, respectively, using again the values of  $J_2$  and  $\theta_M^\circ$  as derived in this section.

The contributions of the magnetic exchange interactions to the specific heat at temperatures much higher than the transition temperature may be calculated from the estimated values of  $J_1$  and  $J_2$ . A value of the exchange specific heat also may be obtained from the experimental values of the total specific heat after subtraction of h.f.s., stark and dipolar contributions. For  $\text{CoNH}_4$ -tutton salt the results are:

$$(CT^2/R)_{\text{tot}} = 43 \times 10^{-4} \text{ deg}^2 \text{ ref. [10] and [11]}$$

$$(CT^2/R)_{\text{h.f.s.}} = 17.4 \times 10^{-4} \text{ deg}^2 \text{ ref. [11]}$$

$$(CT^2/R)_{\text{dip}} = 17.8 \times 10^{-4} \text{ deg}^2 \text{ ref. [6]}$$

$$\text{Left for } (CT^2/R)_{\text{ex}} = 7.8 \times 10^{-4} \text{ deg}^2$$

Nakamura and Uryu calculated the specific heat corresponding to the exchange interactions and obtained  $(CT^2/R)_{\text{ex}} = 12.4 \times 10^{-4} \text{ deg}^2$ . With our

value of the exchange constant  $J_1$  the calculated value of  $(CT^2/R)_{\text{ex}}$  will be about 30 % smaller, and thus of the order of  $9 \times 10^{-4} \text{ deg}^2$ .

For  $\text{MnNH}_4$ -tutton salt the results are:

$$(CT^2/R)_{\text{tot}} = 33 \times 10^{-3} \text{ deg}^2 \text{ (average value, see ref. [4])}$$

$$(CT^2/R)_{\text{h.f.s. + stark}} = 15.4 \times 10^{-3} \text{ deg}^2 \text{ (diluted salt, see ref. [2])}$$

$$(CT^2/R)_{\text{dip}} = 11 \times 10^{-3} \text{ deg}^2 \text{ ref. [4]}$$

$$\text{Left for } (CT^2/R)_{\text{ex}} = 6.6 \times 10^{-3} \text{ deg}^2$$

Using a 23 % smaller value for  $D$ , as we obtained in this section, the exchange part of the specific heat  $(CT^2/R)_{\text{ex}} = 9.1 \times 10^{-3} \text{ deg}^2$ .

A calculation, using formula (5.40) and the estimated values for  $J_1$  and  $J_2$ , gives  $(CT^2/R)_{\text{ex}} = 8.8 \times 10^{-3} \text{ deg}^2$  in fair agreement with the values given above.

### 3. The magnetic structure of $\text{CuNH}_4$ - and $\text{CuK}$ -tutton salt

The free copper ion is in a  ${}^2D_{5/2}$  state. This state is split by the cubic portion of the crystal field into a doublet and a triplet state. Under the joint action of spin-orbit coupling and the tetragonal component of the crystal field a further splitting into five Kramers doublets occurs. Only the lowest one of these is populated. The doublet may be characterized by a fictitious spin  $S = 1/2$  with anisotropic  $g$  values (table IV, I). According to the analysis by ABRAGAM and PRYCE [12] the intrinsic spin part of the magnetic moments has an isotropic  $g$  value 2, the deviation of the total  $g$  value from 2 being due to the orbital part of the copper magnetic moment.

We shall estimate the exchange constants  $J_1$  and  $J_2$  from the deviations from Curie's law and the specific heat measured at relatively high temperatures. Taking the exchange interaction as isotropic we have for a powder the formulae:

$$(5.39) \quad \theta = +4 S(S+1) \mu_B^2 (2 J_1 + 4 J_2) / 3k$$

$$(5.40) \quad (CT^2/R)_{\text{ex}} = 16 S^2(S+1)^2 \mu_B^4 (2 J_1^2 + 4 J_2^2) / 6k^2$$

The specific heat constant  $(CT^2/R)_{\text{tot}}$  contains a nuclear, a dipolar and an exchange part and has been analysed by BENZIE and COOKE [13]. The nuclear and dipolar parts are the same for  $\text{CuNH}_4$ - and  $\text{CuK}$ -tutton salt and given by  $CT^2/R = 1.1 \times 10^{-4}$  and  $1.3 \times 10^{-4} \text{ deg}^2$ , respectively. The exchange contribution equals  $(CT^2/R)_{\text{ex}} = 6.3 \times 10^{-4} \text{ deg}^2$  for  $\text{CuNH}_4$  and  $3.6 \times 10^{-4} \text{ deg}^2$  for  $\text{CuK}$ -tutton salt.

The observed values of  $\theta$ , which is defined by  $\chi = C/(T - \theta)$ , are  $\theta = 0.010^\circ \text{ K}$  for  $\text{CuNH}_4$ -tutton salt (ref. 14) and about  $0.030^\circ \text{ K}$  for  $\text{CuK}$ -tutton salt (see ref. 14-18). From formulae (5.39) and (5.40) we obtain a quadratic equation for the exchange constants. The results are

for  $\text{CuNH}_4$ -tutton salt:

$$\begin{array}{ll} J_2 = +1.22 \times 10^{22} \text{ cm}^{-3} & J_2 = -0.67 \times 10^{22} \text{ cm}^{-3} \\ J_1 = -1.62 \times 10^{22} \text{ cm}^{-3} & \text{or} \quad J_1 = +2.16 \times 10^{22} \text{ cm}^{-3} \end{array}$$

and for  $\text{CuK}$ -tutton salt:

$$\begin{array}{ll} J_2 = +1.26 \times 10^{22} \text{ cm}^{-3} & J_2 = +0.36 \times 10^{22} \text{ cm}^{-3} \\ J_1 = -0.06 \times 10^{22} \text{ cm}^{-3} & \text{or} \quad J_1 = +1.70 \times 10^{22} \text{ cm}^{-3} \end{array}$$

### 3a. $\text{CuNH}_4$ -tutton salt

The experimental results, given in the foregoing chapter have shown that the magnetic behaviour of  $\text{CuNH}_4$ -tutton salt is quite different from the behaviour of  $\text{CoNH}_4$ - and  $\text{MnNH}_4$ -tutton salt. In both the  $K_1$  and  $K_3$  directions the susceptibility has a maximum as a function of the entropy and as a function of an external magnetic field, which suggests the occurrence of an antiferromagnetic ordering. No relaxation effects are present. The second possibility for  $J_1$  and  $J_2$  predicts similarity between  $\text{Cu}$ ,  $\text{Co}$  and  $\text{MnNH}_4$ -tutton salt and we therefore consider the first possibility, with a positive interaction between dissimilar ions and a negative interaction between similar ions as the right one.

As mentioned before, the nearest neighbours of a particular ion are two ions of the similar type in the direction of the  $c$  axis and four ions of the dissimilar type lying in an  $ab$  plane. Using the first possibility for  $J_1$  and  $J_2$  the crystal will contain sheets parallel to the  $ab$  plane where the spins are ordered by a ferromagnetic interaction while neighbouring sheets will be magnetized antiparallel. The corresponding picture is shown in figure 5.3. The angle between the magnetic moments of ions with

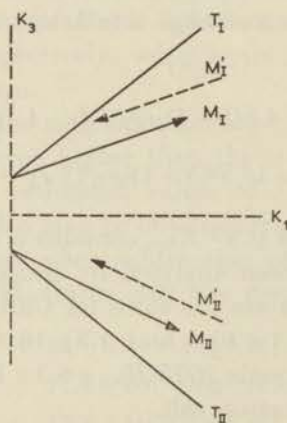


Fig. 5.3 The magnetic sublattices in  $\text{CuNH}_4$ -tutton salt below its transition temperature.

M Magnetization of the copper ions in the  $ab$  plane through  $[0, 0, 0]$  and  $[\frac{1}{2}, \frac{1}{2}, 0]$

M' Magnetization of the copper ions in the  $ab$  plane through  $[0, 0, 1]$  and  $[\frac{1}{2}, \frac{1}{2}, 1]$

different crystal field axes will be determined by an anisotropy energy which may occur, for instance, from dipolar and h.f.s. interactions. As a result we apparently have two systems in which the magnetic moments are antiparallely ordered and of which the alignment axes lie between the  $K_1$  and  $K_3$  directions. Both the  $K_1$  and  $K_3$  axes are neither fully parallel nor perpendicular to the preferential axes of the magnetic ordering. The susceptibility maxima are more pronounced in the  $K_1$  direction (fig. 4.15 and fig. 4.16) which indicates that the angle between  $K_1$  axis and preferential axes is rather small.

### 3b. *CuK-tutton salt*

The magnetic behaviour of CuK-tutton salt is apparently ferromagnetic. In small fields  $\chi_2$  is larger than  $\chi_1$  and  $\chi_3$  and the volume susceptibility in the  $K_2$  direction differs by only 5 percent from  $3/4\pi$  if reduced to a spherical sample.

We may describe the magnetic behaviour using both possibilities for the constants  $J_1$  and  $J_2$ . The first possibility, a strong positive interaction between dissimilar ions and a very weak negative interaction between similar ions predicts a magnetic structure like that found for  $\text{CuNH}_4$ -tutton salt. The  $K_2$  susceptibility will be larger than  $\chi_1$  and  $\chi_3$  and since the negative interaction is so small,  $\chi_2$  may be very large. The observed values of  $\chi_1$  and  $\chi_3$  both show a weak maximum as a function of entropy, which may be expected from the weak negative interaction.

If the second possibility for  $J_1$  and  $J_2$  applies with positive interaction only, the largest susceptibility must be expected in the  $K_2$  direction in agreement with the experimental data. As may be seen from the constants  $G_{1t}$  and  $G_{2t}$  in table VI, I, the dipolar interaction favours the  $K_2$  ( $y$ ) direction if a ferromagnetic arrangement exists. In table VI, I the  $y$  axis corresponds to  $\psi = 40^\circ$  and since in CuK-tutton salt the  $K_2$  axis has  $\psi = 15^\circ$ , the  $K_2$  axis will be preferred above the  $K_1K_3$  plane.

However, we cannot explain the remarkable minimum in the specific heat occurring at an entropy of about  $(1/2)R \ln 2$ . The minimum suggests that a magnetic ordering takes place which needs only half the entropy. This specific heat minimum was found earlier for  $\text{CuSO}_4 \cdot 5\text{H}_2\text{O}$ , which has a similar crystal structure. In both salts two ions are present in the unit cell, each having a crystal field of tetragonal symmetry, the angle between the two crystal field axes being  $90^\circ$  and  $84^\circ$  in  $\text{CuSO}_4 \cdot 5\text{H}_2\text{O}$  and CuK-tutton salt, respectively. GEBALLE and GIAUQUE [19] suggested that in copper sulphate pentahydrate the magnetic interaction exists mainly between similar ions. They suggest that the two systems of magnetic ions have somewhat different environments, such that the magnetic interactions cause different level splittings. The splittings in one system must be at least five times larger than the splittings in the other system in order to explain the observed specific heat.

A minimum in the specific heat at  $S \approx (1/2)R \ln 2$  also has been found

in a solution of copper chloride in propanol (chapter II). In this case the minimum could be explained by assuming an ordering of the electron magnetic moments in pairs, each magnetic ion having only one nearest neighbour. It seems attractive to explain the specific heat minimum in CuK-tutton salt on this basis but since each copper ion has two equivalent neighbours of the similar type and four of the other type, there seems to be no reason for an ordering in pairs.

#### 4. Conclusions

The occurrence of ferromagnetic and antiferromagnetic phenomena in one salt has been reported several times. Examples are  $\text{FeCl}_2$ ,  $\text{FeCO}_3$ ,  $\text{Fe}_2\text{O}_3$ ,  $\text{MnCO}_3$ ,  $\text{NiF}_2$ ,  $\text{CoCO}_3$  and  $\text{CrK}(\text{SO}_4)_2 \cdot 12\text{H}_2\text{O}$  (WOLTJER *e.a.* [20], [21], BECQUEREL *e.a.* [22], NEEL [23], BIZETTE *e.a.* [24], MATARRESE *e.a.* [25], BOROVIK-ROMANOV *e.a.* [26] and BEUN *e.a.* [27]). The magnetic phenomena occurring in these salts are considered as a weak ferromagnetism present in an essentially antiferromagnetic salt, the ferromagnetic moments being small. The moments vary from 0.02 % of the saturation moment for  $\text{Fe}_2\text{O}_3$  to 3 % for  $\text{NiF}_2$ . In most cases the authors explain their results assuming ferromagnetic walls between antiferromagnetic domains. Borovik-Romanov *e.a.* explained the observed anomalies in  $\text{MnCO}_3$  and  $\text{CoCO}_3$  by postulating that these carbonates go over into an antiferromagnetic state in which the moments of the sublattices do not fully compensate but make an angle of a few minutes with each other. It will be clear that the present model used for  $\text{CoNH}_4$ - and  $\text{MnNH}_4$ -tutton salt in fact corresponds to the basic assumption of Borovik-Romanov. Since in the present case the anisotropy energy is of the same order of magnitude as the energy of the magnetic interactions, the angle between the sublattices is not of the order of minutes but  $32^\circ$  in  $\text{MnNH}_4$ - and  $48^\circ$  in  $\text{CoNH}_4$ -tutton salt.

A magnetic behaviour as found for  $\text{CoNH}_4$ - and  $\text{MnNH}_4$ -tutton salt may occur quite generally in crystals which contain two inequivalent lattice sites for the magnetic ions, if these ions have different preferential axes for their magnetic moments and if a negative interaction between dissimilar ions exists. In fact we have found that two other cobalt tutton salts,  $\text{CoK}$ - and  $\text{CoCs}$ -tutton salt (unpublished) also show this combined antiferromagnetic and ferromagnetic behaviour.

The difference between the copper tutton salts on one hand and cobalt and manganese ammonium tutton salt on the other may be due to the fact that the exchange interaction between dissimilar ions is positive in the copper salts.

We may say that the magnetic phenomena in  $\text{MnNH}_4$ ,  $\text{CoNH}_4$  and  $\text{CuNH}_4$ -tutton salt are reasonably described by a molecular field model based on the assumption that the anisotropy of the exchange interaction is only due to the anisotropy of the intrinsic spin part of the magnetic moments. We can give no satisfactory explanation for the results obtained

with CuK-tutton salt, which may suggest that a description with isotropic exchange interaction up to the second neighbours is not justified in this salt.

The values of the exchange constants as proposed in this chapter are collected in table V, IV.

TABLE V, IV

The exchange parameters in the magnetic tutton salts investigated

$J_1$  and  $J_2$  give the interactions between similar and dissimilar ions, respectively. The exchange interaction is defined by

$$\mathcal{H}_{ex} = - \sum_{i>k} J_{ik} \mu_i^S \mu_k^S$$

where  $\mu_i^S$  is the intrinsic spin part of the magnetic moment of an ion  $i$ . Each magnetic ion has four magnetic neighbours with exchange parameter  $J_2$  and two neighbours with exchange parameter  $J_1$ .

Tutton salt	$J_1$	$J_2$
MnNH <sub>4</sub>	+ 0.60	- 0.31
CoNH <sub>4</sub>	+ 0.43	- 0.80
CuNH <sub>4</sub>	-1.62	+ 1.22
CuK	{ - 0.06 + 1.70	{ + 1.26 + 0.36

## REFERENCES

1. ABRAGAM, A. and M. H. L. PRYCE, Proc. Roy. Soc. A 205, 135 (1951).
2. BLEANEY, B. and D. J. E. INGRAM, Proc. Roy. Soc. A 205, 336 (1951).
3. URYU, N., Preprint (1960).
4. KLERK, D. DE, Handbuch der Physik 15, 38 (1956).
5. HOFFMANN, W., Z. Kristallogr. 78, 279 (1931).
6. NAKAMURA, N. and N. URYU, J. Phys. Soc. Japan 11, 760 (1956).
7. ERICSON, R. A. and L. D. ROBERTS, Phys. Rev. 93, 957 (1954).
8. BLEANEY, B. and D. J. E. INGRAM, Proc. Roy. Soc. A 208, 143 (1951).
9. ABRAGAM, A. and M. H. L. PRYCE, Proc. Roy. Soc. A 206, 173 (1951).
10. GARRETT, C. G. B., Proc. Roy. Soc. A 206, 242 (1951).
11. BROEK, J. VAN DEN, L. C. VAN DER MAREL and C. J. GORTER, Commun. Kamerlingh Onnes Lab., Leiden 314c; Physica 25, 371 (1959).
12. ABRAGAM, A. and M. H. L. PRYCE, Proc. Roy. Soc. A 206, 163 (1951).
13. BENZIE, R. J. and A. H. COOKE, Nature 164, 837 (1949).
14. COOKE, A. H., H. MEYER and W. P. WOLF, Proc. Roy. Soc. A 233, 536 (1956).
15. KLERK, D. DE, Commun. 270c; Physica 12, 513 (1946).
16. GARRETT, C. G. B., Proc. Roy. Soc. A 203, 375 (1950).
17. BENZIE, R. J. and A. H. COOKE, Proc. Phys. Soc. (London) A 63, 201 (1950).
18. BOTS, G. J. C. and M. J. F. J. COREMANS, Commun. 320b; Physica 26, 342 (1960).
19. GEBALLE, T. H. and W. F. GIAUQUE, J. Amer. Chem. Soc. 74, 3513 (1952).
20. WOLTJER, H. R., Commun. 173b; Proc. Kon. Acad. Amsterdam, 28, 536 (1925).
21. WOLTJER, H. R. and E. C. WIERSMA, Commun. 201a; Proc. Kon. Acad. Amsterdam, 32, 735 ((1929).

22. BECQUEREL, J. and J. VAN DEN HANDEL, Commun. 316a; J. Phys. Radium 10, 10 (1939).
23. NÉEL, L. and R. PAUTHENET. R., Comt. Rend. 234, 2172 (1952).
24. BIZETTE, H. and D. TSAI, Comt. Rend. 241, 369 (1955).
25. MATARRESE, L. M. and J. W. STOUT, Phys. Rev. 94, 1792 (1954).
26. BOROVIK-ROMANOV, A. S. and M. P. ORLOVA, J.E.T.P. 4, 531 (1957).
27. BEUN, J. A., A. R. MIEDEMA and M. J. STEENLAND, Commun. 305d; Physica 23, 1 (1957).

SOME EXPERIMENTS ON NUCLEAR ORIENTATION IN  
MAGNETICALLY ORDERED TUTTON SALTS

It has been suggested by DAUNT [1] and GORTER [2] that nuclear orientation can be obtained in antiferromagnetically ordered single crystals at low temperatures. Below a transition temperature the electronic moments of the magnetic ions will be aligned along certain preferred directions in the crystals, and this may lead to nuclear orientation by means of magnetic hyperfine structure (h.f.s.) coupling. The first results in producing nuclear alignment by means of antiferromagnetism were reported by DANIELS and LE BLANC [3] who observed an anisotropy in the  $\gamma$ -radiation of  $^{54}\text{Mn}$  nuclei included in  $\text{MnCl}_2 \cdot 4\text{H}_2\text{O}$  and  $\text{MnBr}_2 \cdot 4\text{H}_2\text{O}$  cooled to about  $0.1^\circ \text{K}$  by means of heat conduction. Nuclear alignment in a ferromagnetic material was first achieved by KHUTSISHVILI [4] and GRACE *et al.* [5] who aligned  $^{60}\text{Co}$  nuclei in cobalt metal.

In view of these successful experiments it seemed remarkable that an earlier Leiden experiment by POPPEMA *et al.* [6, 7] on the  $\gamma$ -anisotropy of  $^{60}\text{Co}$  in undiluted  $\text{CoNH}_4$ -tutton salt had given no positive results. Therefore the present investigation on the orientation of  $^{60}\text{Co}$  and  $^{54}\text{Mn}$  in  $\text{CoNH}_4$ - and  $\text{MnNH}_4$ -tutton salt was started together with the magnetic investigations reported in the foregoing.

In the meantime a  $\gamma$ -ray anisotropy  $\epsilon$ , defined by  $[W(K_2) - W(K_1)]/W(K_2)$  (where  $W$  is the  $\gamma$ -intensity), of 0.055 has been reported for  $^{60}\text{Co}$  in  $\text{CoNH}_4$ -tutton salt [8] with a sample cooled to about  $0.04^\circ \text{K}$  by means of an indirect cooling method.

## EXPERIMENTS

1a.  $^{60}\text{Co}$  included in  $\text{CoNH}_4$ -tutton salt

The temperature which can be reached in this salt by means of adiabatic demagnetization is  $0.05^\circ \text{K}$ . The  $\gamma$ -ray anisotropy is small at this temperature and a method for indirect cooling was applied to reach a lower temperature. The apparatus used is described in chapter III (fig. 3.1). The weights of the  $\text{CoNH}_4$ -tutton salt crystals were 0.5 g and 2 g in two different experiments, the weight of the cooling substance being 80 g.

In the decay of  $^{60}\text{Co}$  two gamma rays occur in cascade (fig. 6.1) which are known to have the same directional distribution for oriented nuclei. The sum of the intensities of these gamma rays has been observed in the  $K_2$  and  $K_3$  directions and under a small angle with the  $K_1$  axis. The  $K_1$  axis was placed vertically and the susceptibility in this direction could be measured simultaneously with the counting.

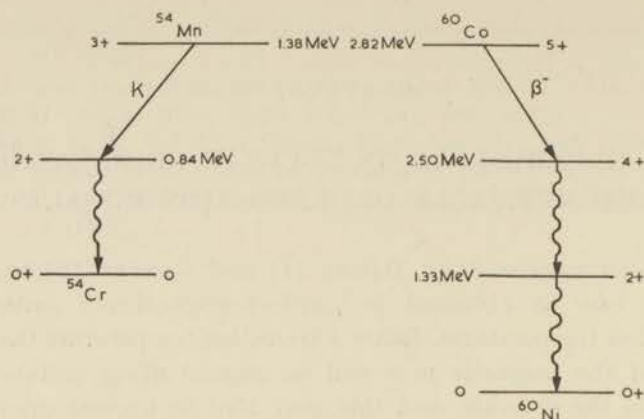


Fig. 6.1 Decay schemes of  $^{60}\text{Co}$  and  $^{54}\text{Mn}$ .

The results of 15 runs under experimentally identical conditions are combined and shown in fig. 6.2. During the first 15 minutes after demagnetization the  $\gamma$ -anisotropy increases while after 15 min. the sample warms up and the anisotropy decreases. The largest value of  $\varepsilon$  observed was 0.085 and was obtained with the 0.5 g crystal.

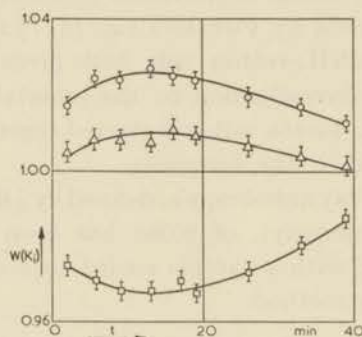


Fig. 6.2  $^{60}\text{Co}$  in  $\text{CoNH}_4$ -tutton salt. The  $\gamma$ -intensities measured in the directions of the three magnetic axes as functions of time. Indirect cooling is applied.

□  $K_1$  axis

○  $K_2$  axis

△  $K_3$  axis

In order to find the relation between the  $\gamma$ -intensities and temperature at higher temperatures a 5 g  $\text{CoNH}_4$  single crystal was demagnetized directly. The  $\gamma$ -anisotropy was not noticeably dependent on time, the warming up time being very long. The maximum value of  $\varepsilon$  observed was 0.045. In the latter experiments the temperatures could be derived from the conditions before demagnetization, using the known  $g$  values and the  $T$ - $S$  relation given by GARRETT [9].

#### 1b. $^{60}\text{Co}$ in $\text{MnNH}_4$ -tutton salt

Using the apparatus of fig. 3.1 a 0.5 g crystal of  $\text{MnNH}_4$ -tutton salt containing  $5\mu\text{C}$  of  $^{60}\text{Co}$  has been cooled. The average of 13 runs is given

in fig. 6.3. The three counters were arranged in the same way as they were in the foregoing experiment. The temperature reached its minimum after 30 minutes.

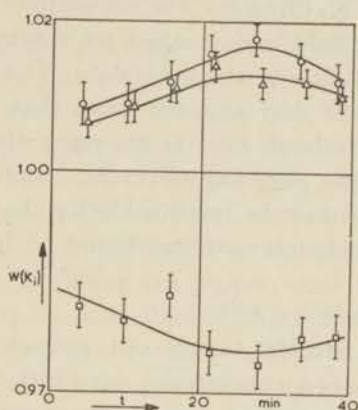


Fig. 6.3  $^{60}\text{Co}$  in  $\text{MnNH}_4$ -tutton salt. The  $\gamma$ -intensity as a function of time. Indirect cooling is applied.

□  $K_1$  axis                      ○  $K_2$  axis                      △  $K_3$  axis

1c.  $^{54}\text{Mn}$  in  $\text{CoNH}_4$ -tutton salt

A single crystal of cobalt ammonium tutton salt was grown containing  $4\mu\text{C}$  of  $^{54}\text{Mn}$ . The decay scheme of  $^{54}\text{Mn}$  is shown in fig. 6.1. By demagnetizing the crystal from various magnetic fields the relation between the magnetization entropy of the cobalt ions and the  $\gamma$ -intensities measured in the directions of the three magnetic axes, was obtained (fig. 6.4).

The  $\gamma$ -ray intensity in the  $K_2$  direction has been studied in magnetic

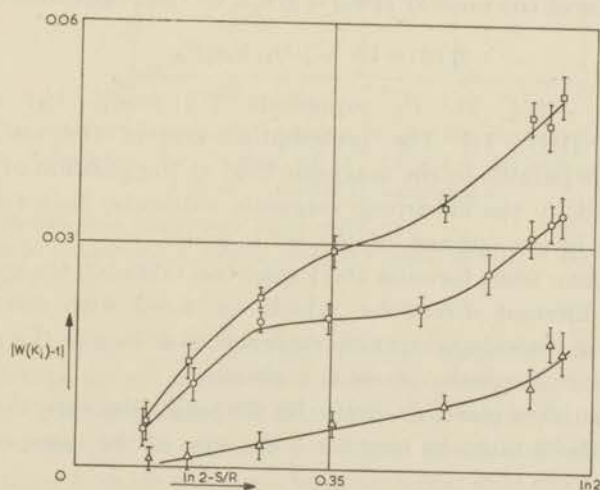


Fig. 6.4  $^{54}\text{Mn}$  in  $\text{CoNH}_4$ -tutton salt. The relation between the  $\gamma$ -intensity of  $^{54}\text{Mn}$  nuclei and the magnetization entropy of the cobalt ions.

□  $K_1$  axis                      ○  $K_2$  axis                      △  $K_3$  axis

fields of up to 500 Oe. A magnetic field in the  $K_3$  direction had little influence on the  $\gamma$ -intensity, the decrease of the effect at increasing field strength apparently being due to a temperature rise. When the magnetic field was applied in the  $K_1$  direction, the normalized  $K_2$  intensity increased slowly with increasing field and reached its maximum value of 1.06 in a field of 400 Oe. According to magnetic data of Garrett the temperature of the  $\text{CoNH}_4$ -tutton salt decreases not more than 20 % and reaches its minimum in a field of about 350 Oe at which the transition from the antiferromagnetic to the paramagnetic state takes place. The decrease of temperature alone cannot be responsible for the increase of  $W(K_2) - 1$  (see next section), which increase was found to be 90 %.

#### 1d. $^{54}\text{Mn}$ in $\text{MnNH}_4$ -tutton salt

A single crystal of  $\text{MnNH}_4$ -tutton salt containing  $7\mu\text{C}$  of  $^{54}\text{Mn}$  was investigated. The observed anisotropies were rather small ( $\epsilon < 0.039$ ) and for that reason the intensities were not measured as functions of temperature. At the temperature reached after demagnetization from  $21 \times 10^3$  Oe (0.07° K) the three values of  $W(K_i) - 1$ , which will be called the effects in the following, were  $-2.40 \pm 0.18$  %,  $+1.28 \pm 0.07$  % and  $+1.22 \pm 0.13$  % for the  $K_1$ ,  $K_2$  and  $K_3$  counters, respectively. With the help of indirect cooling the magnitudes of the effects were doubled, the ratio of the three values remaining the same.

#### 2. Some theoretical aspects

The  $\gamma$ -radiations emitted by both  $^{60}\text{Co}$  and  $^{54}\text{Mn}$  nuclei are quadrupole radiations with  $\Delta I = -2$ . Since in our experiments the  $\gamma$ -anisotropy was always small the  $\gamma$ -effect in a direction which makes an angle  $\beta$  with the preferential axis of the nuclear spins is given by (see, for instance, ref. 10):

$$(6.1) \quad W(\beta) - 1 = -\left(\frac{15}{7}\right) N_2 f_2 P_2$$

in which  $N_2 = I/(2I - 1)$ ,  $P_2$  represents  $\left(\frac{3}{2}\right) (\cos^2 \beta - 1/3)$  and  $f_2$  is  $(1/I^2)[\langle I_z \rangle^2 - (1/3)I(I + 1)]$ . The preferential axis of the nuclear spins, denoted by  $z$ , is parallel to the magnetic field at the position of the nuclei, which is caused by the electronic magnetic moments.  $f_2$  is a function of  $\Delta/T$ , where  $\Delta$  is the spacing of the h.f.s. levels.

It will be clear from formula (6.1) that the ratios of the  $\gamma$ -ray effects measured in different directions, which are fixed with respect to the crystalline axes, are independent of temperature as long as the preferential axis for nuclear orientation does not change.

For three counters placed in mutually perpendicular directions the sum of the  $\gamma$ -ray effects must be zero since the sum of the three  $\cos^2 \beta$  values equals 1.

If cobalt ions are polarized by a strong magnetic field parallel to the crystal field axis,  $2A$  is equal to the well-known h.f.s. constant  $A$ , while  $2A$  equals  $B$  if the polarizing field is perpendicular to the crystal field

axis. If the polarizing field has an arbitrary direction the spacing of the h.f.s. levels is determined by:

$$(6.2) \quad 4\Delta^2 = (A^2 g_{\parallel}^2 \cos^2 \theta_H + B^2 g_{\perp}^2 \sin^2 \theta_H) / (g_{\parallel}^2 \cos^2 \theta_H + g_{\perp}^2 \sin^2 \theta_H)$$

For cobalt ions in  $\text{CoNH}_4$ -tutton salt the difference between  $2\Delta$  and  $A$  will be a few percent if  $\theta_H < 35^\circ$ , as may be concluded from formula (6.2) using the values for  $A$ ,  $B$  and  $g$  measured by BLEANEY *et al.* [11] in the diluted salt. In  $\text{CoNH}_4$ -tutton salt  $A \gg B$  and for this reason the relation between  $f_2$  and  $T$  in the case of crystal field alignment is the same as for polarization in the direction of the crystal field axis. For  $^{60}\text{Co}$  the  $f_2$  versus  $T$  relation has been calculated by POPPEMA [6]. At temperatures where  $A/kT \ll 1$ , the  $f_2$  values are proportional to  $T^{-2}$ .

If manganese nuclei become aligned along the crystal field axis the dependence of  $f_2$  and thus of the  $\gamma$ -effects on temperature can be calculated at relatively high temperatures, by means of a formula given by SIMON *et al.* [12]. Their formula can be used at temperatures where  $A$  and  $D$  are small compared to  $kT$ , but it is possible to derive a formula which is somewhat more generally valid (no restriction for  $D/kT$ ). Curve I of fig. 6.5 gives the relation between  $W(\pi/2) - 1$  and temperature calculated assuming  $A/kT \ll 1$  and using  $I = 3$ ,  $\mu/I = 1.1$  n.m.,  $A/k = 0.0104^\circ \text{K}$  [13].

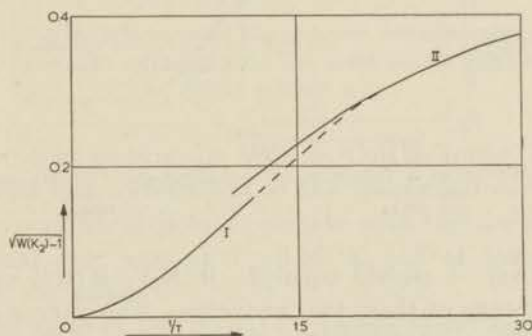


Fig. 6.5 The relation between  $\gamma$ -intensity in the  $K_2$  direction and the absolute temperature calculated by means of  $I = 3$ ,  $\mu/I = 1.1$  n.m.,  $A/k = 0.0104^\circ \text{K}$ ,  $D/k = -0.038^\circ \text{K}$  assuming:

curve I crystal field alignment with  $A/kT \ll 1$

curve II polarization by a strong magnetic field in the  $K_1K_3$  plane or crystal field alignment with  $|D|/kT > 1$

The  $\gamma$ -effect versus temperature relation may also be calculated at very low temperatures, since then only the energy levels with electron spin  $S_z = \pm 5/2$  are populated. This relation is given in fig. 6.5 by curve II. The two curves can be connected without much difficulty.

If manganese ions are polarized by an external field the low temperature curve remains unchanged even if the magnetic field makes a large angle with the crystal field axis since  $\Delta$  is isotropic ( $A = B$  and  $\langle S \rangle$  is always  $5/2$  for negative values of  $D$ ).

### 3. Comparison with theory

In agreement with theory the sum of the  $\gamma$ -ray intensities measured in the directions of the three magnetic axes equals zero within the statistical accuracy of the measurements. A consideration of the ratios of the effects shows that these ratios are not independent of temperature for experiments 1a and 1c as they would be if the preferential directions for nuclear orientation would not change. For  $^{60}\text{Co}$  in  $\text{CoNH}_4$ -tutton salt this may be seen in fig. 6.2. When the sample warms up, after about 15 minutes, the effects of the  $K_1$  and  $K_3$  counters decrease more rapidly than the effect of the  $K_2$  counter. The same behaviour is shown in fig. 6.4 for  $^{54}\text{Mn}$  in the  $\text{CoNH}_4$  salt. At relatively high temperatures (high entropies) the  $K_3$  and  $K_1$  effects are smaller compared to the  $K_2$  effect than at lower temperatures. The ratio of  $W(K_3)-1$  and  $W(K_2)-1$ , denoted by  $W^{(3/2)}$  in the following, is plotted *versus* temperature in fig. 6.6. ( $\text{CoNH}_4$ -tutton

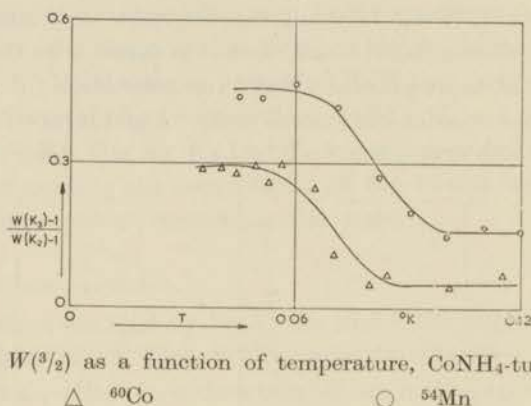


Fig. 6.6  $W^{(3/2)}$  as a function of temperature,  $\text{CoNH}_4$ -tutton salt.

$\Delta$   $^{60}\text{Co}$

$\circ$   $^{54}\text{Mn}$

salt). Since  $W(K_3)-1$  should equal  $2 - W(K_2) - W(K_1)$  we used, in fact the weighted average of these two quantities. The curves show the same behaviour for  $^{60}\text{Co}$  and for  $^{54}\text{Mn}$ .  $W^{(3/2)}$  seems to be independent of temperature for  $T > 0.09^\circ\text{K}$  and for  $T < 0.06^\circ\text{K}$  but it changes considerably between these two temperatures near the transition temperature of  $0.084^\circ\text{K}$ . Above  $0.045^\circ\text{K}$  the temperatures were derived from the known  $T-S$  relation. Temperatures below  $0.045^\circ\text{K}$  ( $^{60}\text{Co}$ ) were reached with an indirect cooling method and were estimated from the  $\gamma$ -ray intensity in the  $K_2$  direction (see fig. 6.7). The lowest temperature reached was about  $0.033^\circ\text{K}$ .

The experimental values of  $W^{(3/2)}$  are at temperatures higher than  $0.09^\circ\text{K}$  in agreement with a calculation for nuclear alignment along the crystal field axes. Assuming that these axes make angles with the  $K_1$  axis as found by means of paramagnetic resonance in the diluted salt, ( $\alpha = 32^\circ$  for Mn and  $\alpha = 34^\circ$  for Co), one expects  $W^{(3/2)} = 0.16$  for Mn and  $W^{(3/2)} = 0.06$  for Co in fair agreement with the experimental values of  $0.16 \pm 0.02$  and  $0.04 \pm 0.02$ , respectively.

The magnitude of the  $\gamma$ -intensity was above  $0.08^\circ\text{K}$  in agreement with the calculation for crystal field alignment. This is shown in fig. 6.7 for  $^{60}\text{Co}$  and the  $\text{K}_2$  counter. The solid line represents the calculated intensity *versus* temperature relation. Below  $0.08^\circ\text{K}$  the  $\text{K}_2$  effect increases less than expected. The temperatures used before (fig. 6.6) for the indirect cooling experiment were derived from the  $\text{K}_2$  intensity by extrapolating the experimental curve in fig. 6.7 to lower temperatures.

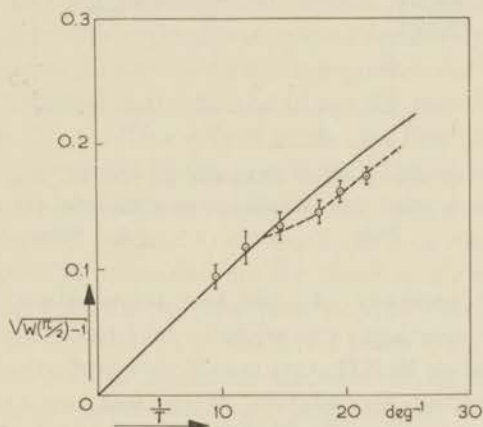


Fig. 6.7  $^{60}\text{Co}$  in  $\text{CoNH}_4$ -tutton salt. The relation between the  $\gamma$ -effect in the  $\text{K}_2$  direction and the absolute temperature. The solid line is calculated by means of  $A/k = 0.0200^\circ\text{K}$ .

The corresponding picture for  $^{54}\text{Mn}$  in  $\text{CoNH}_4$ -tutton salt is given in fig. 6.8. The solid line corresponds to the theoretical curve, discussed in fig. 6.5. The experimental points coincide with the curve for alignment along the crystal field axis at  $T > 0.09^\circ\text{K}$  but at lower temperatures  $W(\text{K}_2) - 1$  gets too small.

In fig. 6.9 the ratio of the  $W(\text{K}_2) - 1$  values found experimentally and the values calculated for crystal field alignment are plotted *versus* temperature. At relatively high temperature their ratio equals 1 within

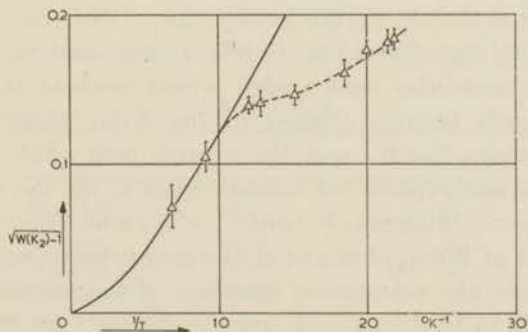


Fig. 6.8  $^{54}\text{Mn}$  in  $\text{CoNH}_4$ -tutton salt. The relation between  $W(\text{K}_2) - 1$  and temperature. The solid line is a theoretical curve, taken from fig. 6.5.



cobalt nuclei values of  $\theta_N$  similar to those just mentioned are very unlikely if the h.f.s. constants as found in the diluted salt ( $A/B=12$ ) describe the interaction. In a molecular field model the following relation between  $\theta_N$  and  $\theta_M$  holds:

$$(6.3) \quad \text{tg } \theta_N = Bg_{11} \text{tg } \theta_M / Ag_{\perp}$$

and for this reason one expects  $\theta_N$  to be smaller than  $2^\circ$ . We checked this formula and also our experimental method to derive  $\theta_N$  for  $^{60}\text{Co}$  in  $\text{ZnNH}_4$ -tutton salt, which crystal was cooled indirectly by gluing it to a  $\text{CeMg}$ -nitrate crystal. The  $\gamma$ -intensities were measured when a magnetic field of 400 Oe was applied in the  $K_1$  and in the  $K_3$  direction. The observed values of  $\theta_N$  were  $1.5 \pm 1^\circ$  for a field in the  $K_1$  direction and  $2.5 \pm 1^\circ$  for a field in the  $K_3$  direction in agreement with formulae (6.3) and (5.29).

In all experiments the values of  $W(K_2)-1$  were much smaller than expected for a direction perpendicular to the axis of nuclear orientation. There are some possible explanations for these small effects:

a. The  $\gamma$ -intensity in the  $K_2$  direction may be less than expected if the nuclear spins are not aligned in the  $K_1K_3$  plane [18]. However, rather large angles between nuclear alignment axes and  $K_1K_3$  plane are required to get agreement with experiment. Such large angles, of the order of  $30^\circ$ , are unlikely, particularly for cobalt nuclei and no indication of these angles has been found in the magnetic experiments. Moreover, if we explain the too small effects found for  $^{54}\text{Mn}$  in  $\text{MnNH}_4$ -tutton salt in this way, we derive from the observed value of  $W(K_3)-1$  that the angle between nuclear spins and  $K_3$  axis must be  $58^\circ$ , which disagrees with the ferromagnetic moments observed in the  $K_3$  direction, since the nuclear and electron spins become oriented in the same direction.

b. The spacing of the energy levels for the nuclear spins may be considerably smaller than in the case of crystal field alignment ( $\Delta$  is too small). If this is the explanation of the experimental results, we see from fig. 6.9 that the values of  $\Delta$  are independent of temperature at the lowest temperatures obtained. The ratio of  $\Delta$ , derived from the experiments and  $\Delta_p$  calculated for crystal field alignment in the paramagnetic state is given in table VI, I. The value of  $\Delta/\Delta_p$  is relatively the smallest for  $^{54}\text{Mn}$  in  $\text{MnNH}_4$ -tutton salt and the largest for  $^{60}\text{Co}$  in  $\text{CoNH}_4$ -tutton salt.

TABLE VI, I

Nucleus	Tutton salt	$\Delta/\Delta_p$	$\theta_N$ deg	$\theta_M^\circ$ deg
$^{54}\text{Mn}$	$\text{MnNH}_4$	0.45	$\geq 21$	16
$^{54}\text{Mn}$	$\text{CoNH}_4$	0.54	$7.5 \pm 1$	
$^{60}\text{Co}$	$\text{MnNH}_4$	0.6	$16 \pm 3$	
$^{60}\text{Co}$	$\text{CoNH}_4$	0.88	$5 \pm 1$	10

The position of the nuclear alignment axes and the magnitude of the nuclear level spacing for Co and Mn nuclei in  $\text{CoNH}_4$ - and  $\text{MnNH}_4$ -tutton salt. It is assumed that the nuclei become aligned in the  $K_1K_3$  plane.

c. The relaxation times for the nuclear spin system are long. A small value of  $\Delta$  may occur if the magnetic moments of the electrons change sign in a time which is short compared with the relaxation time for the nuclear spin system, that is to say that the magnetic domains move rather quickly through the crystal. However, in this case one expects a much larger  $\gamma$ -anisotropy if the ferromagnetism is saturated by a magnetic field in the  $K_3$  direction.

Experimentally this is not found (section 1c). There is another possibility that the nuclear spin relaxation time is so long that the temperature of the nuclear spin system is higher than the temperature of the electron spin system. Since we never found any time dependence of the  $\gamma$ -anisotropy in experiments with a directly demagnetized crystal, this possibility seems unlikely.

### 5. Conclusions

None of the possibilities mentioned above gives a satisfactory explanation of the experimental data. It seems that in magnetically ordered  $\text{CoNH}_4$ - and  $\text{MnNH}_4$ -tutton salt the h.f.s. interaction is not described completely by the usual terms in the spin Hamiltonian [ $AS_zI_z + B(S_xI_x + S_yI_y)$ ] which terms only account for the interaction between the nuclear and the electron magnetic moments of the same ion.

Similar effects have been found by DANIELS [14]. One of his results is that the  $\gamma$ -ray anisotropy of  $^{60}\text{Co}$  nuclei inserted in  $\text{Mn}(\text{SiF}_6)_2 \cdot 6\text{H}_2\text{O}$  is much larger than expected. Other data on the h.f.s. interaction in antiferromagnetic crystals were obtained by COOKE *et al.* [15] who measured the specific heat of  $\text{MnF}_2$  between 0.5 and 2° K. The value of the h.f.s. constant as derived from the specific heat data differs by only five percent from the expected value. This may suggest that the remarkable effects measured in tutton salts and fluosilicates have something to do with the fact that the energy of the magnetic interaction, h.f.s. interaction and crystal field anisotropy are of the same order of magnitude in these salts, whereas in  $\text{MnF}_2$  the magnetic interaction is much larger.

### 6. The crystal field splitting of manganese ions in a tutton salt

A comparison of the position of the crystal field axes and the value of the crystal field parameter  $D$ , observed for manganese ions in several tutton salts, gives rather surprising results.

According to resonance experiments (ref. 16)  $\psi = 58^\circ$ ,  $\alpha = 32^\circ$  and  $D/k = 0.038^\circ \text{K}$  for manganese ions inserted in  $\text{ZnNH}_4$ -tutton salt.

The magnetic data obtained with concentrated  $\text{MnNH}_4$ -tutton salt suggest that  $\psi$  is about  $150^\circ$  and  $D$  is negative in this salt. The analysis of the magnetic susceptibilities below the transition temperature gives an absolute value for  $D$  which is 23 % smaller than measured in the diluted salt. A negative sign for  $D$  in  $\text{MnNH}_4$ -tutton salt is agreement

with deviations from Curie's law observed by DURIEUX [17] on a single crystal between 20 and 1° K.

Also the alignment data obtained on  $^{54}\text{Mn}$  in  $\text{CoNH}_4$ -tutton salt suggest a negative value for  $D$ . The observed  $\gamma$ -anisotropies were above the transition temperature in agreement with  $\psi = 150^\circ$ ,  $\alpha = 32^\circ$  and  $D/k = -0.038^\circ \text{K}$ . If  $D$  was positive the  $\gamma$ -anisotropy would be about two times smaller than observed experimentally.

It seems unplausible, that upon diluting  $\text{MnNH}_4$ - or  $\text{CoNH}_4$ -tutton salt with zinc ions the value of  $\psi$  for manganese ions changes by  $90^\circ$  and the sign of  $D$  reverses while  $\alpha$  remains the same and the change of the absolute value of  $D$  is small. The discrepancy might be explained if there is an error of  $90^\circ$  in the measurement of  $\psi$  in the diluted salt. However, an experiment on the  $\gamma$ -anisotropy of  $^{54}\text{Mn}$  in a  $\text{ZnNH}_4$ -tutton salt single crystal, which was cooled indirectly by gluing it to a  $\text{CeMg}$ -nitrate crystal, gave a  $\gamma$ -anisotropy roughly in agreement with  $\psi = 58^\circ$  and the positive sign for  $D$ . It seems therefore that there really is a change of the sign of the crystal field parameter  $D$ , when diluting  $\text{MnNH}_4$ -tutton salt with Zn ions.

#### REFERENCES

1. DAUNT, J. C., Proc. Int. Conf. Low Temp. Phys. Oxford 157 (1951).
2. GORTER, C. J., Proc. Int. Conf. Low Temp. Phys. Oxford 158 (1951).
3. DANIELS, J. M. and M. A. R. LE BLANC, Canad. J. Phys. 36, 638 (1958).
4. KHUTSISHVILI, G. R., J. Exp. Theor. Phys. U.S.S.R. 29, 894 (1955).
5. GRACE, M. A., C. E. JONHSON, N. KURTI, R. G. SCURLOCK and R. T. TAYLOR, Proc. Int. Conf. Low Temp. Phys. Paris 263 (1955).
6. POPPEMA, O. J., Thesis, Groningen (1954).
7. GORTER, C. J., O. J. POPPEMA, M. J. STEENLAND and J. A. BEUN, Commun. Kamerlingh Onnes Lab. Leiden 287b; Physica 17, 1050 (1951).
8. DANIELS, J. M. and M. A. R. LE BLANC, Canad. J. Phys. 37, 82 (1959).
9. GARRETT, C. G. B., Proc. Roy. Soc. A 206, 242 (1951).
10. STEENLAND, M. J. and H. A., TOLHOEK, Progress in Low Temperature Physics II, North-Holland Publ. Co., Amsterdam 292 (1957).
11. BLEANY, B. and D. J. E. INGRAM, Proc. Roy. Soc. A 208, 143 (1951).
12. SIMON, A., M. E. ROSE and J. M. JAUCH, Phys. Rev. 84, 1155 (1951).
13. JEFFRIES, C. D., Phys. Rev. 117, 1056 (1960).
14. DANIELS, J. M., Proc. Int. Conf. Low Temp. Phys. Toronto (1960).
15. COOKE, A. H. and D. T. EDMONDS, Proc. Phys. Soc. (London) 71, 517 (1958).
16. BLEANEY, B. and D. J. E. INGRAM, Proc. Roy. Soc. A 205, 336 (1951).
17. DURIEUX, M., Thesis, Leiden (1960).
18. This might be due to a term  $D \cdot [\mathbf{S}_1 \times \mathbf{S}_2]$ , as suggested by DZIALOSHINSKI [19] and MORIYA [20].
19. DZIALOSHINSKI, I, J. Phys. Chem. Solids 4, 241 (1958).
20. MORIYA, T., Phys. Rev. Let. 4, 228 (1960).

## SAMENVATTING

De in dit proefschrift beschreven experimenten zijn uitgevoerd bij temperaturen beneden  $1^\circ \text{K}$ , die bereikt worden met behulp van de methode der adiabatische demagnetisatie. Een korte beschrijving van de gebruikte meetmethoden wordt gegeven in hoofdstuk I.

Metingen, die verricht zijn aan alcoholische oplossingen van chroom, ijzer en koperzouten worden besproken in hoofdstuk II. De gebruikte oplosmiddelen zijn gemakkelijk te onderkoelen vloeistoffen en bij zeer lage temperaturen verkrijgt men een glasachtige substantie, waarin de magnetische ionen vrijwel gelijkmatig verdeeld zullen zijn. De wisselwerking tussen de magnetische momenten van de ionen en het elektrische veld, veroorzaakt door omringende alcohol en water moleculen, blijkt in het algemeen veel groter te zijn dan gewoonlijk voor deze ionen gevonden wordt in kristallen. Bij oplossingen van lage concentratie blijken irreversibele processen op te treden tijdens het demagnetiseren, hetgeen wijst op het bestaan van lange relaxatietijden tussen de magnetische momenten en de thermische roostergolven.

Hoofdstuk III is gewijd aan het probleem van warmteoverdracht bij zeer lage temperaturen. Gebruik makend van alcoholische oplossingen als koelsubstanties zijn eenkristallen afgekoeld. Uit de analyse van de warmteoverdracht, gemeten tussen  $0.6$  en  $0.015^\circ \text{K}$ , blijkt dat de door verschillende auteurs belangrijk geachte contactweerstand in onze experimenten geen rol van betekenis vervult. Bij de laagste temperaturen werd de warmtestroom voornamelijk bepaald door de beperkte warmtegeleiding in het te koelen eenkristal. De gemeten warmtestroom is vergeleken met de theorie over warmtetransport door middel van phononen. Verschillende methoden voor indirecte afkoeling, die in gebruik zijn, worden in hoofdstuk III vergeleken. Het gebruik van een koelzout, dat bestaat uit een groot aantal schijfjes van een magnetisch eenkristal geplakt op koperen plaatjes, wordt aanbevolen. Dit koelzout zal relatief grote hoeveelheden warmte relatief snel kunnen opnemen.

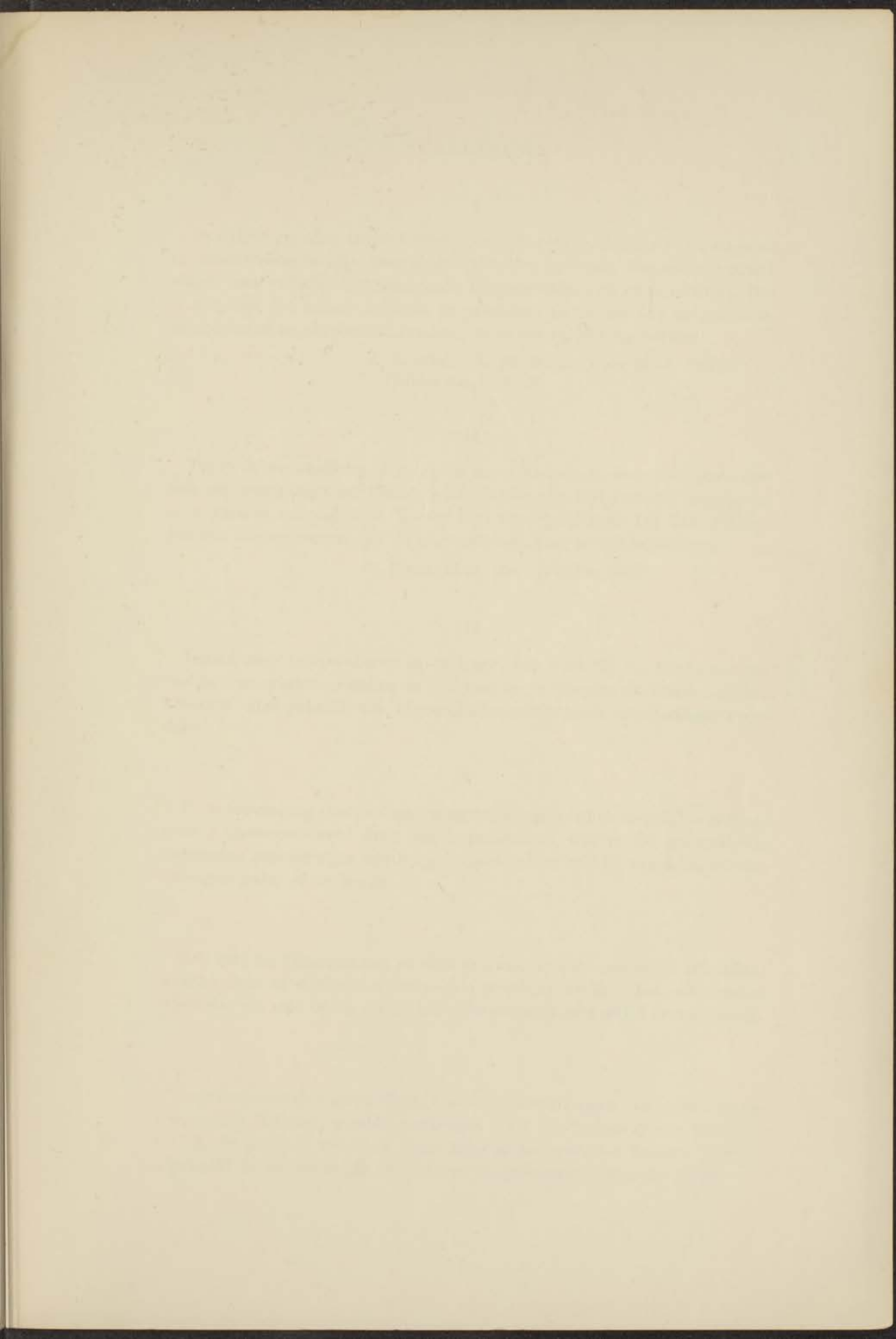
Het magnetisch gedrag van kristallen van  $\text{MnNH}_4$ -,  $\text{CoNH}_4$ -,  $\text{CuNH}_4$ - en  $\text{CuK}$ -tutton zout is beschreven in hoofdstuk IV. De twee eerstgenoemde kristallen vertonen een zeer anisotroop magnetisch gedrag. In één richting wijst het magnetisch gedrag op een antiferromagnetische ordening, in een richting loodrecht hierop op een ferromagnetische ordening.

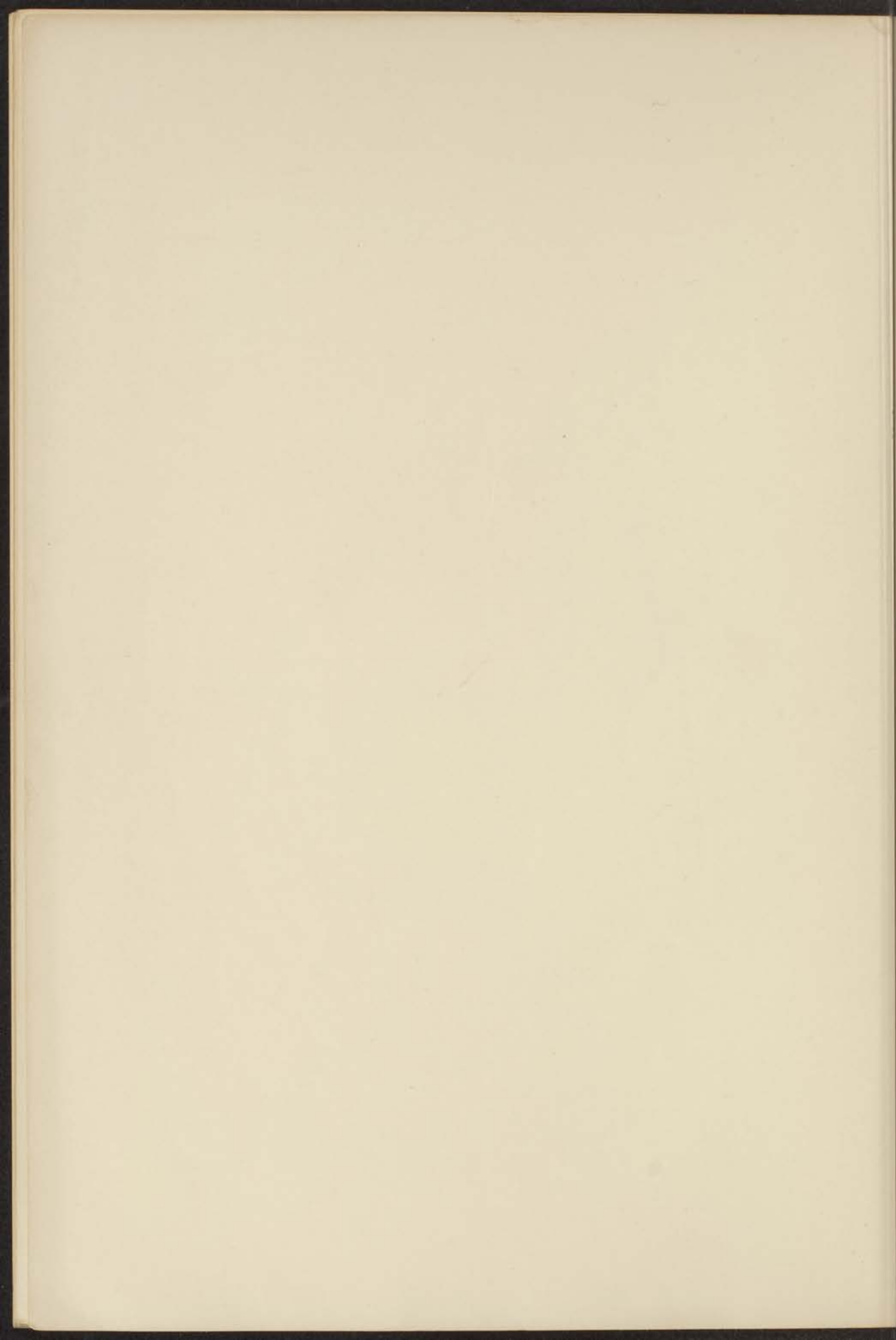
De beide onderzochte koperzouten vertonen een geheel verschillend magnetisch gedrag.  $\text{CuNH}_4$ -tutton zout lijkt duidelijk antiferromagnetisch te zijn terwijl in  $\text{CuK}$ -tutton zout zeer hoge waarden voor de susceptibiliteit gemeten worden, die op ferromagnetisme wijzen.

In hoofdstuk V worden de resultaten vergeleken met een model, dat van een moleculair veld gebruik maakt, hetwelk zowel de dipool-dipool wisselwerking als de exchange wisselwerking tussen de magnetische ionen in rekening brengt. Op grond van röntgenonderzoekingen kan men verwachten dat ieder magnetisch ion exchange wisselwerking heeft met twee soorten buurionen. De bijdragen van deze twee soorten buuren worden geschat uit de experimenteel verkregen gegevens.

De hyperfijnstructuur wisselwerking in magnetisch geordend  $\text{CoNH}_4$ - en  $\text{MnNH}_4$ -tutton zout is onderzocht met behulp van de anisotrope intensiteitsverdeling der gammastralen van axiaal gerichte  $^{60}\text{Co}$  en  $^{54}\text{Mn}$  kernen (hoofdstuk VI). De gevonden  $\gamma$ -straal anisotropieën zijn kleiner dan men verwachtte en ook de orientering van de voorkeursas is niet zonder meer in overeenstemming met de magnetische metingen.







A. R. Miedema

## STELLINGEN

### I

In enkele gevallen is het ferromagnetisch gedrag, dat als bijverschijnsel in antiferromagnetisch geordende kristallen optreedt, toegeschreven aan elkaar niet volledig compenserende magnetisaties van onderroosters. Het is mogelijk dat andere bekende gevallen van parasitair ferromagnetisme, bijvoorbeeld in chroomkaliumaluin, dezelfde verklaring hebben.

J. A. BEUN, A. R. MIEDEMA en M. J. STEENLAND,  
*Physica* 23, 1 (1957).

### II

Tegen de verwachting in zijn geen supergeleidende elementen gevonden met een overgangspunt beneden  $0.3^{\circ}$  K. Zo zijn bijvoorbeeld molybdeen en wolfram ook bij  $0.02^{\circ}$  K nog niet supergeleidend. Dit kan wellicht worden toegeschreven aan de aanwezigheid van verontreinigingen.

D. PINES, *Phys. Rev.* 109, 280 (1959).

### III

Indien men temperaturen in de buurt van  $0.01^{\circ}$  K wil bereiken door middel van warmtegeleiding is één van de problemen de keuze van het koelzout. Het gebruik van chroomkaliumaluin heeft verscheidene voordelen.

### IV

Door toevoeging van geringe verontreinigingen is het mogelijk een magnetisch geconcentreerd zout als koperacetaat, waarin de magnetische momenten paarsgewijze worden gekoppeld, door middel van adiabatische demagnetisatie af te koelen.

### V

Men mag bij metingen aan poeders van magnetisch anisotrope kristallen, waarbij deze in sterke magneetvelden gebracht worden, het oriënterend effect dat dit veld op de poederkristalletjes heeft niet altijd verwaarlozen.

### VI

Gegevens over de wisselwerking tussen roostertrillingen van verschillende frequenties kunnen worden verkregen door bij temperaturen beneden  $0.1^{\circ}$  K de snelheid waarmee paramagnetische kristallen kunnen worden afgekoeld in verschillende uitwendige magnetische velden te meten.

## VII

Het is praktisch uitvoerbaar om de anisotropie in de ruimtelijke hoekverdeling van  $\gamma$ -straling, geëmitteerd door georiënteerde atoomkernen, tussen 0.1 en 0.01 °K als thermometrische parameter te gebruiken. Een gunstige keuze is  $^{54}\text{Mn}$  opgenomen in magnesiumfluosilicaat.

O. J. POPPEMA, Academisch Proefschrift Groningen, Stelling II (1954).

## VIII

In aansluiting op metingen over het warmtetransport door een grenslaag bij zeer lage temperaturen zijn experimenten over de absorptie van ultrageluid in laagjes, die enkele golfengten dik zijn, interessant.

## IX

Uit het feit dat onder isolatoren vrijwel alleen subroosters met tegengesteld gerichte magnetisaties gevonden zijn mag men niet zonder meer concluderen dat magnetische superexchange bijna altijd het antiferromagnetische teken heeft.

P. W. ANDERSON, *Phys. Rev.* **115**, 2 (1959).

## X

Het valt te betwijfelen of VAN STRATEN e.a. er inderdaad in zijn geslaagd om cumulus-wolken van ongeveer 1 km<sup>3</sup> met behulp van kleine hoeveelheden koolstof te doen oplossen.

F. W. VAN STRATEN, R. E. RUSKIN, J. E. DINGER en H. J. MASTENBROOK, *U.S. Nav. Res. Rep.*, 5235 (1958).

## XI

De door SCORER opgezette en door LEVINE verder uitgewerkte theorie over opwaartse bewegingen in cumulus-wolken is in haar huidige vorm niet in overeenstemming met experimentele gegevens over menging van wolkenlucht met de omringende droge lucht.

R. S. SCORER, *J. Fluid Mechanics* **2**, 583 (1957).  
J. LEVINE, *J. Meteor.* **16**, 653 (1959).

## XII

Het is principieel onjuist dat GOLD e.a. en PEARSON hun metingen betreffende thermokrachten analyseren met behulp van de additieregels van KOHLER.

A. V. GOLD, D. K. C. MAC DONALD, W. B. PEARSON en I. M. TEMPLETON, *Phil. Mag.* **5**, 765 (1960).  
W. B. PEARSON, *Phys. Rev.* **119**, 549 (1960).

### XIII

Het is niet inconsequent te noemen dat COSSEE de kleine waarden van de magnetische verzadiging in het systeem  $\text{Co}_{1-x}\text{Zn}_x\text{Co}_2\text{O}_4$  toeschrijft aan covalente binding en niet aan antiferromagnetisme.

R. WARD, *Progress in Inorganic Chemistry* I, 488 (1959).  
P. COSSEE, *Academisch Proefschrift Leiden*, (1956).

### XIV

Indien men, zoals KNESE, „voorgespannen beton” als model gebruikt bij de interpretatie van de fijne structuur van beenelementen is het onjuist om de collagene fibrillen met de betonmassa te vergelijken.

K. H. KNESE, *Knochenstruktur als Verbundbau*, 16 (1958).

### XV

De bij paardenraces in gebruik zijnde totalisator biedt de mogelijkheid tot het bestaan van een spelsysteem, dat winst garandeert.

